Synthetic Cannabinoid Activation of hTRPA1 and Naturally Occurring Channel Variants

Saarin Pearson (BMedSc)

MACQUARIE University

Department of Biomedical Sciences

Faculty of Medicine and Health Sciences

Macquarie University

2017

A thesis submitted in fulfilment of the requirements for the degree of

Master of Research in Medicine and Health Sciences

To my mum. Everything I am is because of you.

CONTENTS

DECLARATION

I certify that this work contains no material which has been accepted for the award of any other degree or diploma in my name, in any university or other tertiary institution and, to the best of my knowledge and belief, contains no material previously published or written by another person, except where due reference has been made in the text. In addition, I certify that no part of this work will, in the future, be used in a submission in my name, for any other degree or diploma in any university or other tertiary institution without the prior approval of Macquarie University.

I give consent to this copy of my thesis, when deposited in the University Library, being made available for loan and photocopying, subject to the provisions of the Copyright Act 1968.

I also give permission for the digital version of my thesis to be made available on the web, via the University's digital research repository, the Library Search and also through web search engines, unless permission has been granted by the University to restrict access for a period of time.

Saarin Pearson
Department of Biomedical Sciences
Faculty of Medicine and Health Sciences
Macquarie University

ACKNOWLEDGEMENTS

I would like to thank the funding bodies that made this work possible. This work was funded in part by the NHMRC Project Grant APP 1107088 awarded to Mark Connor. I would also like to acknowledge the support I have received for my research through the provision of an Australian Government Research Training Program Scholarship.

I would like to thank my supervisors, Mark Connor and Marina Santiago, who were truly better supervisors than I could have ever hoped. Mark, thanks for your patience, guidance, support and everything else I can't put words to. Cheers. Marina, thank you also for your support and guidance, particularly in early stages of this project. I owe much of what I learned in the lab to you.

Thank you to Michael Kassiou, Sam Bannister and colleagues, for supplying many of the drugs used in this project.

I extend my thanks to all members of the Connor group, those who were there when I arrived, and those who I came to know later in the year. Each and every member made me feel welcome from the very first day, and I appreciate all the great chats we had, the volume of which may have brought the ire of the rest of the office, sorry! In particular, I'd like to thank Rochelle Boyd and Shivani Sachdev. Rochelle, thanks for all the little things you helped me out with over the course of the project, and your technical guidance along the way. Shivani, thanks for the ever present reminder that my experimental design was quite simple, regardless of how much I may have thought it wasn't. I would also like to thank the technical staff in CBMS, Faculty of Science and Engineering, for providing a supportive environment to work in while I completed my thesis. In particular, thank you to Elsa Mardones!

Thank you to all my friends from home, (all the s p i c y b o i s, you know who you are) who never strayed too far from me, despite my increasing reclusiveness as the thesis deadline loomed. I look forward to catching up with everyone in the very near future. My MRes companions Tom and Christine, you were there from the start and there till the end. Thanks for being around for a quick lunch, a chat and a break from the office when I needed it. I owe great thanks to my partner, Amalia, who supported me and put up with the highs and lows of the year without batting an eyelid. We're due for a nice dinner soon, my shout. My sisters; Jazzy, Tab and Krystal; and my gran and gramps, who were always curious about my work and supported me no matter what choices I made. And finally, my mum, for her unwavering support in life, my education and beyond. I love you.

LIST OF FIGURES

LIST OF TABLES

LIST OF TERMS AND ABBREVIATIONS

2-AG	2-arachinodoyl glycerol
5-OH	5-hydroxypentyl metabolite of UR-144
AEA	Anandamide
AITC	Allyl isothiocyanate
ANKTM1	Ankyrin like with Transmembrane domain
ARD	Anykrin Repeat Domain
CA	Cinnamaldehyde
Ca_i	Intracellular Calcium
CaM	Calmodulin
CFA	Coal fly ash
CHO	Chinese Hamster Ovary
COX-2	Cyclooxygenase-2
CRIB	CaM-and IP3R-Binding
DEA	Drug Enforcement Administrations
DMSO	Dimethyl sulfoxide
DTBP	3,5-ditert butylphenol
EC50	Half maximal effective concentration
EMCDDA	European Monitoring Centre for Drugs and Drug Addiction
FBS	Fetal Bovine Serum
FLIPR	Fluorescent Imaging Plate Reader
GPCR	G protein coupled receptor
HBSS	Hanks Buffered Salt Solution
HEK	Human Embryonic Kidney
hTRPA1	Human TRPA1
ICL	Intracellular Loop
IP3	Inositol 1,4,5-triphosphate
IP3R	Inositol 1,4,5-triphosphate Receptor
MAPK	mitogen-activated protein kinase
MDMA	Methylenedioxymethamphetamine
NFLIS	National Forensic Laboratory Information System
NMM	N-methyl malemide
P/S	Penicillin/Streptomycin
PAR-1	Protease Activated Receptor 1
PBS	Phosphate buffered saline
PPAR	Peroxisome Proliferator-Activated Receptor
RFU	Relative Fluorescence Units
S4	Transmembrane segment 4
SCRA	Synthetic Cannabinoid Receptor Agonist
SEM	Standard Error of the Mean
SNP	Single Nucleotide Polymorphism
THC	(–)-Δ-9-trans-tetrahydrocannabinol
TRP	Transient Receptor Potential
TRPA	Transient Receptor Potential Ankyrin
TRPC	Transient Receptor Potential Canonical
TRPM	Transient Receptor Potential Melastatin
TRPML	Transient Receptor Potential Mucolipin
TRPN	Transient Receptor Potential NOMPC (no mechanoreceptor potential C)
TRPP	Transient Receptor Potential Polycystin
TRPV	Transient Receptor Potential Vanilloid

SUMMARY

THC, the primary psychoactive compound in cannabis, is a low efficacy agonist of the CB_1 receptor. Synthetic cannabinoids (SC's) are compounds structurally unrelated to THC, which also function as agonists of the CB receptors. Recreational SC products have been monitored since the emergence of JWH-018 in 2008, with new compounds rapidly developed to evade legislation and detection. SC consumption, including mass intoxication events, is associated with a range of adverse effects uncharacteristic of plant derived cannabinoids, such as psychomotor agitation, aggression, cardiac arrhythmias, seizures and death. The mechanisms of SC toxicity are not established, however, some SCs are higher efficacy agonists of CB receptors than common research cannabinoids, and have the potential to act at non-CB receptor targets. Polymorphic variants of these targets may influence individual toxicity. Transient receptor potential ankyrin 1 (TRPA1) is a calcium-permeable ion channel highly expressed in the brain, sensory neurons and the epithelium of the lungs. TRPA1 is activated by THC and some synthetic cannabinoids, with several naturally occurring polymorphic variants in humans. HEK293 cells stably transfected with human TRPA1 and five select SNP variants were studied by measuring changes in intracellular $[Ca^{2+}]$ in response to selected high concern SCs and some natural ligands. The SC's MDMB-CHMICA, PB-22, 5F-PB-22, UR-144, XLR-11 and 5-OH-UR-144 activate hTRPA1 and each mutant, although they exhibited varying degrees of efficacy between the mutants. The R58T variant resulted in increased activation by PB-22 and 5F-PB-22 compared to the WT. R3C, E179K, H1018R and R3C+R58T resulted in decreased activated compared to the WT by UR-144 and XLR-11. The 5-hydroxypentyl metabolite common to both remained unaffected by hTRPA1 polymorphisms, as did MDMB-CHMICA and two prototypic ligands, cinnamaldehyde and allyl isothiocyanate. At hTRPA1, XLR-11 was relatively more potent than the structurally similar UR-144. The common 5-OH metabolite exhibited greater relative potency than both parents at some hTRPA1 variants. THC was shown to be a more potent agonist at hTRPA1 than all synthetic cannabinoids tested. These data show that the efficacy of SCs varies at naturally occurring hTRPA1 polymorphisms, but that different drugs are affected in distinct ways. If SC toxicity is related to actions at non-CB proteins such as TRPA1, mechanisms of drug toxicity may be highly individualized.

1 INTRODUCTION

1.1 CANNABIS AND CANNABINOIDS

1.1.1 Background

The Cannabis plant has a long and storied history, being one of the oldest continually cultivated plants by man [1]. The plant is part of a family with only one genus, Cannabis, and three species, sativa, indica and ruderalis [1]. The differences are a matter of geography, with *C. sativa* originating in present day Kazakhstan, *C. indica* from the Western Himalayas, and *C. ruderalis* in Central Asia [1]. From their geographic origins, the plants gradually spread West, reaching Egypt and eventually Europe with the slave trade [1].

The plant itself has been used as food stock and as a textile material for hundreds of years, however, pharmacological preparations of cannabis are perhaps the most well-known and interesting [2]. The history of cannabis use as medicine reaches as far back as 2700 BCE, where an oral preparation was noted in a Chinese farmers manual for its hallucinatory, appetite stimulating, tonic and antisenility effects [3]. Since then, it has been purported for its antibacterial, anti-inflammatory, antitumor and analgesic effects, among others [3]. With the recognition of the therapeutic potential of cannabinoids came a search for synthetic compounds that avoid the psychoactivity, while retaining the benefits of plant based cannabinoids [4]. Several compounds made their way to clinical trials, but so far no synthetic cannabinoid therapeutic has made it to market [5-8]. In recent years, cannabis based medicines have made it to market. Dronabinol, a synthetically derived THC, has been in use since the 1980's as a treatment for nausea [9]. Sativex®, a mixture tetrahydrocannabinol and cannabidiol, has been approved in a number of countries for the treatment of pain and nausea, and muscle spasticity in multiple sclerosis (MS) [10-13].

1.1.2 Cannabinoids and their Receptors

Cannabinoids refer to the C21 terpenophenolic compounds isolated from Cannabis sativa, their derivatives and transformation products [2]. The term "phytocannabinoid" is given to those that originate from the plant itself [2]. These compounds fall in to 11 classes, one of which is Δ9-THC (referred to as THC henceforth). THC is the most well-known cannabinoid, and the primary psychoactive component of cannabis [14].

Two cannabinoid receptors have been discovered so far, CB_1 and CB_2 [15]. Both are G protein coupled receptors (GPCRs), which are coupled through $G_{i/o}$ proteins and less commonly through G_s and $G_{q/11}$ [15, 16]. CB_1 receptors are expressed mainly in the central nervous system, on the terminals of central and peripheral nerves where they mediate the inhibition of neurotransmitter release via interaction with a large variety of ion channels and protein kinases [15, 16]. There is also evidence of non-neuronal CB_1 expression, in the digestive tract, liver, fat and muscle cells [17]. Evidence for CB_2 expression in the brain is limited and its role is yet to be firmly established, however, it is found expressed in cells throughout the immune system [15, 16]. Two endogenous derivatives of arachidonic acid are known to function as agonists of the CB receptors, and are known as endocannabinoids [15]. These compounds are anandamide (AEA), and 2-arachinodoyl glycerol (2-AG), discovered in the mid 1990's [18-20]. These compounds, and the CB receptors, form part of the endocannabinoid system, whose functions include homeostasis, neuroprotection, the modulation of nociception, regulation of motor activity, memory processing, immunity and inflammation [17, 21-24]. THC exerts its psychotropic effects as an agonist of CB_1, but is a low efficacy agonist compared to AEA and 2-AG [16].

1.1.3 Modern Cannabis Usage

In modern times, cannabis is most famous in the preparation, marijuana, a recreational drug. Marijuana has a substantial amount of global users, with 182.5 million active users reported in

2014 (2.5% of the global population in 2014) [25]. Additionally, the recently released results of the 2017 Global Drug Survey position marijuana as the most popular illicit drug in the world. 77.8% of survey respondents (n>115,000) report having used marijuana at least once in their lifetime, with the next most popular drug being MDMA (Methylenedioxymethamphetamine, commonly referred to as ecstasy) at 33.5% [26]. Furthermore, cannabis users (n=69,299) report an average of 135.4 days out of the year where they consumed cannabis [26]. In Australia, 35% of people over the age of 14 have reported using cannabis at least once, and 10% report being active users in 2013 [27]. The reasons for cannabis use among users vary, however, most often users seek to experience disinhibition, dreaminess, euphoria, enhance otherwise mundane experiences and socialise with other smokers [27, 28]. Cannabis use is often reported in those at risk of, or suffering mental illnesses, who report that they use to self-medicate, and regulate their disorders, despite awareness that cannabis usage may exacerbate negative symptoms [29, 30]. Marijuana has a track record and perception as a safe drug when compared to other popular drugs such as nicotine and alcohol [31]. This is also, in part, due to the rarity of deaths that can be attributed solely to cannabis consumption [32, 33]. However, there is still great potential for incidents causing bodily harm due to the effects of cannabis. Consumption of cannabis can lead to short term tiredness, dizziness and tachycardia, which increase the risk of trips, falls and motor vehicle accidents [32, 34]. In Metropolitan Melbourne, Australia, cannabis is implicated in 4 ambulance call outs per day [35]. Of these callouts, 73% result in conveyance to hospital, often for persons between 25-30 years old suffering psychosis resulting from long term drug use, and have usually consumed more than one drug prior to the callout [35, 36]. The most acute, adverse reactions to cannabis in the literature take the form of serious cardiac dysfunctions, such as tachyarrhythmia, requiring immediate hospitalisation. These cases have been documented in both persons young and old, with and without history of cardiovascular complications [37, 38].

1.2 SYNTHETIC CANNABINOIDS

1.2.1 Background

Synthetic cannabinoids are structures that interact with CB receptors, either as agonists or antagonists, which are synthesised in a laboratory. Synthetic cannabinoids began as derivatives of the structure of THC, for development of cannabinoid analgesics [39]. A number of compounds from diverse structural classes were created to find suitable, potent CB_1 CB_2 selective ligands [39]. Four basic structural classes exist; classical, THC like cannabinoids which feature a dibenzopyran moiety; non-classical cannabinoids, bi and tricyclic derivatives of THC that lack a pyran ring; aminoalkylindoles, with structures that differ markedly from the classical and non-classical groups, consisting of an indole core, substituted with an aroyle group at C3 and aminoalkyl sidechain at N1; and eicosanoids, which differ markedly from the previous 3 and feature the endocannabinoids AEA and 2-AG [40-42].

In the mid 2000's, derivatives of these structures began to appear in products sold to human consumers. These synthetic cannabinoids are synthesised in clandestine labs, mostly in China, and sprayed on to plant material which is then packaged for retail [39, 43]. The consumer name for these products is often a derivative of "Spice", Spice Silver, Spice Gold, Spice Diamond, etc. [44]. These products went under formal investigation in 2008, by German and Austrian authorities who sought to ascertain the psychoactive ingredients of Spice [44]. The compound JWH-018 was notified to the European Monitoring Centre for Drugs and Drug Addiction (EMCDDA) on the 19th of December, 2008 by Austrian authorities, following independent identifications in Austria and Germany in the days prior [44]. JWH-018 is an aminoalkylindole, first synthesised by John W. Huffman in 1995, as a high affinity CB receptor agonist for CB receptor research [44, 45]. The following year, reports of novel synthetic cannabinoid compounds in Spice products increased. Derivatives of CP 47,497, a non-classical research cannabinoid developed in the 1980's, were reported in Spice products

from Germany, Slovakia, Finland and the UK [44, 46]. HU-210, a classical cannabinoid research compound developed in the 1980's, and other members of the JWH family were found in products seized in the US, Denmark and the Netherlands [44, 47]. A rapid proliferation of synthetic cannabinoid compounds followed. The first seized synthetic cannabinoid was reported to the EU Early Warning System [EMCDDA] in 2008. In 2015, 30 novel compounds were identified, with a total of 160 individual compounds identified in synthetic cannabinoid products seized since 2008 [43, 48]. In the US, 2009, the first 2 synthetic cannabinoid products were reported to the Drug Enforcement Administrations (DEA) National Forensic Laboratory Information System (NFLIS) [49]. Novel reports continued year on year, with 84 individual compounds entered into NFLIS by 2015 [49]. NFLIS data also highlights the rapidly changing nature of synthetic cannabinoid products. In 2013, XLR-11 made up 60% of reported synthetic compounds. In 2015, this was only 24%, with AB-CHMINACA taking 26%, a compound that went unreported in 2013 [49].

Several national and international surveys on synthetic cannabinoid users have been conducted to ascertain a picture of the average user, and their reasons for usage. The average synthetic cannabinoid user tends to be a young, white male, with a history of poly drug use [50]. The primary route of administration appears to be inhalation, either via traditional combustion and smoking, or by vaporisation [51-53]. Commonly reported reasons for usage include, but are not limited to; curiosity, increased effect compared to normal cannabis, legality, perceived safety, value for money, and availability compared to normal cannabis [53-55]. Synthetic cannabinoids are also popular among persons subject to regular workplace drug testing, such as military personnel and those in the mining industry [50, 54]. The dynamic and rapidly evolving nature of consumer synthetic cannabinoid products allows consumers to stay ahead of and evade drug screens, which take time to develop and validate for a particular substance.[56]. In Australia, synthetic cannabinoid products are typically purchased from

either drug paraphernalia stores, or the internet, where a wide variety of vendors can be found[54].

Synthetic cannabinoid use in Australia is decreasing, with 0.3% of Australians aged 14 years and over consuming synthetic cannabinoid products in 2016, compared to 1.2% in 2013 [27]. In comparison, the United Kingdom estimates synthetic cannabinoid use at 0.1% in those aged 16-64 in 2011/2012, compared to 0.2% in 2010/2011 [57]. Synthetic cannabinoid use among prisoners in the United Kingdom is much higher than the general population. A 2016 survey found that 33% of prisoners (n = 625) had consumed a synthetic cannabinoid product in the last month [57]. Of those users, 46% reported almost daily use [57]. In Spain, a national survey estimated synthetic cannabinoid usage at 0.5% in those aged 15-64 [57]. In France, lifetime use of synthetic cannabinoids in those aged 18-64 is estimated at 1.7% [57]. In Frankfurt, Germany, the use of synthetic cannabinoids has remained relatively high in those aged 15-18, between 6 to 9% in 2010-2015[57]. Synthetic cannabinoid use is also declining in the US. 6% of 17 to 18 year old reported synthetic cannabinoid use in 2014, compared to 8% in 2013 and 11% in 2012 [58].

1.2.2 The Danger of Synthetic Cannabinoids

Synthetic cannabinoids, unlike their plant derived counterparts, have been implicated in a host of reported acute intoxication events. These have produced adverse effects including, but not limited to, psychomotor agitation, aggression, delirium, loss of consciousness, tachycardia, bradycardia and seizures [43, 48, 49, 55, 59-95]. Mass poisonings with synthetic cannabinoids have gained significant public attention in the US, with 33 persons in a New York block found standing in a “zombie like” state, after consuming a synthetic cannabinoid product containing AMB-FUBINACA [75]. Examples of deaths following acute synthetic cannabinoid intoxication can be found in the literature. The compounds 5F-ADB and ADB-CHMINACA were found during the autopsy of a man who had died of asphyxia as a result of vomiting while unconscious [87, 92]. 5F-PB-22 was found post mortem in 4 young adults

between July-October 2013, whose causes of death were ruled as accidental, with extreme intoxication and loss of conscious common to all cases [94]. A 20-year-old man died due to anoxic brain injury after being found unconscious without medical care for 24 hours. MAB-CHMINACA was the main toxicological finding [70]. MDMB-CHMICA was implicated in the deaths of several global citizens, many young adults found unconscious with anoxic brain damage [62, 67, 77]. Similar cases have been reported with the compounds ADB-FUBINACA, 5F-AMB, AB-CHIMINACA and MDMB-FUBINACA, with brain death occurring after serious cardiovascular complications [65, 80, 86]. A common theme in these cases appears to be death via anoxic brain damage, either as the result of asphyxia upon loss of consciousness, a cardiovascular complication or a combination of both.

1.2.3 Hypotheses Regarding Synthetic Cannabinoid Toxicity

The mechanisms of synthetic cannabinoid toxicity are not well established, however, a number of theories have been put forward. Synthetic cannabinoid receptor agonists (SCRA's) and their metabolites may act at CB receptors to produce toxicity, or, they may act at non-CB receptors and ion channels to produce toxicity. SNPs in SCRA targets may modify agonist activity, and lead to exaggerated responses in those harbouring the mutation.

SCRA's have been shown to be far more potent at CB_1 than THC, anywhere from 4 to 380 fold so [96-99]. SCRA's also possess greater efficacy than THC, that is, the maximal response achieved at CB_1 is greater than that which can be achieved by THC [96-99]. Limited data illustrates the potential for SCRA's to elicit toxic effects in rats consistent with acute synthetic cannabinoid intoxication in humans. Administration of SCRA's to rats has been shown to bradycardia, hypothermia and seizures [96-99]. These effects are inhibited by pre-treatment of a CB_1 but not a CB_2 antagonist, suggesting that these toxic effects are CB_1 mediated [96-99].

Secondly, synthetic cannabinoids may act at receptors other than CB_1 and CB_2, and these interactions alone or in combination with CB receptors contribute to their toxicity. While the psychoactive effects of THC are mediated by CB_1 activity, it is only a low efficacy agonist, and has been reported to interact with a handful of other targets in the body [100]. Such targets include; the G protein-coupled receptors GPR18 and GPR55; PPARγ, a nuclear receptor which plays a role in the regulation of metabolism; TRPA1, TRPV2 and TRPM8, ion channels which belong to the Transient Receptor Potential (TRP) family [101-105]. The interaction between THC and TRPA1 has been shown to mediate the analgesic effects of cannabis [106]. Additionally, some early generation SCRA's, HU-331, CAY 10429, and WIN 55,212-2 , have been shown to function as more potent agonists of TRPA1 than THC [107].

Thirdly, gain of function mutations in any of these targets may exacerbate toxicity in persons harbouring the mutation. Mutations that alter ligand mediated channel activation exist in a number of the aforementioned cannabinoid targets, such as TRPA1, TRPM8 and CB_1 [108-111]. Mutations that increase ligand mediated channel activation might contribute to toxicity in an individual.

This work will focus on TRPA1, a known target of THC and a number of synthetic cannabinoids, and which has a range of important polymorphic variants [104, 107, 110-117].

1.3 Transient Receptor Potential (TRP) Channels

1.3.1 TRP Family and Structure

TRP channels are the constituents of the TRP superfamily of ion channels, organised in to 2 groups and 7 subfamilies [118, 119]. TRPC (canonical), TRPV (vanilloid), TRPM (melastatin), TRPA (ankyrin), and TRPN (nompC, no mechanoreceptor potential C) belong to group 1, while TRPP (polycystin) and TRPML (mucolipin) belong to group 2 [118]. TRPC channels are so named as they most closely resemble the original trp locus of Drosophila, which encodes a membrane protein required for signal transduction, identified in a mutant fly

in 1969 and successfully cloned in 1989 [120, 121]. The names of TRPV, TRPM, TRPA and TRPN are derived from the names originally given to the first member characterised of each family [118]. TRPP and TRPML were discovered and subsequently named after mutations in their gene products were found to cause polycystic kidney disease and mucolipidosis type IV, respectively [122-125]. TRPN was originally identified as “no mechanoreceptor potential C” (nompC) in Drosophila with abolished mechanosensory signalling [126]. TRPN proteins are not found in mammals but are, however, found in insects and some vertebrates [118]. An eighth subfamily of TRP channels exist in yeast, known as TRPY, related to human TRP channels. Yeast Yvc1 shows structural and functional homology to human TRP channels, where it forms a Ca^{2+} permeable channel in the internal vacuolar membrane [127-129]. Additionally, a gene essential for cell growth and cell wall synthesis in some yeast bears the name pkd2, for its distant similarity to the human TRPP2 ion channel [118, 128, 130, 131].

TRP channel structure varies between subfamily, however, each share common elements. All TRP feature 6 transmembrane spanning helices, which are designated S1-S6 [119, 132]. A loop between transmembrane segments S5-S6 forms a cation permeable pore, which displays high selectivity for Ca^{2+} and Mg^{2+} ions in some subfamily members [118, 119, 132]. Both the N and C terminal tails are intracellular, and contain motifs which differentiate subfamilies from each other. TRPA and TRPN channels are distinctive in having a large number of ankyrin repeat domains (ARD) at their N terminal end, up to 29 in Drosophila TRPN and 18 in human TRPA1 [119, 126, 132, 133]. Ankyrin repeats are 33 residue, helix-loop-helix-hairpin motifs, which mediate protein/protein interactions and may function as mechanoreceptive units [134, 135]. TRPC and TRPV contain a smaller amount of ankyrin repeats, between 4-6 [132, 136-141]. TRPC and TRPV, along with TRPM feature calmodulin (CaM) binding sites in their N and C termini [142-145]. In some TRPC channels, the CaM binding site can also bind inositol 1,4,5-triphosphate (IP3) receptors (IP3R), earning the name CaM-and IP3R-binding (CRIB) site [143, 146]. Members of the TRPM family (TRPM 2,

TRPM6 and TRPM7) are unique in their inclusion of an α-kinase domain at their C terminal, whose function is debated but may play a role in aldosterone signalling and autoregulation via ATP [132, 147-149]. The group 2 TRP channels, TRPP and TRPML, are differentiated by their longer extracellular loop 1 (ECL-1) and an EF hand domain on their C terminal tail [119, 150, 151].

1.3.2 Function, Distribution and Polymodality

The function of individual TRP channels vary, however, there is a consensus that they act as cellular receptors for a range of varied environmental stimuli, including pain and nociceptive stimuli. These channels react to ligands, both naturally occurring and synthetic, as well as stimuli such as cold, heat, pH and mechanical force [118, 152]. TRP channels are expressed in a wide variety of tissues, examples include; the endothelium of the lungs, where they function as chemoreceptors, the vasculature, where they mediated vasodilation, on nociceptive neurons, where they respond to noxious and nociceptive stimuli and in the gut, where they mediate motility, secretion and play a role in gastrointestinal disease [152-163]. TRP channels are also expressed on cell types including macrophages, monocytes and taste receptor cells [153, 164, 165].

1.3.3 Ligands – Natural Products

TRP channels are modulated by a variety of ligands, many of them naturally occurring in herbs, spices and aromatic plants, which are encountered in the environment. The sensitivity of TRP channels to naturally occurring ligands provided an important part of the driving force to the discovery of several distinct channels, such as TRPV1, TRPA1 and TRPM8 [166]. Perhaps the most famous example is the identification of TRPV1 as the receptor for capsaicin, the active component responsible for the perceived heat of chilli [166, 167]. TRP channel activation accounts for the pungency of many other food items. Eugenol, responsible for the distinctive smell of cloves, has been shown to activate TRPV1, TRPV3, and TRPA1 [168-

171]. Piperine, the pungent component of black pepper, is a less potent, but apparently higher efficacy agonist of TRPV1 [172]. Much like TRPV1, TRPM8 was identified due to the cooling sensation of its prototypical ligand, menthol [173, 174]. The pungent, burning sensation from wasabi, mustard and horseradish is due to compounds of the isothiocyanate class, which bind to TRPA1 [112, 171]. Thiosulfinates from onions and garlic also activate TRPA1 [175].

A number of aromatic compounds isolated from plants have been shown to interact with TRP channels. Monoterpenes such as 6-tert-butyl-m-cresol, carvacrol, dihydrocarveol, thymol, carveol, (+)-borneol and camphor activate TRPV3 but not TRPM8 [176]. TRPV4 is activated by the diterpenoids 4α-phorbol 12,13-didecanoate and bisandrographolide, although neither are particularly potent [177, 178]. TRPM8 is activated by a number of compounds including menthol, isopulegol, geraniol, linalool, eucalyptol and hydroxy-citronellal [179]. Linalool has also been shown to activate TRPA1 [180].

TRP channels also interact with cannabinoids. Cannabidiol, virtually inactive at CB receptors, activates both TRPV1 and TRPV2 [107, 181]. Additionally, TRPV2 is activated by cannabinol [107]. THC is a ligand of both TRPV2 and TRPA1 [112, 166, 182].

1.3.4 Other Modes of Activation

1.3.4.1 Voltage

The six-transmembrane segment structure of TRP channels resembles that of voltage-gated potassium channels, and as such, most members of the TRP channel family exhibit voltage sensitivity [152, 153]. Charged residues in the transmembrane segment 4 (S4) react to changes in the electric field across the cell membrane, causing the segment to move, providing a mechanism by which the channel is gated [183]. The voltage sensitivity of TRP channels is weak when compared to voltage gated K channels, however, owing to the relatively low amount of charged arginine residues in the S4 [153, 184-187]. Secondly, the

activation threshold of TRP channels is often well outside of normal physiological range under standard conditions. The half-activation voltage of temperature dependent channels TRPV1 and TRPM8 is near +100mV, however, this can be shifted to -50mV with changes in temperature or by ligand binding, a voltage which can be easily reached by a sensory neuron [152, 184].

1.3.4.2 Temperature

Since the discovery of TRPV1 and its sensitivity to heat, many TRP channels have been analysed and classified as highly temperature sensitive [152, 167]. These channels are referred to as "thermoTRPs". Along with TRPV1, TRPV2-TRPV4, TRPM8 and TRPC5 fall in to this category. TRPV1 is activated by temperatures above 43°C, TRPV2 above 52°C, with TRPV3 and TRPV4 activated by slightly cooler temperatures, around 30°C [188-191]. TRPM8, on the other hand, is a cold sensitive channel, which responds to temperatures below 20°C [173, 174, 192]. TRPC5 is also cold sensitive, activating at temperatures below 37°C, to around 25°C [193].

1.3.4.3 Mechanical Force

Transmembrane proteins are subject to mechanical force caused by the motion of the cell membrane, as a cell swells and contracts with changes in extracellular fluid osmolarity. TRPV4 has been shown to react to these changes directly, being activated by decreases in extracellular osmolarity, and inhibited by increases [194, 195]. Extracellular hypotonicity and membrane stretch is also known to effect TRPM7, TRPV2, TRPM7, TRPC1 and TRPC6 [196-200].

1.4 TRPA1

1.4.1 Structure

Transient Receptor Potential Ankyrin 1 (TRPA1, also known as ANKTM1) is a Ca^{2+} ion channel and the sole member of the TRPA subfamily, originally identified as one of several proteins repressed in virally transformed fibroblasts [133]. The protein consists of 1119 residues, with a mass of 127.4kDa and two N linked glycosylation sites on the first extracellular loop [133, 201]. TRPA1 shares the common 6 transmembrane domain structure of all TRP channels, owing its name to the chain of 18 ankyrin like repeats at its N terminal (Figure 1:1) [133]. Due to the amount of ankyrin repeats, the intracellular N terminal of TRPA1 accounts for over two thirds of the total residues of the protein (719/1119) [201]. The linker region between the last ARD and first transmembrane domain is characterised by a number of reactive cysteine residues [202]. Electrophilic agonists (which account for the bulk of TRPA1 agonists) interact with conserved cysteine residues, through covalent modification, in this region to activate the channel [203, 204]. Cysteine dependant activation of the channel was first demonstrated using cysteine reactive electrophiles, N-methylmaleimide and iodoacetamide. While both are structurally unrelated to known TRPA1 agonists, the latter is used in mass spectrometry to bind free cysteines and avoid protein aggregation, both produced TRPA1 activation like that of known agonists [203, 204]. Additionally, TRPA1 mutants lacking C415, C422, C619, C622, C639 and C663 show lessened or abolished responses to agonists, suggesting electrophilic agonists interact with these residues directly [203, 204]. The ARD of TRPA1 is thought to regulate the open probability of the channel, by reacting to temperature, mechanical strain, and participating in ligand/calcium binding directly [134, 205, 206]. Like other TRP channels, TRPA1 functions as a homotetramer in the cell membrane [207].

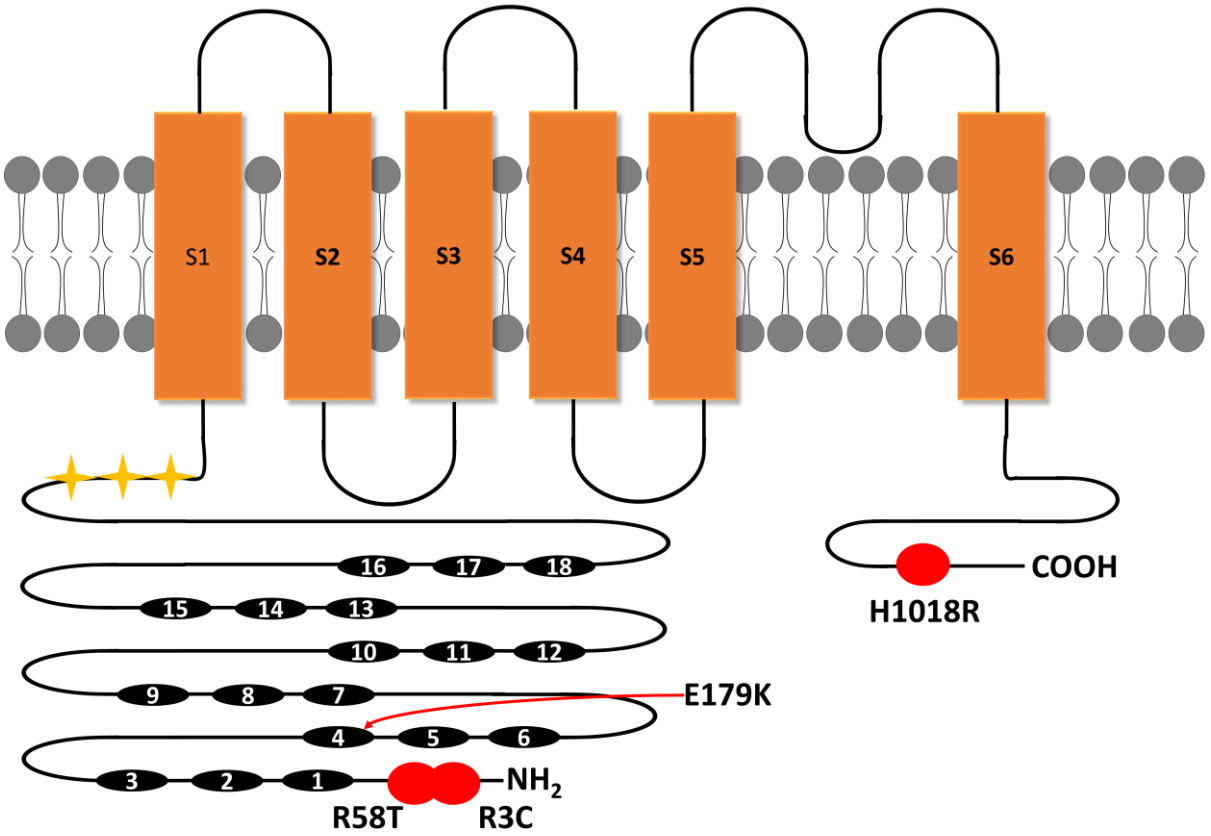

Figure 1:1 – A representation of hTRPA1 structure: The numbered oval sections at the N-terminal denote the ankyrin repeats, while the starred region indicates the position of the reactive cysteines in the linker region. There are 6 transmembrane domains, S1-S6 left to right, with a pore forming loop between the 5th and 6th. Marked in red are the locations of the point mutations selected for characterisation in this study.

1.4.2 Expression and Function

The channel was originally described as being expressed in nociceptive neurons of the dorsal root, trigeminal and nodose ganglia, where it could respond to noxious cold and irritants [153, 208, 209]. TRPA1 expression has been found in esophageal nociceptors, whose cell bodies are located in the nodose ganglia, where they respond to distention and chemical irritants [210]. Vagal nerve fibres which enervate the heart express TRPA1, and activation of the channel has been shown to influence changes in blood pressure and local blood flow [211]. In the surrounding cardiovascular system, TRPA1 is expressed on endothelial cells of the vasculature and mediate vasodilation [209]. Both sensory nerves and epithelial cells in the lung express TRPA1. Here, TRPA1 is poised to react to environmental irritants such as cigarette smoke, chlorine, aldehydes and other pollutants [212, 213]. In the airways, TRPA1 is also thought to mediate inflammation and cytokine release, contributing to airway

hyperreactivity in asthma [212]. In the gut, TRPA1 is expressed on enterochromaffin cells, where it regulates gastrointestinal motility [214].

1.4.3 Ligands

As mentioned previously, TRP channels are known for the abundance of ligands with which they are activated. The most well characterized agonists of TRPA1 are pungent culinary compounds, which were, and are still used as prototypical agonists in laboratory experiments. Allyl isothiocyanate (AITC), the pungent component of wasabi and mustard, activates TRPA1 with a half maximal effective concentration (EC_{50}) of ~11-22μM [112, 171]. The pungent components of garlic, allicin and diallyl disulphide, activate TRPA1 with an EC_{50} of ~1-8μM and ~192μM, respectively [175, 215]. Finally, cinnamaldehyde (CA) has been shown to activate TRPA1 with an EC_{50} of ~61μM. A handful of other natural plant products activate TRPA1, including gingerol (ginger), thymol (thyme), oleocanthal (olive oil), eugenol (cloves), methyl salicylate (wintergreen), and carvacrol (oregano) [112, 153, 171, 202]. Additionally, TRPA1 is activated by acrolein, crotonaldehyde (components of exhaust fumes, cigarette smoke and teargas) and endogenous products of oxidative stress (H2O2, 4-hydroxynonenal, 4-oxo-nonenal, 4-hydroxyhexenal and 15-deoxy-Δ12,14-prostaglandin J2) [216-220].

Perhaps the most interesting is the discovery that the cannabinoid THC activates TRPA1 in 2004 [112]. In the years prior to this, the cannabinoids cannabinol and THC were shown to cause vasodilation by activating receptors on sensory nerves enervating the smooth muscle [221]. The effect was preserved in the presence of GPCR antagonists, but abolished by ruthenium red, a TRP channel inhibitor [221]. Furthermore, the effect was dependent on extracellular calcium and persisted in TRPV1-deficient mice [221]. This was identical to the effects of isothiocyanates observed in the smooth muscle of blood vessels and in TRPV1-deficient mice [222-224]. TRPV1 and TRPA1 are often coexpressed in sensory neurons, drawing attention to TRPA1 (then referred to as ANKTM1) as a potential candidate [112,

208, 225]. THC activated Xenopus oocytes with an EC_{50} of 12 µM [112], while subsequent studies with rat TRPA1 expressed in HEK293 cells reported EC_{50} values between 230 nM [226] and 33 µM [107] for elevations in intracellular calcium. The quantitative differences between these experiments are not readily explicable, but the agonist activity of THC at TRPA1 is firmly established.

Research into synthetic cannabinoid activation of TRP channels and TRPA1 began in the context of pain and inflammation. Cannabis has historically been used for the treatment of pain, however the psychotropic effects of THC limit its clinical viability [227]. The implication of TRP channels in nociception and their CB receptor independent activation by cannabinoids (synthetic, natural and non-psychoactive) makes them attractive drug targets. Qin et. al. 2008 found the synthetic cannabinoids HU-331, CAY 10429, WIN 55,212-2 and WIN 55,212-3 were more potent agonists of rat TRPA1 than THC (EC_{50} = 3 µM, 9 µM, 9 µM, 22 µM respectively, compared to 32 µM) [228]. These data were reaffirmed by Akopian et. al. (2008), who showed that WIN 55,212-2 and AM1241 inhibited the response of trigeminal neurons to capsaicin and mustard oil, by activating and desensitising TRPA1 [229]. More recently, illicit synthetic cannabinoid compounds, found in products sold to consumers, have been shown to activate TRPA1 [230]. These compounds include UR-144, XLR-11, PB-22, ADB-FUBICA and AB-FUBINACA [230].

1.4.4 TRPA1 Mutants

More than 10 SNPs for TRPA1 have been identified, which result in amino acid changes to the protein, and the possibility of subsequent functional changes. These TRPA1 have been associated with a variety of phenotypic changes in humans who carry the variant. Two SNPs (rs13268757 and rs16937976), with minor allele frequencies of 0.10 have been associated with the overall control and impact on quality of life in childhood asthma [110]. Specifically, children with these mutations reported their asthma to be less well-controlled than those without, in survey regarding frequency of coughing, night awakenings, asthma related

hospitalisation and overall impact on normal activity [110]. These SNPs result in an R3C (rs13268757) and R58T (rs16937976) amino acid substitution, respectively, in the N-terminal of the protein. The R3C mutation had been reported earlier, in a separate study, along with an E179K substitution (found in the 4th ARD, SNP rs920829, minor allele frequency of 0.20), in association with menthol preference in smokers [117]. Further support for the involvement of R58T in asthma was provided by Gallo et. al. (2016), who associated the R58T mutation once more with asthma, along with E179K and a handful of other SNPs with as yet uncharacterised amino acid substitutions, in a longitudinal study of parents and children in Avon, UK [114]. E179K has also been implicated in paradoxical heat sensation in patients with neuropathic pain [231]. The SNP rs7819749 (resulting in a K186N mutation in the 4th ARD) is found heterozygous in the parents of children suffering from glioblastoma, who are homozygous for this mutation [113]. Patients with neuropathic pain and the SNP rs959976, which results in a H1018R substitution (C terminal), are found to have higher overall pain sensation [232].

The effect of some SNPs on TRPA1 function been assessed in HEK293 and SH-SY5Y cells expressing the channel. R3C and R58T, located before the 1st ARD, have been shown to increase sensitivity to single concentrations of AITC by 170% and 200% respectively, as well as other non-electrophilic agonists of TRPA1, while a double mutant of the two increases sensitivity by 20% [110]. E179K, in the 4th ARD, results in a negligible change to agonist sensitivity [110]. Y69C (rs377324180), located in the 1st ARD, was shown to be activated by AITC, cinnamaldehyde, carvacrol and menthol, with EC_{50} values 5 fold lower than the WT [116]. Similarly, R797T (rs200192163) in the 1st intracellular loop (ICL) and N855S, in the second ICL (rs398123010) were activated by these agonists, with EC_{50} values approximately 3 and 1.3 fold lower than the WT, respectively [116]. Conversely, the variants A366D in the 9th ARD (rs771347444), E477K in the 13th ARD (rs61753711) and D573A 15th ARD (rs140846916) exhibited poor to non-existent responses to prototypic TRPA1 agonists [116]. N855S, characterised as a higher sensitivity mutant by Morgan et. al., is the only recognised

pathogenic mutant of TRPA1. This gain of function mutant has been shown to cause a rare familial episodic pain syndrome, in a family from Colombia, South America [115].

Limited pharmacological data exists on the activity of TRPA1 mutants. The studies by Deering Rice et. al.2015 and Morgan et. al. 2015 represent the only two where mutants are both identified, expressed in vitro and characterised with agonists. Therefore, this study presents an opportunity to study both the activity of synthetic cannabinoids and prototypical TRPA1 agonists on TRPA1 mutants. This study will focus on a subset of the above TRPA1 mutants, summarised in Table 1.

Table 1:1 – TRPA1 mutants selected for characterisation: This table shows the 5 mutants selected for characterisation in this study. These mutants are presented with their SNP ID, as well as the frequency of the minor allele in the population (MAF)

ID	AA Substitution	MAF	Domain	Reference
rs13268757	R3C	0.1004	N-terminal	Deering-Rice et. al. 2015 Uhl et. al. 2011
rs16937976	R58T	0.1016	N-terminal	Deering-Rice et. al. 2015
rs920829	E179K	0.1999	ANK 4	Gallo et. al. 2016 Binder et. al. 2011 Uhl et. al. 2011
rs959976	H1018R	0.1601	C-Terminal	Jihong Zhu 2009
N/A	R3C + R58T	N/A	N-terminal	Deering-Rice et. al. 2015

1.5 AIMS

The aim of this project is to characterise the effect of synthetic cannabinoids on non-CB receptor targets. Transient receptor potential channels are one of several non-CB receptor candidates, with evidence existing in the literature of synthetic cannabinoid activity at these channels. TRPA1 was chosen for two reasons: firstly, the large body of evidence surrounding synthetic cannabinoid activity at this channel and secondly, its expression and role in the body makes it a good candidate to play a physiological role in synthetic cannabinoid toxicity.

Aim 1 – Characterise the activity of several, recently identified, high concern synthetic cannabinoids at the TRPA1 receptor.

Aim 2 – Determine the effect of TRPA1 polymorphisms in the channels sensitivity to agonists, both synthetic cannabinoids and traditional.

2 MATERIALS AND METHODS

2.1 CELL CULTURE

2.1.1 General Cell Culture

Cells were grown in 75 cm^2 tissue culture flasks (Corning, Inc.) with Dulbecco's Modified Eagle's Medium – high glucose (Sigma-Aldrich Pty. Ltd.), supplemented with 10% foetal bovine serum (FBS) (SAFC Biosciences Pty. Ltd.) and 100 U/100 µg.mL^{-1} of penicillin/streptomycin (P/S) (Life Technologies Australia Pty. Ltd.). Cells were incubated at 37°C, 5% CO_2 in a humidified atmosphere. To passage, solutions were warmed to 37°C in a water bath. The cells were washed with 3mL of phosphate buffered saline (PBS) (Life Technologies Australia Pty. Ltd.) before addition of 1mL of trypsin/EDTA (Sigma-Aldrich Pty. Ltd.). The trypsin was allowed to coat the bottom of the flask briefly, before being aspirated and the flask left to incubate at room temperature for 3 minutes, or until the cells begun to detach with little force. The cells were washed from the bottom of the flask and resuspended in 3mL of culture media. Six drops of this suspension were then transferred to 10mL of culture media in a fresh 75 cm^2 flask.

2.1.2 HEK-293 Flp-In™ T-REx™ WT

Routine cell culture of wild type HEK-293 Flp-In™ T-REx™ (Life Technologies Australia Pty. Ltd.) cells was performed as outlined above. For these cells, routine culture media was supplemented with 10 µg.mL^{-1} Blasticidin and 100 µg.mL^{-1} Zeocin™ (InvivoGen) for selection purposes.

2.1.3 HEK-293 Flp-In™ T-REx™ hTRPA1

Routine cell culture of HEK-293 Flp-In™ T-REx™ cells stably transfected with hTRPA1 was performed as outlined above. For these cells, routine culture media was supplemented with

10 µg.mL^{-1} Blasticidin and 80 µg.mL^{-1} Hygromycin B Gold (InvivoGen) for selection purposes.

2.2 TRANSFECTIONS

2.2.1 DNA Products

Mutant hTRPA1 constructs were synthesised by GenScript (GenScript HK Limited) in the pcDNA™5/FRT/TO vector (Invitrogen Corporation). Before use, contents were centrifuged at 6000 x g for 1 minute at 4°C and reconstituted in 20 µL of filter sterilised Milli-Q® water. pOG44 Flp-recombinase expression vector was purchased from Life Technologies (Life Technologies Australia Pty. Ltd.). Construct and mutant gene of interest sequences can be found in Appendix A

2.2.2 Transfection Protocol

Wild type HEK-293 Flp-In™ T-REx™ cells were stably transfected with mutant hTRPA1 using the FuGENE® HD Transfection Reagent (Promega Corporation). HEK-293 cells grown as per general protocol to 80% confluency were seeded in 2mL of general culture media supplemented with 80 µg.mL^{-1} Zeocin™ and 15 µg.mL^{-1} Hygromycin B Gold, in a 6-well cell culture cluster (Corning, Inc.). Cells were seeded diagonally opposite to each other, 2 per plate, to minimise risk of contamination and incubated overnight at 37°C, 5% CO_2 in humidified room air. On the day of the transfection, the media on the cells was changed to 2 mL pre-warmed general culture media. The transfection mixture was prepared, as follows, in sterile 1.5 mL microcentrifuge tubes: 3µg of DNA at a ratio of 9 parts pOG44 to 1 part pcDNA™5/FRT/TO, 12µL FuGENE® HD and DMEM – high glucose (additive free) to a volume of 100 µL. The mixture was incubated at room temperature for 15 minutes before being added, drop-wise, to the cells. The cells were then incubated at 37°C, 5% CO_2 in humidified room air for 48 hours. Following incubation, each well was passaged to its own 75 cm^2 flask in general culture media with no selection antibiotics and incubated overnight.

Following incubation, the media was changed to general culture media with 100 µg.mL^{-1} Hygromycin B Gold and 15 µg.mL^{-1} Blasticidin. The media was changed every 3rd day until resistant foci were observed, at which point the cells were passaged, as per general protocol. Passaging continued, using 100 µg.mL^{-1} Hygromycin B Gold and 15 µg.mL^{-1} Blasticidin, until passage 5, at which point the cells were frozen down (in DMEM – high glucose, no additives +20% FBS, +10% DMSO [Sigma-Aldrich Pty. Ltd.]) and subsequent passages continued as per HEK-293 Flp-In™ T-REx™ hTRPA1 protocol.

HEK-293 Flp-In™ T-REx™ hTRPA1 WT cells were transfected previously, and provided by Marina Santiago to compare against the mutant TRPA1.

2.3 Calcium Assay

2.3.1 Assay Procedure

Changes in intracellular calcium were measured using the FLIPR® Calcium 5 Assay Kit (Molecular Devices). Cells were grown to 90% confluency and detached from the flask as per general cell culture. The cells were resuspended in 10 mL of Leibovitz's L-15 Medium (Life Technologies Australia Pty. Ltd.), supplemented with 1% FBS, 1% P/S and 15 mM glucose. Eighty microliters of this suspension per-well was plated out in a black, clear bottomed, poly-D-lysine coated (10 µg/mL/well) 96-well plate (Corning, Inc.) 96-well plate and incubated overnight at 37°C, 1% CO_2 in humidified room air. On the day of the experiment, 20 µL of tetracycline solution in L-15 was added to each well (4 µg.mL^{-1} final in-well concentration), and the cells incubated for 3 hours at 37°C, 1% CO_2 in humidified room air to induce protein expression.

Following incubation, the cells were loaded with assay dye. Five hundred microliters of dye was reconstituted in Hanks Balanced Salt Solution (HBSS), containing (in mM): NaCl 145, HEPES 22, Na_2HPO_4 0.338, $NaHCO_3$ 4.17, KH_2PO_4 0.441, $MgSO_4$ 0.407, $MgCl_2$ 0.493, $CaCl_2$ 1.26 and 1mg/mL glucose (pH 7.4, osmolarity 315 ± 5), to a total volume of 10 mL

Probenecid (Biotium, Inc.) was added to the dye to a concentration of 2.5 mM and 80 µL per-well was added to the cells, for an initial assay volume of 180 µL (1 mM final in-well probenecid concentration). The cells were then incubated for one hour at 37°C. Following dye incubation, the cells were transferred to a FlexStation® 3 Multi-Mode Microplate Reader (Molecular Devices) set to an internal temperature of 37°C. Fluorescence readings were taken at 2 second time intervals for the duration of the experiment (λ excitation/emission = 485/525 nm). Baseline readings were taken for 60 seconds prior to drug addition. Twenty microliters of drug solution per-well was added to the cells at 60 seconds, with readings continuing no longer than 10 minutes, unless otherwise noted.

2.3.2 Drugs

All drugs are aliquoted and stored at -80°C until needed. All synthetic cannabinoids, unless otherwise stated, were synthesized by Sam Bannister or Shane Wilkerson in the lab of Michael Kassiou at Sydney University (Sydney, NSW, Australia). Synthetic cannabinoids were made up in dimethyl sulfoxide (DMSO) (Sigma-Aldrich Pty. Ltd.) at 30 mM. Cinnamaldehyde and AITC were purchased from Sigma-Aldrich Pty. Ltd. and made up in DMSO. Carvacrol was purchased from Toronto Research Chemicals, and made up in DMSO. PAR-1 agonist (H-TFLLR-NH_2) was purchased from Auspep Pty. Ltd. and made up in HBSS. For an experiment, drugs were serially diluted in HBSS containing 0.01% BSA (Sigma-Aldrich Pty. Ltd.) and 1% DMSO, such that the final in-well concentration of DMSO was kept at 0.1%. The drugs were transferred to a clear, V-bottomed 96-well plate (Greiner Bio-One GmbH) and placed in the FlexStation® 10 minutes prior to experiment start to warm to 37°C. A list of all hTRPA1 ligands and cannabinoids used can be found in Table 2:1

Table 2:1 – hTRPA1 ligands and cannabinoids: This table provides a list, including IUPAC name and CAS # of all ligands used in this study. Information was taken from the ChemSpider database (http://www.chemspider.com)

Common Name	IUPAC Name	CAS #
Cinnamaldehyde	(2E)-3-Phenylacrylaldehyde	14371-10-9
Allyl Isothiocyanate	3-Isothiocyanato-1-propene	57-06-7
Carvacrol	5-Isopropyl-2-methylphenol	499-75-2
THC	(6aR,10aR)-6,6,9-Trimethyl-3-pentyl-6a,7,8,10a-tetrahydro-6H-benzo[c]chromen-1-ol	1972-08-3
MDMB-CHMICA	Methyl (2*S*)-2-{[1-(cyclohexylmethyl)-1*H*-indol-3-yl]formamido}-3,3-dimethylbutanoate	1971007-95-0
PB-22	1-Pentyl-1H-indole-3-carboxylic acid 8-quinolinyl ester	1400742-17-7
5F-PB-22	1-pentyfluoro-1H-indole-3-carboxylic acid 8-quinolinyl ester	1400742-41-7
UR-144	(1-pentylindol-3-yl)-(2,2,3,3-tetramethylcyclopropyl)methanone	1199943-44-6
XLR-11	[1-(5-Fluoropentyl)-1H-indol-3-yl](2,2,3,3-tetramethylcyclopropyl)methanone	1364933-54-9
UR-144/XLR-11 5-hydroxypentyl metabolite	[1-(5-hydroxypentyl)-1H-indol-3-yl](2,2,3,3-tetramethylcyclopropyl)-methanone	895155-95-0

2.4 DATA ANALYSIS

SoftMax® Pro software version 5.4 (Molecular Devices) was used to set up the FlexStation® and export experimental data as a .txt file consisting of time points in seconds and their corresponding fluorescence readings for each well. The data were expressed as a % change in fluorescence over baseline using Microsoft Excel 2016. Microsoft Excel was also used to collate the peak responses measured for each concentration of drug and normalise them to the response of 100µM. These data were then copied in to GraphPad Prism version 7.02 for Windows (GraphPad Software). Agonist concentrations were transformed to log form, and the data analysed using four parameter non-linear regression (bottom constrained to 0) to fit concentration-response curves, with each data point representing the mean ± standard error of the mean (SEM). Concentration response curve and raw trace figures were output from GraphPad Prism using a colour-blind friendly colour palette [233]. GraphPad Prism was also used for all statistical analysis. ANOVA tables can be found in Appendix B.

3 METHOD VALIDATION

3.1 THE EFFECT OF PROBENECID ON CALCIUM 5 ASSAY

3.1.1 Introduction

For measuring the activity of hTRPA1 in a high throughput assay, recording increases in intracellular calcium is an obvious choice [234, 235]. To visualise changes in intracellular Ca concentration (Ca_i), a Ca indicator is used. The most widely used Ca indicators are the high affinity dyes. These are offered by a range of companies for a range of different purposes. The Calcium 5 dye, as part of the FLIPR® Calcium 5 Assay Kit, is a high affinity dye which is used as part of a no-wash FLIPR assay [236, 237]. Dye is loaded in to the intracellular space during incubation, where it responds to changes in Ca_i. A proprietary masking agent quenches the fluorescence of dye in the extracellular space.

In some cell lines, an anion exchange protein actively pumps the dye and Ca out of the cell, which decreases the dynamic range of the assay. For this reason, the use of an organic anion transport inhibitor such as probenecid, at a concentration of 2.5mM, is recommended in the Calcium 5 assay protocol. [238-240]. The use of probenecid significantly reduces dye sequestration into organelles and efflux from the cell [239]. However, there are differing reports in the literature regarding potential interaction between probenecid and TRPA1. Several papers have found that probenecid either abolishes the activity of, or increases the EC_{50} for agonists of hTRPA1 [111, 240]. We have previously used probenecid in fluorometric assays of TRPA1 function, and have obtained large responses to channel agonists [234, 235]. We have never investigated probenecid interaction with TRPA1 or whether we needed it to record a robust signal from HEK293 cells. Given the discrepancies in the literature regarding the use and effect of probenecid, it was important to validate the use of probenecid in our workflow.

3.1.2 Results

Activation of hTRPA1 was analysed in the presence or absence of 2.5mM probenecid, as outlined in Section 2.3 of the methods.

Addition of cinnamaldehyde to HEK293 cells expressing TRPA1, incubated in the presence of probenecid, produced a robust, concentration dependant increase in Ca_i (Figure 3:1). The maximum increase in fluorescence after addition of cinnamaldehyde is approximately 3 fold greater in cells incubated in the presence of probenecid compared to those without (Figure 3:1). The potency of cinnamaldehyde at TRPA1 was not affected by the presence of probenecid, with EC_{50} values of 31 ± 2 µM in cells with probenecid and 32 ± 2 µM in cells without [two-tailed $t(10) = 0.06$, $p = 0.95$), Figure 3:2].

The inclusion of probenecid in the Calcium 5 assay significantly increase the dynamic range, with the maximum response to cinnamaldehyde is approximately 3 fold greater with the inclusion of probenecid [two-tailed $t(10) = 23.96$, $p < 0.0001$ (Figure 3:1)]. Additionally, the separation in signal intensity between 1 mM – 10 µM can clearly be seen in Figure 3:1A, whereas in Figure 3:1B, this is not as clear. The maximum increase in fluorescence elicited by 100 µM and 30 µM cinnamaldehyde appear the same. No increase in fluorescence can be seen after the addition of 10 µM cinnamaldehyde in the assay time frame.

Under our assay conditions, probenecid does not appear to inhibit agonist activity at TRPA1 and is necessary to increase the dynamic range of the Calcium 5 dye. As a result of these data, we used dye supplemented with 2.5 mM probenecid, unless stated otherwise.

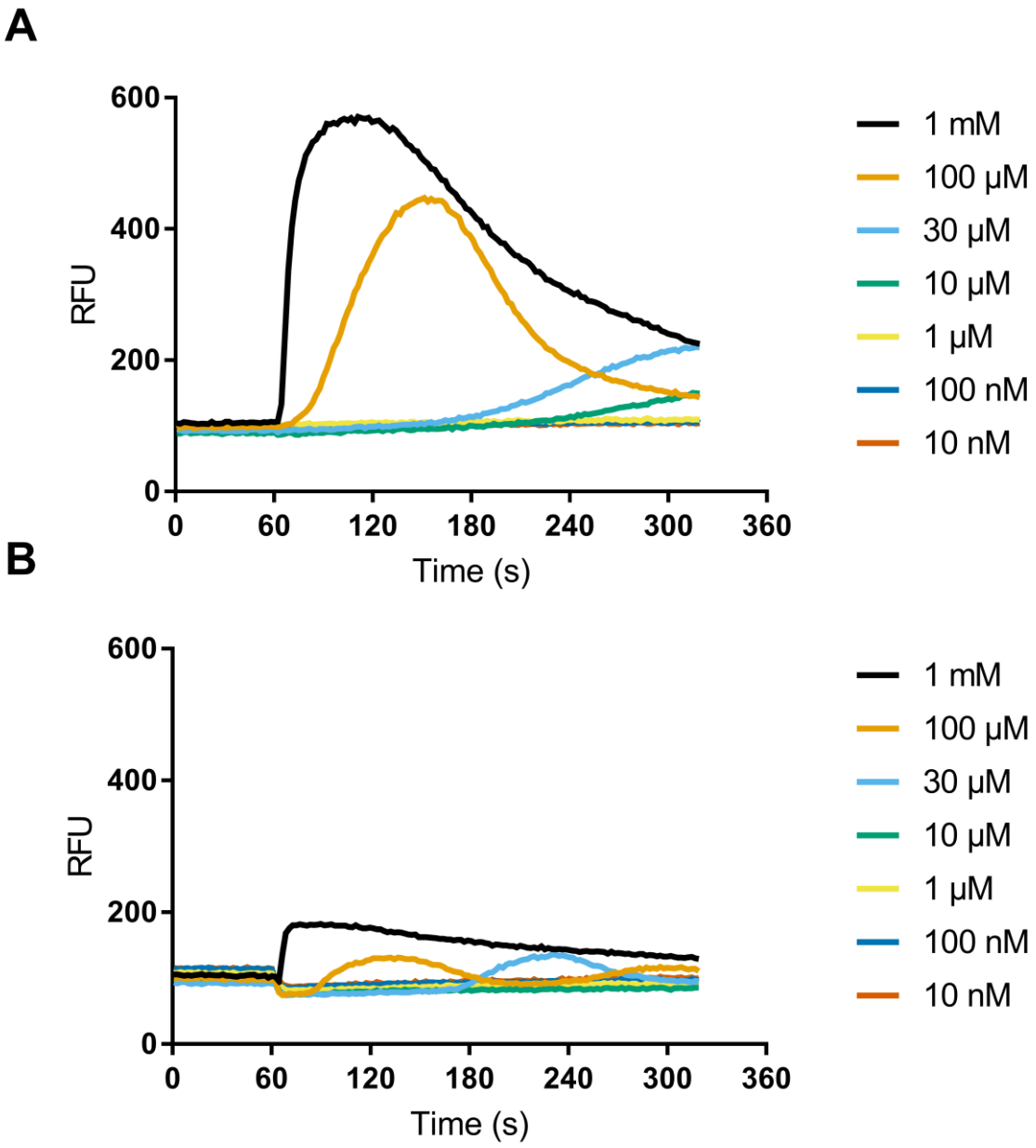

Figure 3:1 – Raw traces of hTRPA1 response to cinnamaldehyde in varying probenecid concentrations: A – representative raw trace of cinnamaldehyde on hTRPA1 in dye loaded with 2.5 mM probenecid. B – representative raw trace of cinnamaldehyde on hTRPA1 in dye not supplemented with probenecid. RFU = Relative Fluorescence Units

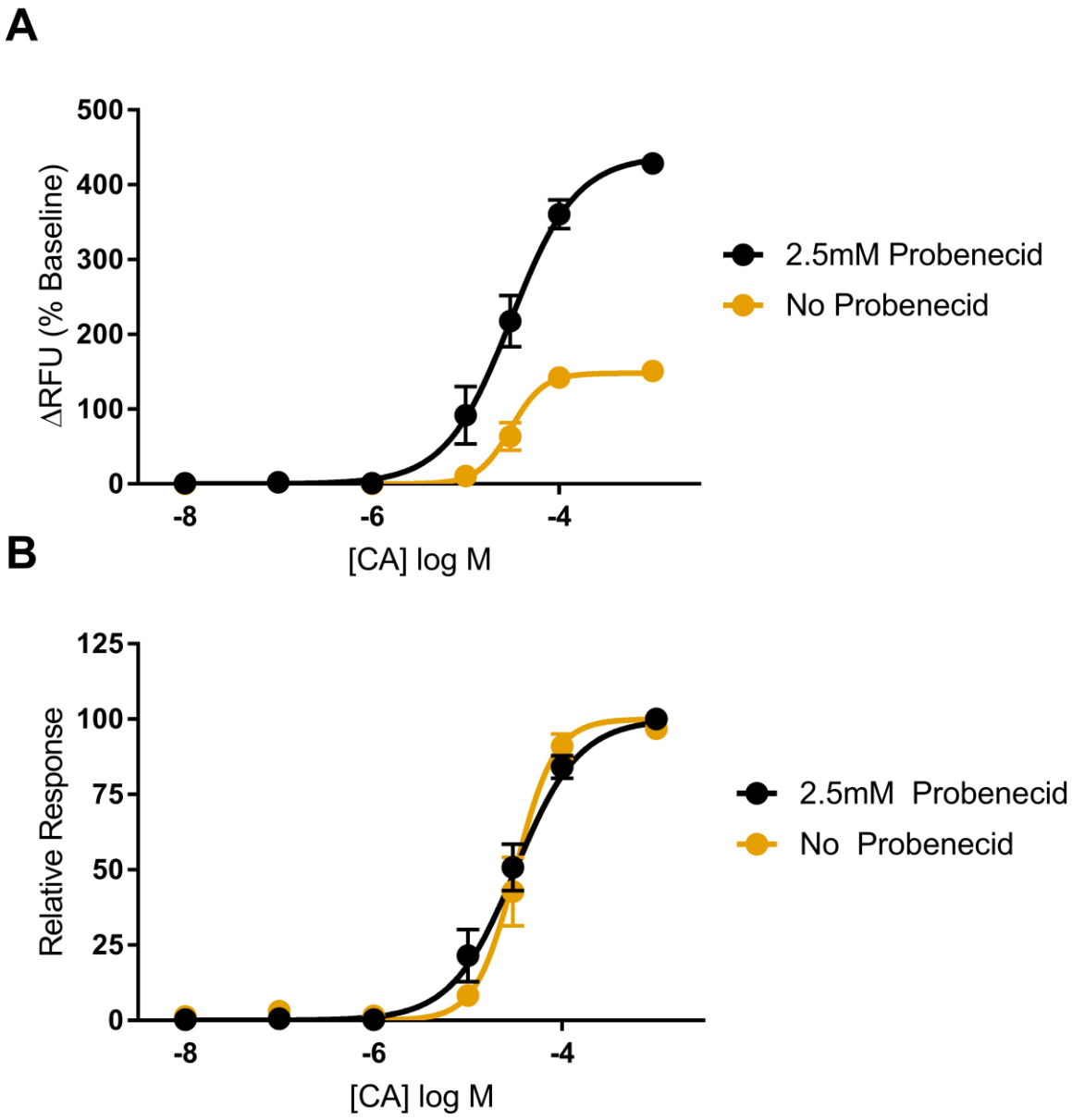

Figure 3:2 – Concentration response curves of cinnamaldehyde on hTRPA1 in varying probenecid concentrations: A – Concentration response curves for cinnamaldehyde in dye with 2.5 mM probenecid or no probenecid added. B – Concentration response curve using the data from A, normalised such that 0 and 100 = the smallest and largest value in each dataset. Each data point represents the mean ± SEM of six independent determinations performed in duplicate.

3.2 VALIDATING A CONTROL COMPOUND

3.2.1 Introduction

When investigating the effects of unknown compounds on potential targets, the response is often normalised against a well characterised agonist of that channel, or some other compound that elicits a consistent, measurable response. This is to control for variance within the assay, and between replicates. For TRPA1, the choices are often the max response produced by cinnamaldehyde or allyl isothiocyanate [110, 230, 241]. Additionally, an ionophore can be used to elicit a response to normalise to [110, 111].

To investigate the role mutations in TRPA1 play in the channels sensitivity to synthetic cannabinoids, the use of cinnamaldehyde or AITC as a control would not be appropriate. We expect that the mutations may influence the potency of all agonists, therefore, the response to a reference agonist will not be a constant across each mutant cell line. HEK-293 cells express a number of endogenous GPCR's, many of which are linked to calcium signalling pathways, including the Gq coupled protease activated receptor 1 (PAR-1) [242]. PAR-1 is activated in vivo by a tethered peptide, SFLLRN, which can be synthesised and used in an assay as H_2-TFLLR-NH_2 [243-245]. We evaluated the consistency of the response elicited by H-TFLLR-NH_2 across the TRPA1 WT and variant cell line for use as a control in later assays.

3.2.2 Results

The consistency of cinnamaldehyde and PAR-1 across the various cell lines was examined as outlined in the methods (Section 2.3). Cells were assayed using cinnamaldehyde or H-TFLLR-NH_2 as an agonist, with concentration response curves constructed from at least 5 replicates.

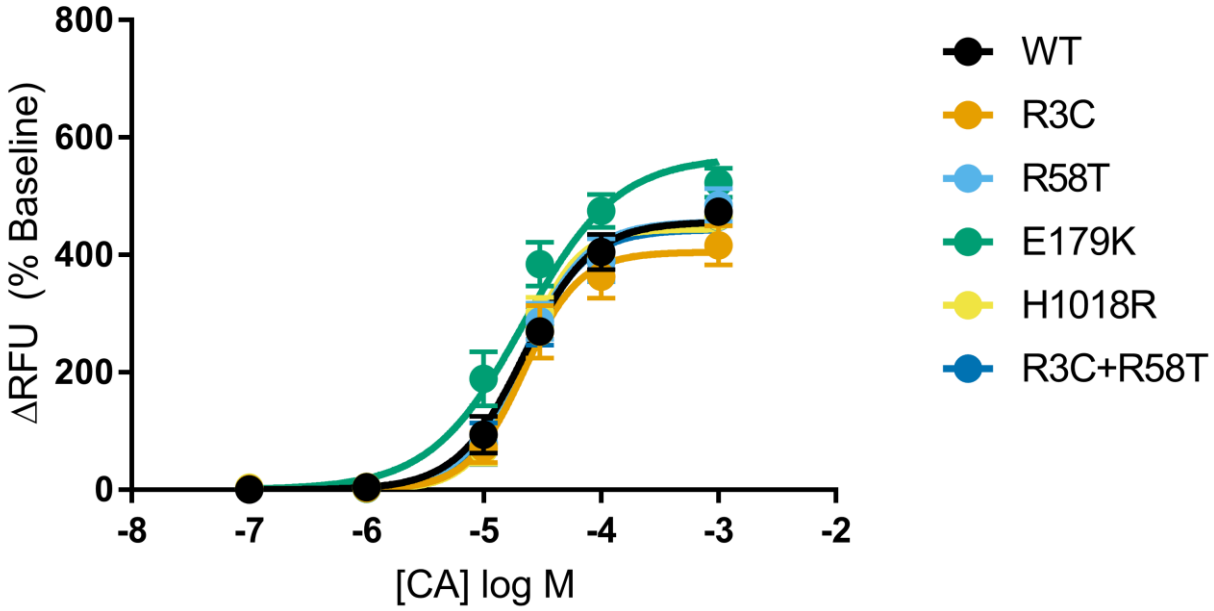

Figure 3:3 – Concentration response curves for cinnamaldehyde on WT hTRPA1 and variants: This figure illustrates the concentration-response relationship of cinnamaldehyde on 5 hTRPA1 variants compared to WT hTRPA1. Each data point represents the mean ± SEM of 5 independent determinations performed in duplicate.

Addition of cinnamaldehyde to HEK293 cells expressing hTRPA1 produced a concentration dependant increase in Ca_i. Figure 3:3 illustrates the concentration response relationship of cinnamaldehyde on the 5 hTRPA1 variants, as well as WT hTRPA1. These data show the response to cinnamaldehyde across the TRPA1 variants is consistent. EC_{50} values at the hTRPA1 variants were between 14 ± 2 in E179K and 27 ± 3 µM in R58T (Table 3:1). Additionally, the peak fluorescence elicited by cinnamaldehyde ranged from 416 ± 33 RFU in R3C to 523 ± 25 RFU in E179K (Table 3:1). There was no significant effect of the hTRPA1 variants on the maximal effect of cinnamaldehyde [One-way ANOVA, $F(5,24) = 2.12$, $p = 0.10$]. Additionally, there was no effect of the hTRPA1 variants on the EC_{50} of cinnamaldehyde [One-way ANOVA, $F(5,24) = 1.97$, $p = 0.12$].

Table 3:1 – Maximal effect and EC50 values for cinnamaldehyde and H-TFLLR-NH$_2$ at hTRPA1 and variants: Maximal effect and EC_{50} values were calculated individually for each replicate and pooled together. Data represent the mean ± SEM of at least 5 independent determinations performed in duplicate.

TRPA1	Maximal Effect (ΔRFU % Baseline)		EC_{50} (µM)	
	CA	H-TFLLR-NH$_2$	CA	H-TFLLR-NH$_2$
WT	474 ± 24	522 ± 13	25 ± 2	5 ± 0.7
R3C	416 ± 33	531 ± 20	25 ± 5	5 ± 0.6
R58T	485 ± 28	517 ± 21	27 ± 3	4 ± 0.8
E179K	523 ± 25	542 ± 18	14 ± 2	5 ± 0.9
H1018R	466 ± 11	533 ± 13	24 ± 2	5 ± 0.5
R3C+R58T	465 ± 13	539 ± 18	25 ± 4	4 ± 0.6

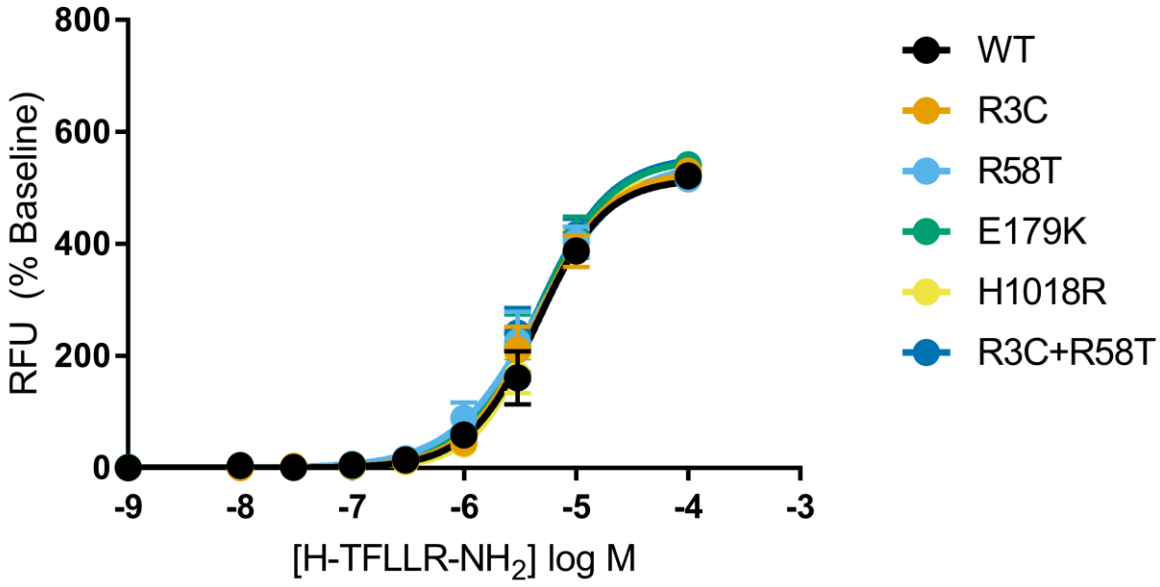

Figure 3:4 – Concentration response curves for PAR-1 agonist on WT hTRPA1 and variants: This figure illustrates the concentration response relationship of PAR-1 agonist on 5 TRPA1 variants compared to WT hTRPA1.Each data point represents the mean ± SEM of at least 5 independent determinations performed in duplicate.

Addition of H-TFLLR-NH_2 to hTRPA1 expressing cell lines elicited a concentration dependant increase in Ca_i. Figure 3:4 shows the concentration response relationship of H-TFLLR-NH_2 on the 5 hTRPA1 variants as well as WT hTRPA1. The range of EC_{50} values is between 4 ± 0.6 µM at R3C+R58T and 5 ± 0.9 µM at E179K (Table 3:1). Additionally, the peak response elicited by 100 µM H-TFLLR-NH_2 spans from 517 ± 21 RFU in R58T to 542 ± 18 RFU in E179K. There was no significant effect in the maximal effect [One-way ANOVA, $F(5,30) = 0.32$, $p = 0.90$] or the EC_{50} [One-way ANOVA $F(5,30) = 0.67$, $p = 0.65$] of H-TFLLR-NH2 in the cells expressing the TRPA1 variants. In light of these data, 100 µM H-TFLLR-NH_2 was chosen to normalise further experiments. The consistency of the PAR-1 response indicates the process of transfection did not significantly alter non TRPA1 mediated calcium signalling. Therefore, we can be confident that any alteration in drug potency observed is due to changes in the channel itself.

4 EFFECT OF HTRPA1 POLYMORPHISMS ON PROTOTYPIC AGONISTS

4.1 INTRODUCTION

Limited pharmacological data exists on the effect of TRPA1 polymorphisms on well characterised agonists, let alone synthetic cannabinoids. For this reason, it was important to begin by characterising the mutants chosen for this study with well characterised, prototypic agonists.

We selected 3 prototypic agonists to characterise the TRPA1 mutants, 2 electrophilic and 1 non-electrophilic. Cinnamaldehyde and AITC were chosen as the electrophilic agonists and carvacrol chosen as a non-electrophilic agonist. Experiments were prepared as per Section 2.3, and all agonist responses were normalised to 100µM H-TFLLR-NH_2.

4.2 RESULTS

4.2.1 Cinnamaldehyde

Cinnamaldehyde was assayed a second time, with all responses normalised to 100 µM H-TFLLRN-H_2. Cinnamaldehyde displayed agonist activity in all TRPA1 expressing cell lines, but did not elevate Ca_i in HEK293 WT cells (Figure 4:1). Table 4:1 shows the calculated values for the maximal effect and EC_{50} at all variants tested. Maximal effect ranged from 108 ± 7 % 100 µM H-TFLLR-NH_2 at R58T to 97 ± 3 at the WT. EC_{50} values ranged from 13 ± 2 µM at R58T to 35 ± 2 µM at R3C. There was no significance at the $p < 0.05$ level between the efficacy and potency of cinnamaldehyde at hTRPA1 variants compared to the WT.

Table 4:1 – Maximal effect and EC_{50} of cinnamaldehyde at variants of hTRPA1: Maximal effect and EC_{50} were calculated individually for each replicate and pooled together. Data represent the mean ± SEM of 5 independent determinations performed in duplicate. Fold change values are presented as variant/WT pending the results of a t test, ns = not significant.

TRPA1	Maximal Effect (% 100 µM H-TFLLR-NH_2)	Fold Change	EC_{50} (µM)	Fold Change
WT	97±3	ns	17±4	ns
R3C	85±4	ns	35±2	ns
R58T	108±7	ns	13±2	ns
E179K	95±6	ns	25±10	ns
H1018R	101±5	ns	21±5	ns
R3C+R58T	99±10	ns	27±1	ns

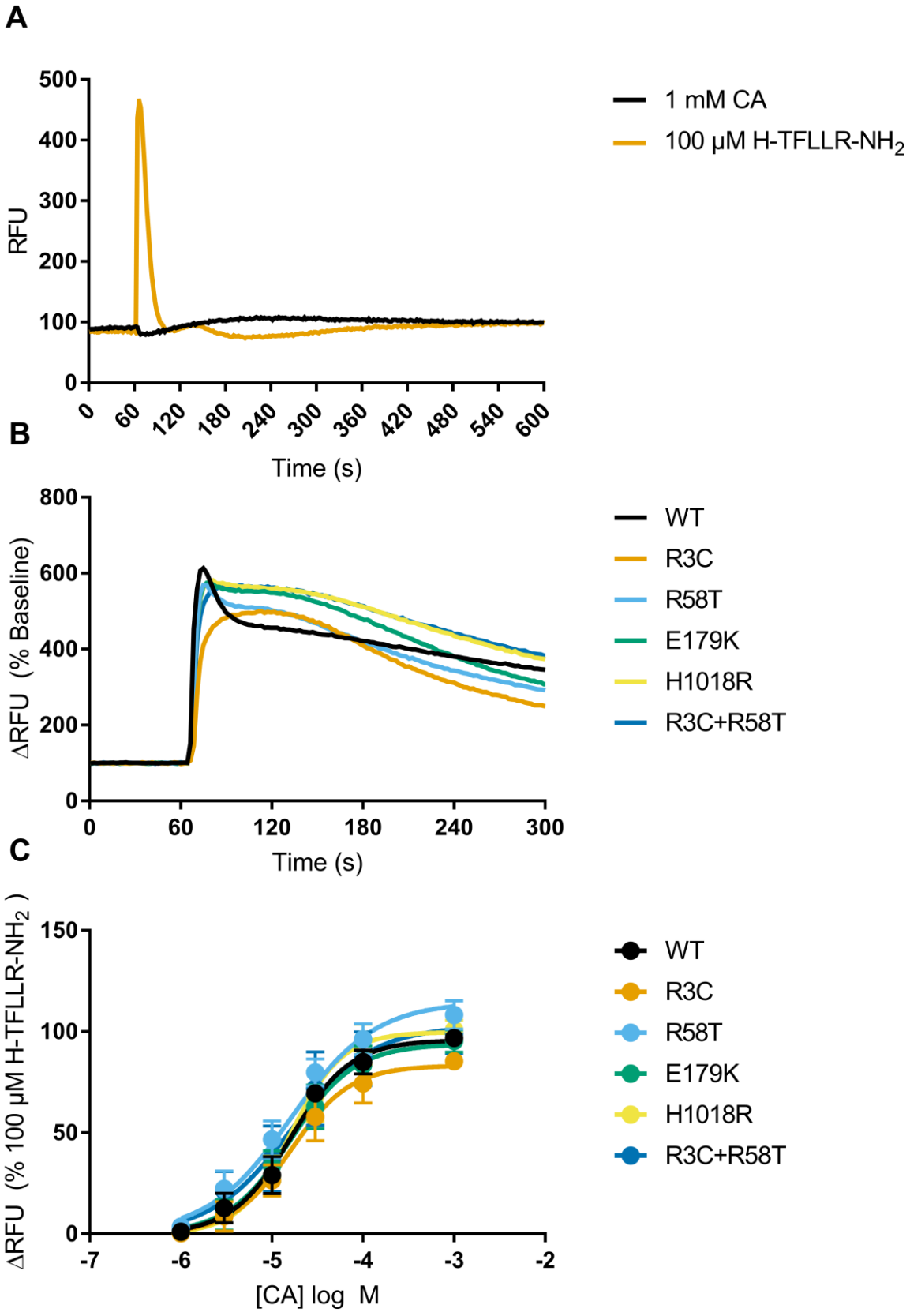

Figure 4:1 – Activation of hTRPA1 variants by cinnamaldehyde: A – Raw trace data illustrating the response of HEK293 WT cells to cinnamaldehyde and H-TFLLR-NH_2. B – Baseline normalised trace data illustrating the response of hTRPA1 WT and variants to 1mM cinnamaldehyde. C – Concentration response relationship of cinnamaldehyde at WT and hTRPA1 variants, illustrating little variation in maximal effect and EC50. Data represent the mean ± SEM of 5 independent determinations performed in duplicate.

4.2.2 AITC

AITC displayed agonist activity in all TRPA1 expressing cell lines, but did not elevate Ca_i in HEK293 WT cells. We did not have the opportunity to construct a full CRC for AITC, however, we were able to compare the activation of hTRPA1 at [AITC] of 10 µM, which produced a robust response in WT hTRPA1 (Figure 4:2). The maximal effect elicited from AITC ranged from 109 ± 3 % H-TFLLR-NH_2 at H1018R to 163 ± 25 at the WT (Table 4:2). At [ATIC] of 10 µM, the increase in Ca_i ranged from 12 ± 10 % H-TFLLR-NH_2 at R3C to 45 ± 20 at R3C+R58T (Table 4:2). There was no significant difference at the $p < 0.05$ level for between the efficacy and potency of AITC at hTRPA1 variants compared to the WT.

Table 4:2 – Maximal effect at 1mM and 10µM for AITC at WT TRPA1 and selected polymorphisms: Maximal effect at 1mM and 10µM were calculated individually for each replicate and pooled together. Data represent the mean ± SEM of 5 independent determinations performed in duplicate. Fold change values are presented as variant/WT pending the result of a two-tailed t test, ns = not significant.

TRPA1	Maximal Effect (% 100 µM H-TFLLR-NH_2)	Fold Change	Effect at 10 µM (% 100 µM H-TFLLR-NH_2)	Fold Change
WT	163±25	ns	19±11	ns
R3C	137±22	ns	12±10	ns
R58T	136±11	ns	36±20	ns
E179K	141±20	ns	23±23	ns
H1018R	109±3	ns	38±13	ns
R3C+R58T	130±7	ns	45±20	ns

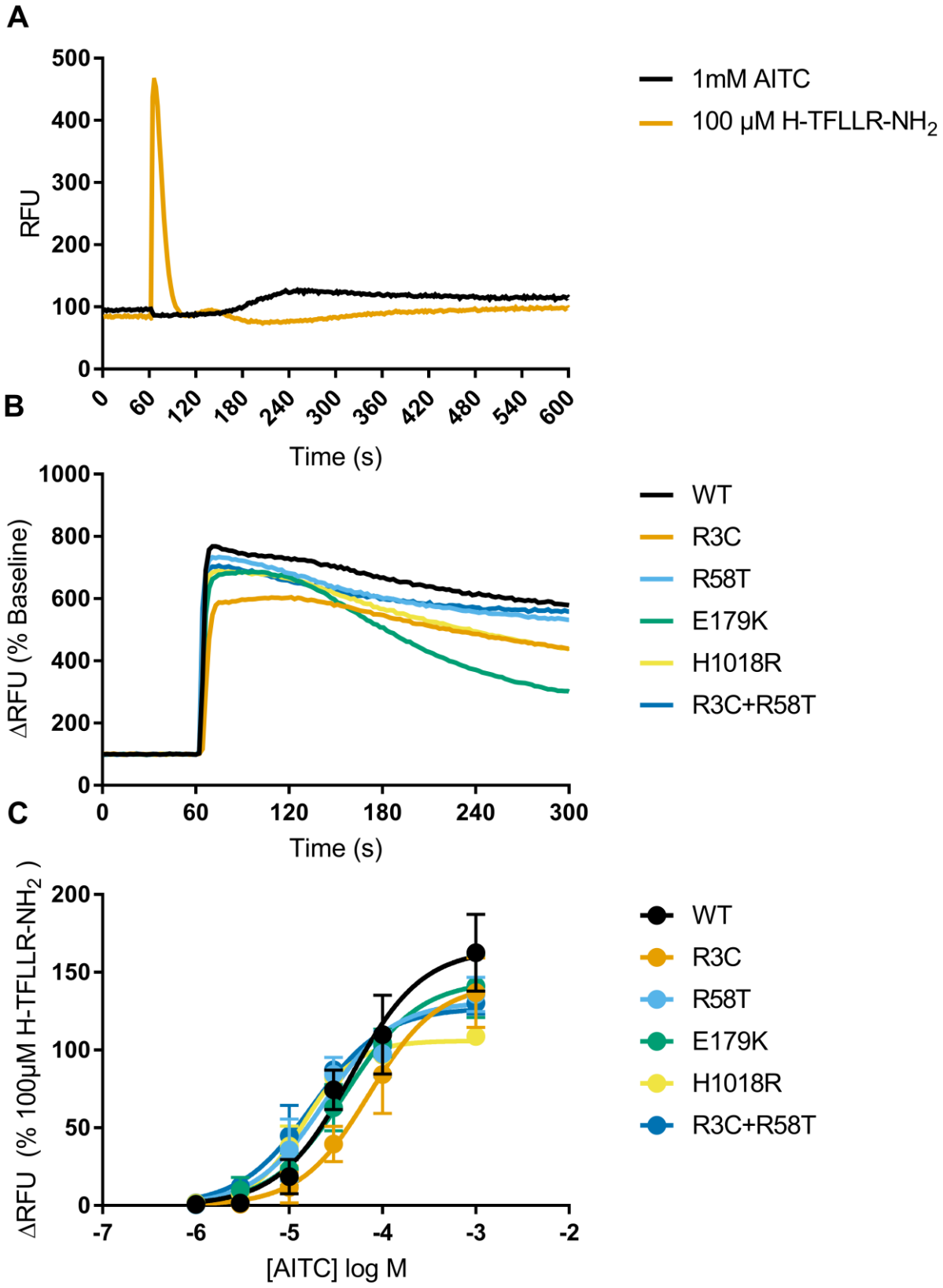

Figure 4:2 – Activation of hTRPA1 variants by AITC: A – Raw trace data illustrating the response of HEK293 cells to AITC and H-TFLLR-NH_2. B – Baseline normalised trace data illustrating the response of hTRPA1 variants to 1mM AITC. C – Concentration response relationship of AITC at hTRPA1 variants. Data represent the mean ± SEM of 5 independent determinations performed in duplicate.

AITC appeared to be a higher efficacy agonist than cinnamaldehyde in our assay. There was significant effect of the agonist on the observed difference in maximal effect at 1mM [$F(1, 41) = 29.73$, $p < 0.0001$]. Sidak's multiple comparisons test was used to compare the difference in maximal effect at 1mM between each variant (Table 4:3). From these data, AITC displays significantly greater efficacy than cinnamaldehyde at TRPA1 WT (1.68 fold) and R3C (1.60 fold) (Table 4:3, Figure 4:3).

Table 4:3 – Sidak's multiple comparisons test for the maximal effect of AITC compared to CA at each hTRPA1 variant: A two-way ANOVA with Sidak's multiple comparisons was conducted on the pooled data from the experiments on the maximal effect at 1 mM of AITC and cinnamaldehyde. Fold change was calculated as AITC/CA where statistically significant, ns = not significant

CA vs. AITC	t (df = 41)	p	Fold Change
WT	3.43	0.0077	1.68
R3C	2.85	0.0386	1.60
R58T	1.53	0.5745	ns
E179K	2.53	0.0858	ns
H1018R	0.44	0.9986	ns
R3C+R58T	1.73	0.4307	ns

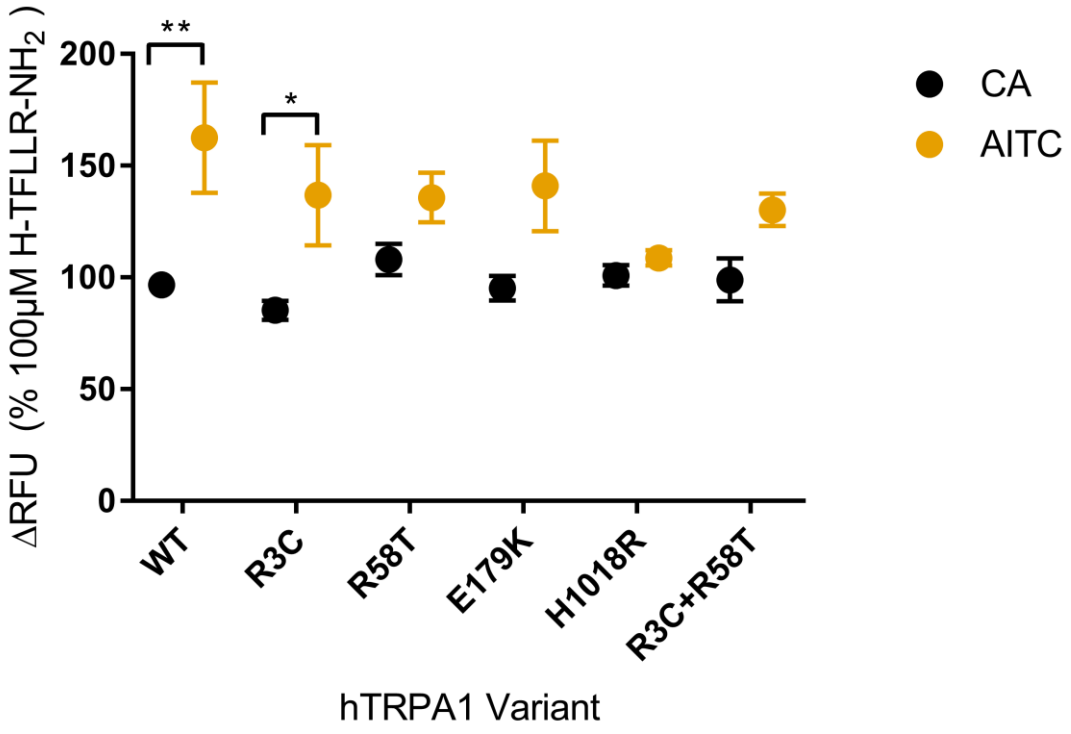

Figure 4:3 – Effect of cinnamaldehyde and AITC at hTRPA1 variants: This figure illustrates the maximal effect observed at each hTRPA1 variant for cinnamaldehyde and AITC at 1 mM. Data represent the mean ± SEM of 5 independent determinations performed in duplicate. Asterisks indicate significance at the $p < 0.05$ level.

4.2.3 Carvacrol

Addition of carvacrol to HEK293 cells expressing hTRPA1 produced a concentration dependant elevation in Ca_i (Figure 4:4). However, addition of carvacrol to HEK293 WT cells produced a sharp elevation in Ca_i, followed by a rapid desensitisation (Figure 4:4). For this reason, maximal response to carvacrol was instead calculated using the fluorescence value at 180 seconds, rather than the peak immediately after drug addition. At 180 seconds, the maximal effect from 1 mM carvacrol ranged from 97 ± 8 % 100 µM H-TFLLR-NH_2 at H1018R to 158 ± 18 at the WT (Table 4:4). There was a statistically significant difference between the Ca_i change at 180s at H1018R compared to the WT, representing a 0.61 fold change (Table 4:4). Due to the unexpected off target effect of carvacrol, we did not analyse these data any further.

Table 4:4 – Ca_i change at 180s for 1 mM carvacrol at hTRPA1 variants: Ca_i change at 180 seconds was calculated individually for each replicate and pooled together. Data represent the mean ± SEM of 5 independent determinations performed in duplicate. Fold change is presented as variant/WT pending the results of a two-tailed t test, ns = not significant.

TRPA1	Ca_i Change @ 180s (% 100 µM H-TFLLR-NH_2)	t (df = 8)	p	Fold Change
WT	158 ± 18	NA	NA	NA
R3C	129 ± 22	1.031	0.3325	ns
R58T	134 ± 15	1.018	0.3385	ns
E179K	118 ± 19	1.535	0.1632	ns
H1018R	97 ± 8	3.036	0.0162	0.61
R3C+R58T	122 ± 12	1.655	0.1364	ns

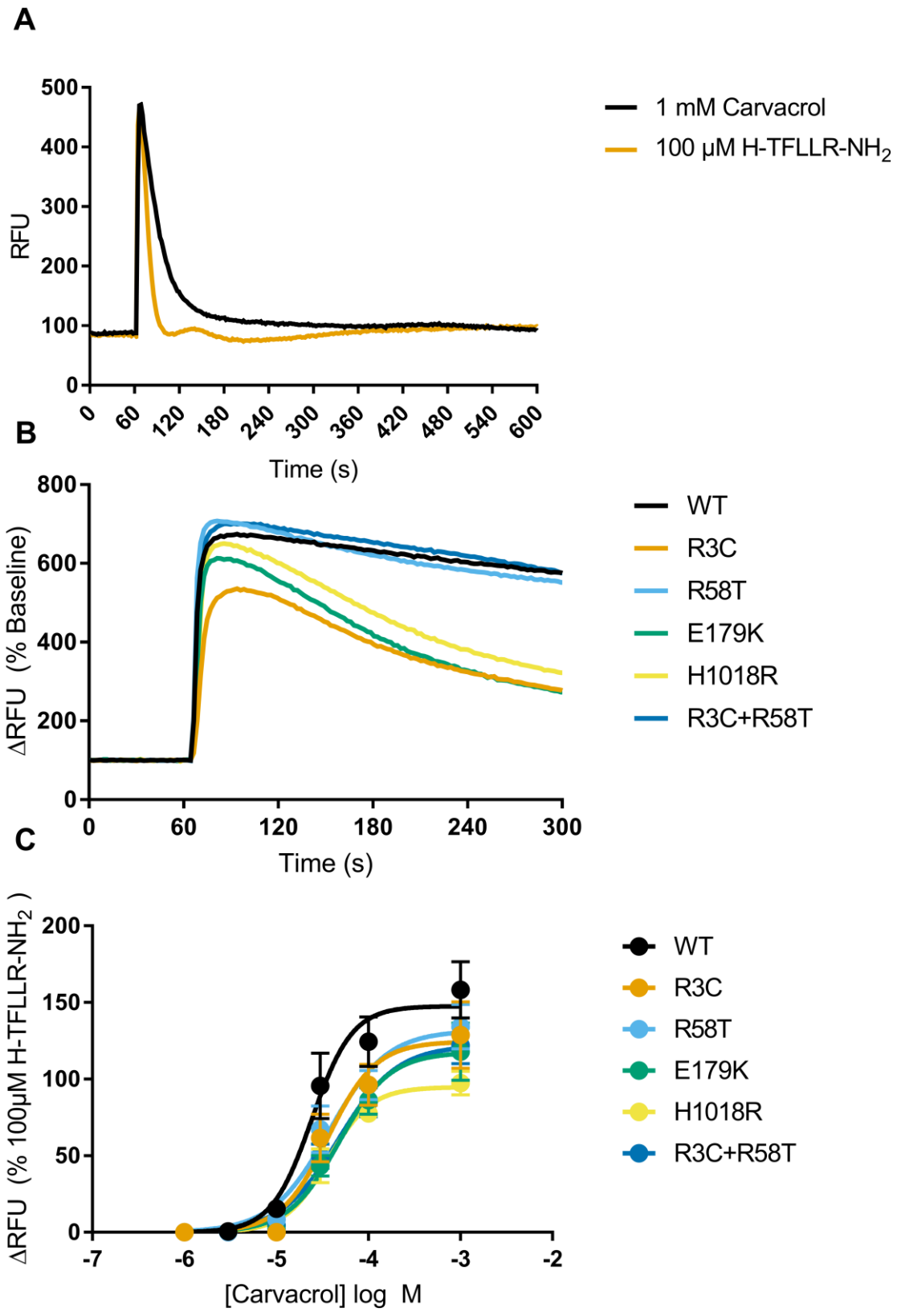

Figure 4:4 – Activation of hTRPA1 variants by carvacrol: A – Raw trace data illustrating sharp elevation in Ca_i after addition of 1 mM carvacrol and 100 µM H-TFLLR-NH_2. B – Baseline normalised trace data illustrating the response of hTRPA1 variants to 1 mM carvacrol. C – Concentration response relationship of carvacrol at hTRPA1 variants. Data represent the mean ± SEM of 5 independent determinations performed in duplicate.

5 THE EFFECT OF HTRPA1 POLYMORPHISMS ON SYNTHETIC CANNABINOIDS

5.1 INTRODUCTION

No pharmacological data exist on the effect of hTRPA1 variants on synthetic cannabinoid activity. To investigate this, we selected a number of recently identified, high concern synthetic cannabinoids. The compounds were selected after a search of recent literature, identifying cases of acute synthetic cannabinoid toxicity resulting in the hospitalisation or death of at least one person. Seven compounds were chosen; THC, 5 synthetic cannabinoids (MDMB-CHMICA, PB-22, 5F-PB-22, UR-144 and XLR-11), and the 5-hydroxypentyl (5-OH) metabolite common to both UR-144 and XLR-11. Experiments were prepared as per Section 2.3, and all agonist responses were normalised to 100 µM H-TFLLR-NH_2. Due to the limits of solubility of these drugs in HBSS, a final concentration of 30 µM was the highest we could achieve in the assay. We did not have the opportunity to construct full CRC's for these drugs, however, we were able to compare the activation of hTRPA1 at both a drug concentration of 30 µM and 10 µM. The chemical structure for each compound tested can be found below in Figure 5:1. The IUPAC name and CAS # for each compound tested can be found in Table 2:1.

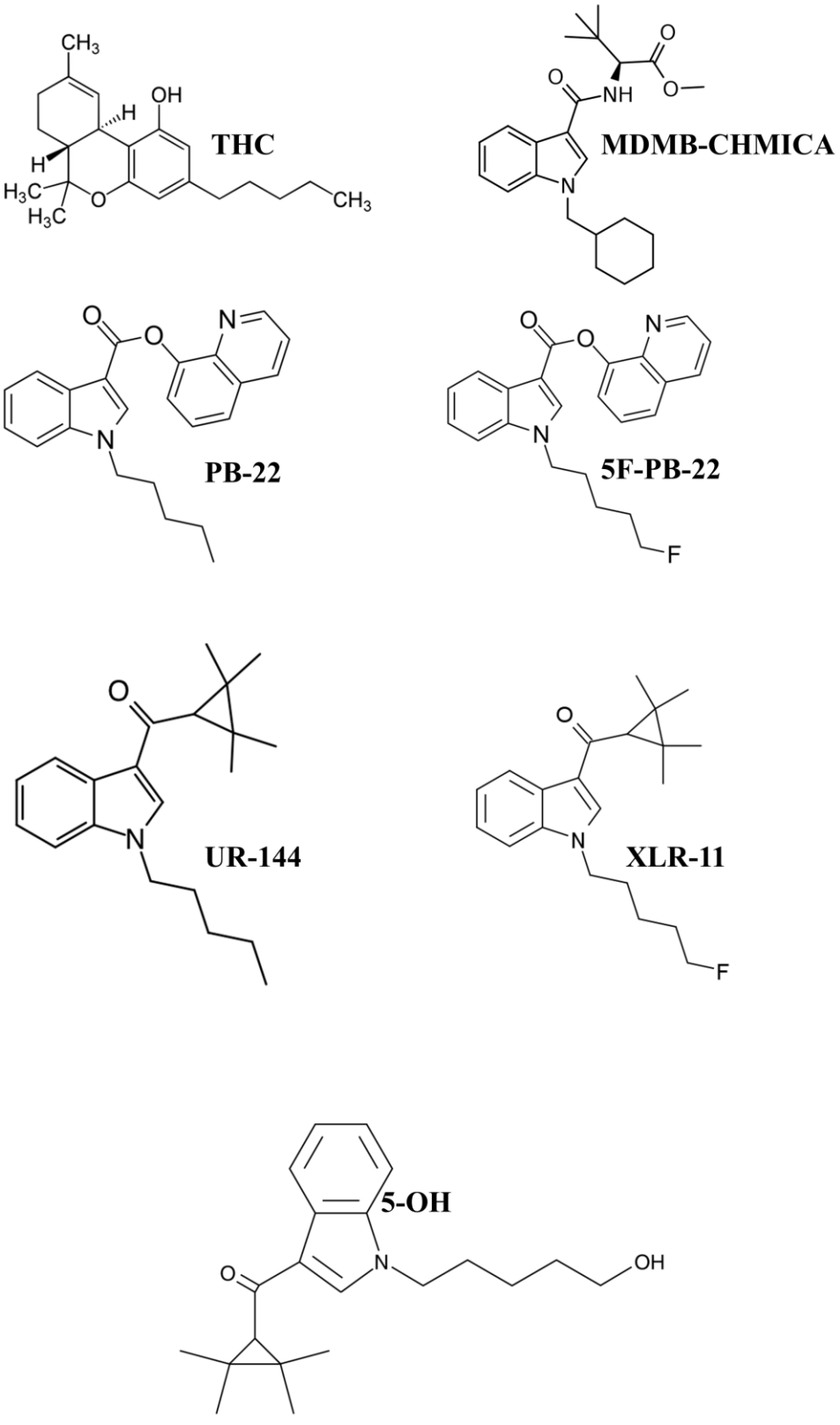

Figure 5:1 – Common names and chemical structures of all cannabinoid compounds tested: This figure illustrates the chemical structures of THC and the 6 synthetic cannabinoid compounds tested. Original structures generated for papers published by our lab [96, 98].

5.2 RESULTS

5.2.1 THC

Addition of THC to HEK293 cells expressing hTRPA1 variants produced a concentration dependant elevation in Ca_i (Figure 5:2). In HEK293 WT cells, THC produced a small elevation in Ca_i of 13 ± 2 of % H-TFLLR-NH_2 (Figure 5:2). The effect at THC (30 µM) ranged from 62 ± 6 % of 100 µM H-TFLLR-NH_2 at R3C to 101 ± 20 at the WT (Table 5:1). There was no statistically significant difference between the maximal effect observed at any hTRPA1 variant compared to the WT (Table 5:1).

Table 5:1 – Effect of 30 µM THC at hTRPA1 variants: Effect at 30 µM was calculated individually for each variant and pooled together. Data represent the mean ± SEM of 5 independent determinations performed in duplicate. Fold change was calculated as variant/WT where significant, indicated by a two-tailed t test, ns = not significant.

TRPA1	Effect at 30 µM (% 100 µM H-TFLLR-NH_2)	t (df = 8)	p	Fold Change
WT	101 ± 20	NA	NA	NA
R3C	62 ± 6	1.869	0.0986	ns
R58T	82 ± 11	0.848	0.4211	ns
E179K	60 ± 4	1.988	0.082	ns
H1018R	75 ± 6	1.235	0.2518	ns
R3C+R58T	79 ± 11	0.9513	0.3693	ns

Effect at [THC] of 10 µM ranged from 26 ± 7 % of 100 µM H-TFLLR-NH_2 at E179K to 56 ± 11 at the WT (Table 5:2). There was a statistically significant difference between the effect of 10 µM THC at R3C and E179K when compared to the WT. These represent at 0.48 and 0.46 fold change, respectively (Table 5:2).

Table 5:2 – Effect of 10 µM THC at hTRPA1 variants: Effect at [THC] of 10 µM was calculated individually for each replicate and pooled together. Data represent the mean ± SEM of 5 independent determinations performed in duplicate. Fold change was calculated as variant/WT where significant, indicated by a two-tailed t test, ns = not significant.

TRPA1	Effect at 10 µM (% 100 µM H-TFLLR-NH_2)	t (df = 8)	p	Fold Change
WT	56 ± 11	NA	NA	NA
R3C	27 ± 3	2.558	0.0338	0.48
R58T	46 ± 9	0.7615	0.4682	ns
E179K	26 ± 7	2.36	0.046	0.46
H1018R	24 ± 10	2.238	0.0556	ns
R3C+R58T	39 ± 11	1.155	0.2815	ns

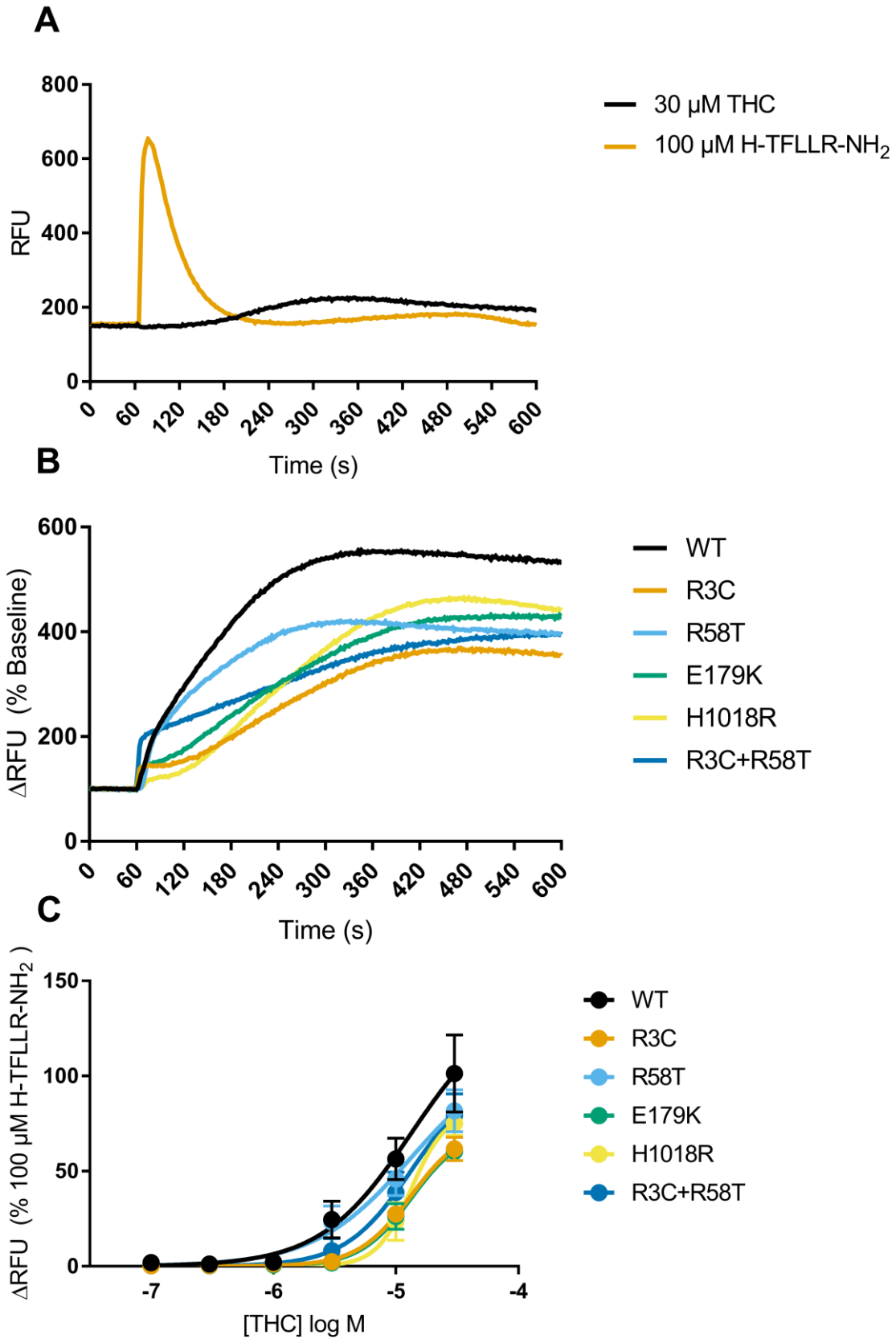

Figure 5:2 – Activation of hTRPA1 variants by THC: A – Raw trace data illustrating the response of HEK293 WT cells to 30 µM THC and 100 µM H-TFLLR-NH_2. B – Baseline normalised trace data illustrating the response of hTRPA1 variants to 30 µM THC. C – Concentration response relationship of THC at hTRPA1 variants. Data represent the mean ± SEM of 5 independent determinations performed in duplicate.

5.2.2 MDMB-CHMICA

Addition of MDMB-CHMICA to HEK293 cells expressing hTRPA1 variants produced a concentration dependant elevation in Ca_i but did not increase Ca_i in HEK293 WT cells (Figure 5:3). The effect at [MDMB-CHMICA] of 30 µM observed from MDMB-CHMICA at hTRPA1 variants ranged from 52 ± 4 % of 100 µM H-TFLLR-NH_2 at R3C+R58T to 73 ± 8 at E179K (Table 5:3). There was no statistically significant difference between the effect at [MDMB-CHMICA] of 30 µM at any hTRPA1 variant compared to the WT (Table 5:3).

Table 5:3 – Effect of 30 µM MDMB-CHMICA at hTRPA1 variants: Effect at [MDMB-CHMICA] of 30 µM was calculated individually for each replicate and pooled together. Data represent the mean ± SEM of 5 independent determinations performed in duplicate. Fold change was calculated as variant/WT where significant, indicated by a two-tailed t test, ns = not significant.

TRPA1	Effect at 30 µM (% 100 µM H-TFLLR-NH_2)	t (df = 8)	p	Fold Change
WT	68 ± 10	NA	NA	NA
R3C	60 ± 6	0.7605	0.4688	ns
R58T	60 ± 5	0.7875	0.4537	ns
E179K	73 ± 8	0.3966	0.7021	ns
H1018R	62 ± 9	0.4963	0.633	ns
R3C+R58T	52 ± 4	1.501	0.1718	ns

Effect at [MDMB-CHMICA] of 10 µM at hTRPA1 variants spanned 39 ± 4 % of H-TFLLR-NH_2 at R3C+R58T to 57 ± 6 at E179K (Table 5:4). There was no statistically significant difference between the effect of 10 µM MDMB-CHMICA at any hTRPA1 variant compared to the WT (Table 5:4).

Table 5:4 – Effect of 10 µM MDMB-CHMICA at hTRPA1 variants: Effect at [MDMB-CHMICA] of 10 µM was calculated individually for each replicate and pooled together. Data represent the mean ± SEM of 5 independent determinations performed in duplicate. Fold change was calculated as variant/WT where significant, as indicated by a two-tailed t test, ns = not significant.

TRPA1	Effect at 10 µM (% 100 µM H-TFLLR-NH_2)	t (df = 8)	p	Fold Change
WT	54 ± 8	NA	NA	NA
R3C	45 ± 6	0.8976	0.3956	ns
R58T	44 ± 5	1.03	0.3329	ns
E179K	57 ± 6	0.3046	0.7685	ns
H1018R	47 ± 7	0.6353	0.543	ns
R3C+R58T	39 ± 4	1.558	0.1579	ns

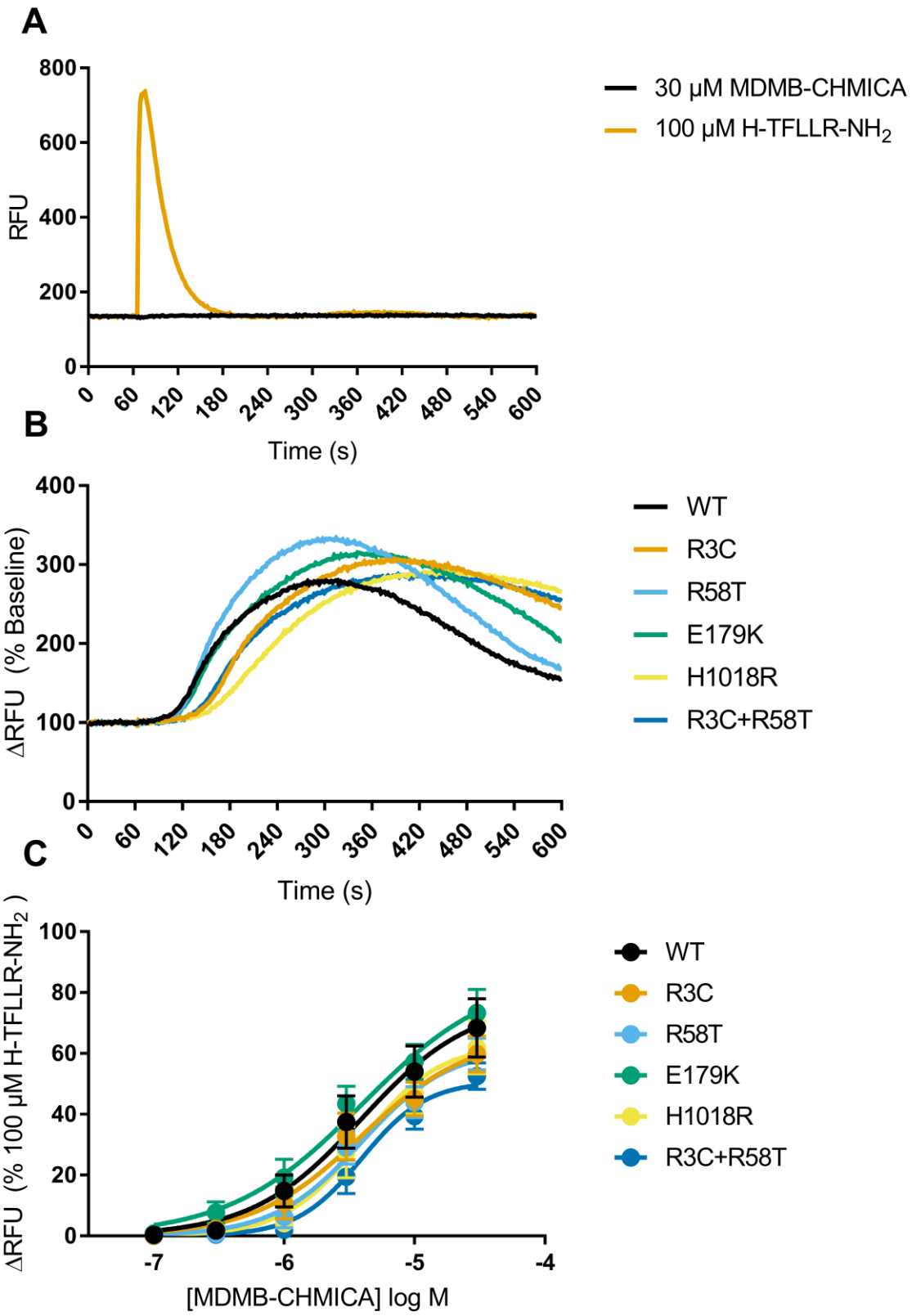

Figure 5:3 – Activation of hTRPA1 variants by the synthetic cannabinoid MDMB-CHMICA: A – Raw trace data illustrating the response of HEK293 WT cells to 30 µM MDMB-CHMICA and 100 µM H-TFLLR-NH_2. B – Baseline normalised trace data illustrating the response of hTRPA1 variants to 30 µM MDMB-CHMICA. C – Concentration response relationship of MDMB-CHMICA at hTRPA1 variants. Data represent the mean ± SEM of 5 independent determinations performed in duplicate.

5.2.3 PB-22

Addition of PB-22 to HEK293 cells expressing hTRPA1 variants elicited a robust, concentration dependant increase in Ca_i, but did not elevate Ca_i in HEK293 WT cells (Figure 5:4). The effect observed at [PB-22] of 30 µM ranged from 17 ± 5 % of 100 µM H-TFLLR-NH_2 at R3C+R58T to 43 ± 3 at R58T (Table 5:5). There was a statistically significant difference between the maximal effect observed at R58T compared to the WT, representing a 1.54-fold change (Table 5:5).

Table 5:5 – Effect of 30 µM PB-22 at hTRPA1 variants: Effect at [PB-22] of 30 µM was calculated individually for each replicate and pooled together. Data represent the mean ± SEM of 5 independent determinations performed in duplicate. Fold change was calculated as variant/where significant, indicated by a two-tailed t test, ns = not significant

TRPA1	Effect at 30 µM (% 100 µM H-TFLLR-NH_2)	t (df = 8)	p	Fold Change
WT	28 ± 4	NA	NA	NA
R3C	30 ± 2	0.3465	0.7379	ns
R58T	43 ± 3	2.761	0.0247	1.54
E179K	29 ± 6	0.0999	0.9229	ns
H1018R	31 ± 7	0.3912	0.7059	ns
R3C+R58T	17 ± 5	1.767	0.1152	ns

The effect observed at [PB-22] of 10 µM ranged from 5 ± 2 % of 100 µM H-TFLLR-NH_2 at the WT to 28 ± at R58T (Table 5:6). There was a statistically significant difference between the effect observed at R58T compared to WT, representing a 5.6-fold change (Table 5:6).

Table 5:6 – Effect of 10 µM PB-22 at hTRPA1 variants: Effect at [PB-22] of 10 µM was calculated individually for each replicate and pooled together. Data represent the mean ± SEM of 5 independent determinations performed in duplicate. Fold change was calculated as variant/WT where significant, indicated by a two-tailed t test, ns = not significant.

TRPA1	Effect at 10 µM (% 100 µM H-TFLLR-NH_2)	t (df = 8)	p	Fold Change
WT	5 ± 2	NA	NA	NA
R3C	11 ± 2	2.029	0.077	ns
R58T	28 ± 5	2.965	0.018	5.6
E179K	10 ± 4	1.009	0.3426	ns
H1018R	11 ± 4	1.358	0.2116	ns
R3C+R58T	5 ± 3	0.1651	0.873	ns

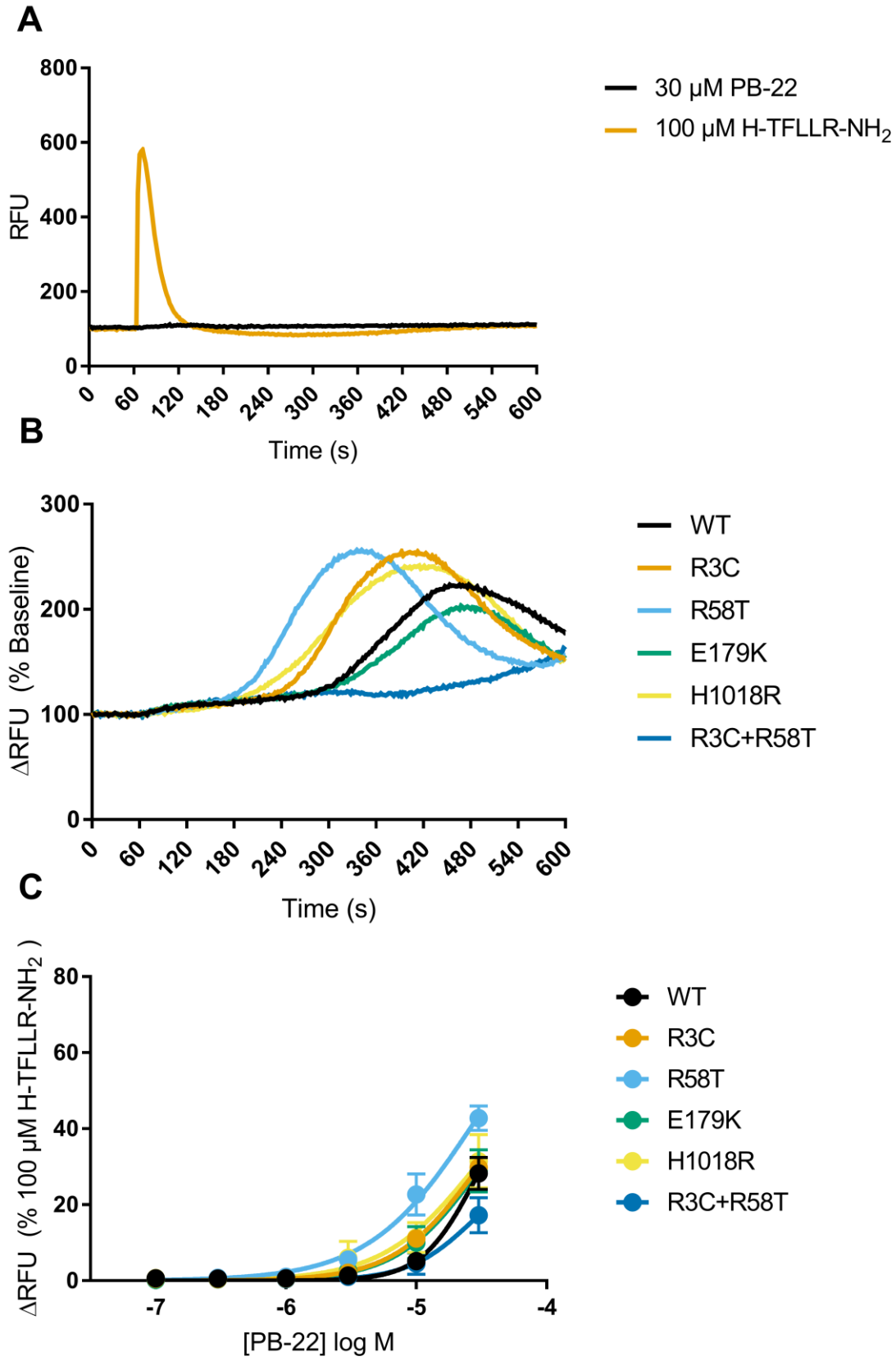

Figure 5:4 – Activation of hTRPA1 variants by the synthetic cannabinoid PB-22: A – Raw trace data illustrating the response of HEK293 WT cells to 30 µM PB-22 and 100 µM H-TFLLR-NH_2. B – Baseline normalised trace data illustrating the response of hTRPA1 variants to 30 µM PB-22. C – Concentration response relationship of PB-22 at hTRPA1 variants. Data represent the mean ± SEM of 5 independent determinations performed in duplicate

5.2.4 5F-PB-22

Addition of 5F-PB-22 to HEK293 cells expressing hTRPA1 variants produced a concentration dependant elevation in Ca_i, but did not elevate Ca_i in HEK293 WT cells (Figure 5:5). The effect observed at [5F-PB-22] of 30 µM ranged from 28 ± 6 % of 100 µM H-TFLLR-NH_2 at R3C+R58T to 55 ± 4 at R58T (Table 5:7). There was a statistically significant difference between the maximal effect at R58T compared to the WT, representing a 1.72-fold change (Table 5:7).

Table 5:7 – Effect of 30 µM 5F-PB-22 at hTRPA1 variants: Effect at [5F-PB-22] of 30 µM was calculated individually for each replicate and pooled together. Data represent the mean ± SEM of 5 independent determinations performed in duplicate. Fold change was calculated as variant/WT where significant, indicated by a two-tailed t test, ns = not significant.

TRPA1	Effect at 30 µM (% 100 µM H-TFLLR-NH_2)	t (df = 8)	p	Fold Change
WT	32 ± 7	NA	NA	NA
R3C	34 ± 5	0.2406	0.8159	ns
R58T	55 ± 4	2.69	0.0275	1.72
E179K	30 ± 5	0.2256	0.8272	ns
H1018R	45 ± 6	1.293	0.232	ns
R3C+R58T	28 ± 6	0.4824	0.6424	ns

The effect observed at [5F-PB-22] of 10 µM ranged from 13 ± 4 % of 100 µM H-TFLLR-NH_2 at R3C+R58T to 36 ± 4 at R58T (Table 5:8). There was no statistically significant difference between the effect of 10 µM 5F-PB-22 at any hTRPA1 variant compared to the WT (Table 5:8).

Table 5:8 – Effect of 10 µM 5F-PB-22 at hTRPA1 variants: Effect at [5F-PB-22] of 10 µM was calculated individually for each replicate and pooled together. Data represent the mean ± SEM of 5 independent determinations performed in duplicate. Fold change was calculated as variant/WT where significant, indicated by a two-tailed t test, ns = not significant.

TRPA1	Effect at 10 µM (% 100 µM H-TFLLR-NH_2)	t (df = 8)	p	Fold Change
WT	19 ± 7	NA	NA	NA
R3C	20 ± 6	0.1204	0.9071	ns
R58T	36 ± 4	2.096	0.0694	ns
E179K	15 ± 5	0.5371	0.6058	ns
H1018R	21 ± 7	0.2388	0.8173	ns
R3C+R58T	13 ± 4	0.8201	0.4359	ns

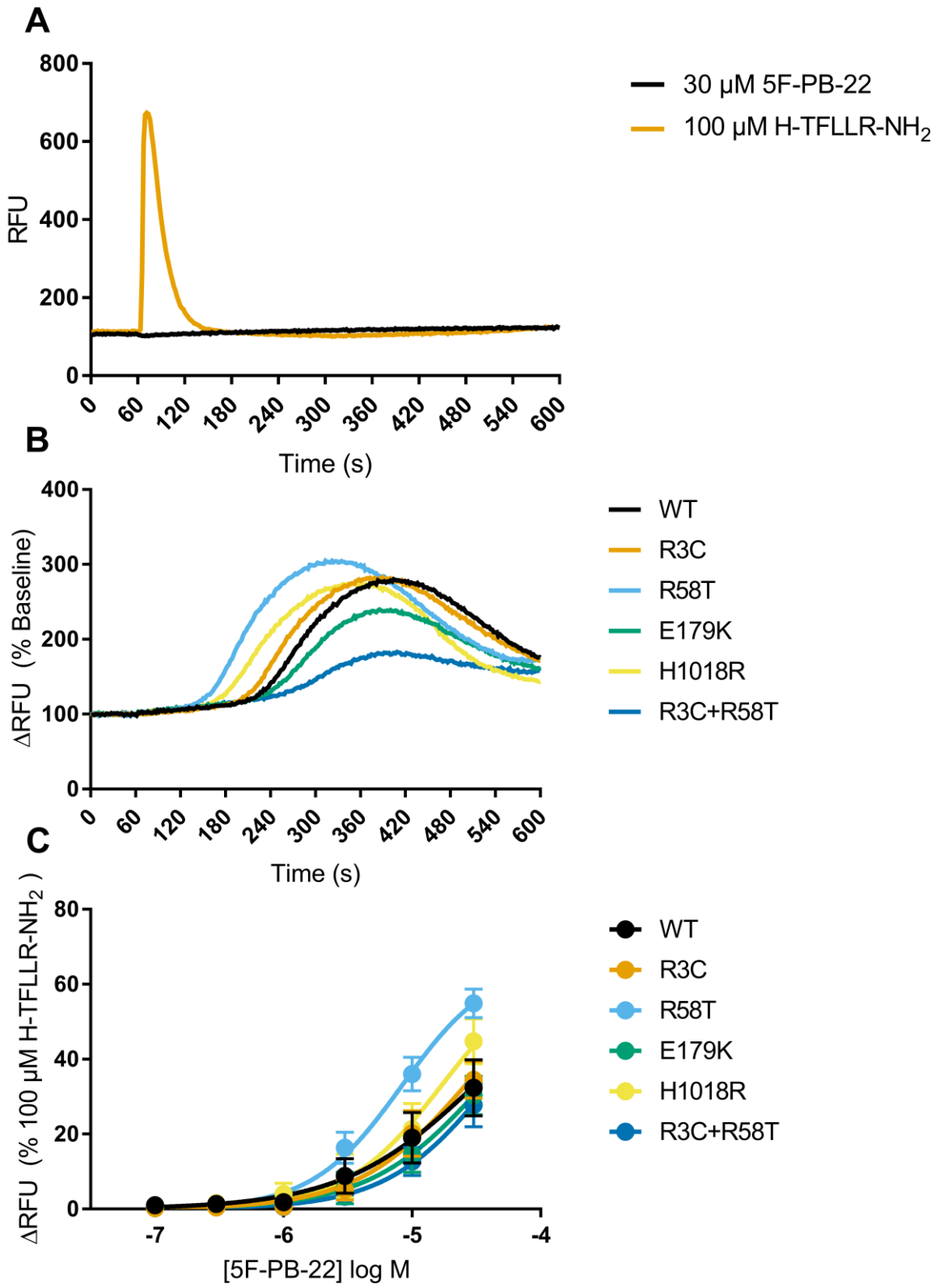

Figure 5:5 – Activation of hTRPA1 variants by the synthetic cannabinoid 5F-PB-22: A – Raw trace data illustrating the response of HEK293 WT cells to 30 µM 5F-PB-22 and 100 µM H-TFLLR-NH_2. B – Baseline normalised trace data illustrating the response of hTRPA1 variants to 30 µM 5F-PB-22. C – Concentration response relationship of 5F-PB-22 at hTRPA1 variants. Data represent the mean ± SEM of 5 independent determinations performed in duplicate.

5.2.5 PB-22 Compared to 5F-PB-22

5F-PB-22 appeared to exhibit greater relative potency at some hTRPA1 variants in our assay (Table 5:9, Figure 5:6). A two-way ANOVA with Sidak's test for multiple comparisons indicated no significant difference between PB-22 and 5F-PB-22 at any hTRPA1 variant (Table 5:9).

Table 5:9 – Effect at 30 µM and 10 µM of PB-22 and 5F-PB-22 at hTRPA1 variants: Effect at 30 µM and 10 µM was calculated individually for each replicate and pooled together. Data represent the mean ± SEM of 5 independent determinations performed in duplicate. Fold change was calculated as 5F-PB-22/PB-22 where statistically significant, indicated by Sidak's test for multiple comparisons, ns = not significant.

TRPA1	Effect at 30 µM (% 100 µM H-TFLLR-NH_2)			Effect at 10 µM (% 100 µM H-TFLLR-NH_2)		
	PB-22	**5F-PB-22**	**Fold Change**	**PB-22**	**5F-PB-22**	**Fold Change**
WT	28 ± 4	32 ± 7	ns	5 ± 2	19 ± 7	ns
R3C	30 ± 2	34 ± 5	ns	11 ± 2	20 ± 6	ns
R58T	43 ± 3	55 ± 4	ns	28 ± 5	36 ± 4	ns
E179K	29 ± 6	30 ± 5	ns	10 ± 4	15 ± 5	ns
H1018R	31 ± 7	45 ± 6	ns	11 ± 4	21 ± 7	ns
R3C+R58T	17 ± 5	28 ± 6	ns	5 ± 3	13 ± 4	ns

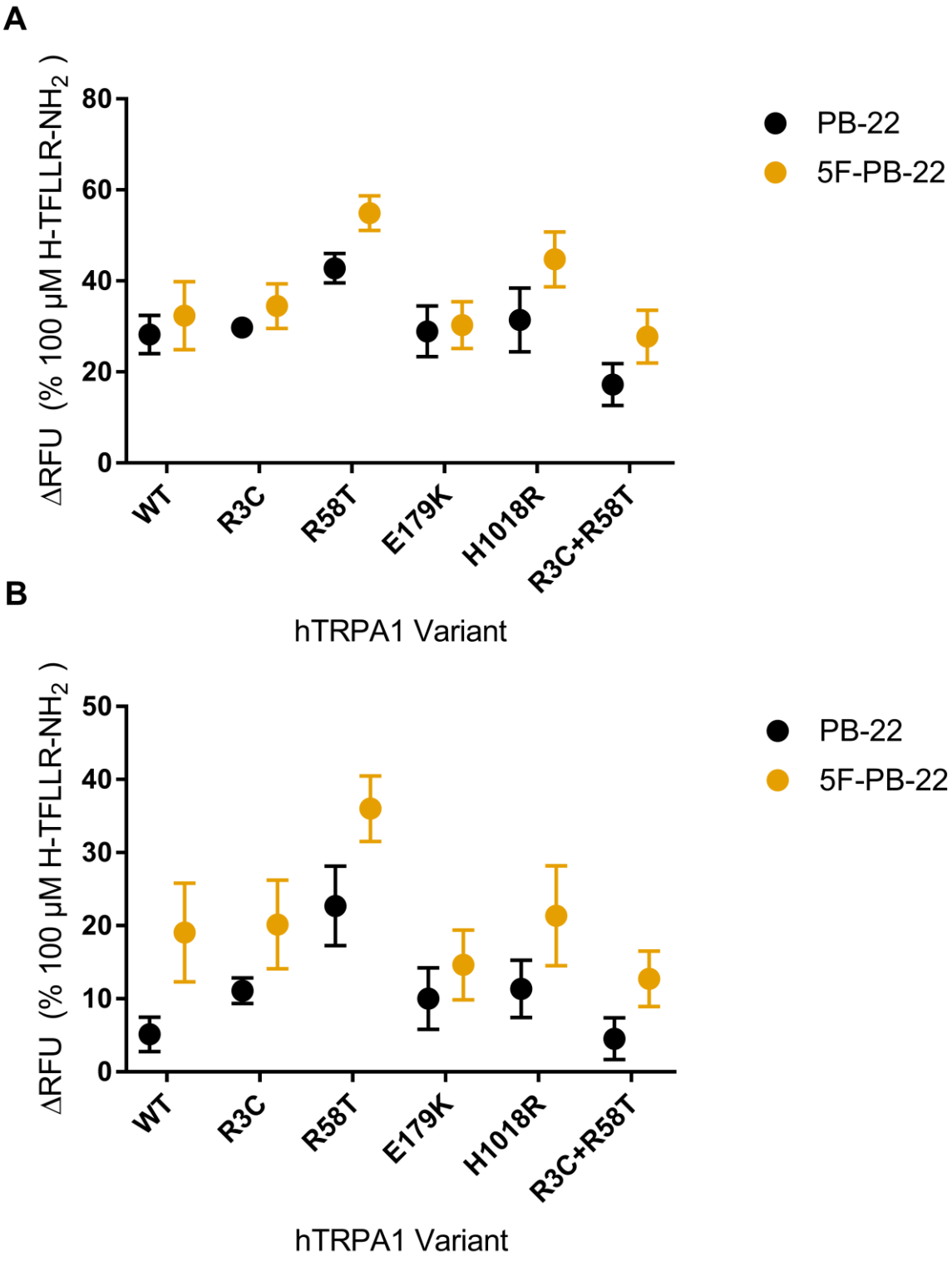

Figure 5:6 – Effect of PB-22 and 5F-PB-22 at hTRPA1 variants: A – The effect of PB-22 and 5F-PB-22 at 30 µM on hTRPA1 variants. B – The effect of PB-2 and 5F-PB-22 at 10 µM at hTRPA1 variants. Data represent the mean ± SEM of 5 independent determinations performed in duplicate.

5.2.6 UR-144

Addition of UR-144 to HEK293 cells expressing hTRPA1 variants produced a robust, concentration dependant increase in Ca_i, and did not elevate Ca_i in HEK293 WT cells (Figure 5:7). Effect at [UR-144] of 30 µM at hTRPA1 variants ranged from 14 ± 4 % of H-TFLLR-NH_2 at H1018R to 50 ± 10 at the WT (Table 5:10). There were statistically significant differences observed between the maximal effect at R3C, E179K and H1018R compared to the WT. These represent a 0.32, 034 and 028-fold change, respectively (Table 5:10).

Table 5:10 – Effect of 30 µM UR-144 at hTRPA1 variants: Effect at [UR-144] of 30 µM was calculated individually for each replicate and pooled together. Data represent the mean ± SEM of 5 independent determinations performed in duplicate. Fold change was calculated as variant/WT where significant, indicated by a two-tailed t test, ns = not significant.

TRPA1	Effect at 30 µM (% 100 µM H-TFLLR-NH_2)	t (df = 8)	p	Fold Change
WT	50 ± 10	NA	NA	NA
R3C	16 ± 5	2.936	0.0188	0.32
R58T	28 ± 6	1.86	0.0999	ns
E179K	17 ± 4	3.027	0.0164	0.34
H1018R	14 ± 4	3.264	0.0115	0.28
R3C+R58T	27 ± 4	2.077	0.0714	ns

The effect observed at [UR-144] of 10 µM ranged from 1 ± 0.4 % of 100 µM H-TFLLR-NH_2 at H1018R to 22 ± 7 at the WT (Table 5:11). There was a statistically significant difference between the effect observed at E179K and H1018R compared to the WT. These represent a 0.09 and 0.05-fold change, respectively (Table 5:11).

Table 5:11 – Effect of 10 µM UR-144 at hTRPA1 variants: Effect at [UR-144] of 10µM was calculated individually for each replicate and pooled. Data represent the mean ± SEM of 5 independent determinations performed in duplicate. Fold change was calculated as variant/WT where significant, indicated by a two-tailed t test, ns = not significant.

TRPA1	Effect at 10 µM (% 100 µM H-TFLLR-NH_2)	t (df = 8)	p	Fold Change
WT	22 ± 7	NA	NA	NA
R3C	4 ± 3	2.266	0.0532	ns
R58T	10 ± 5	1.369	0.2082	ns
E179K	2 ± 0.6	2.754	0.0249	0.09
H1018R	1 ± 0.4	2.819	0.0225	0.05
R3C+R58T	9 ± 3	1.564	0.1564	ns

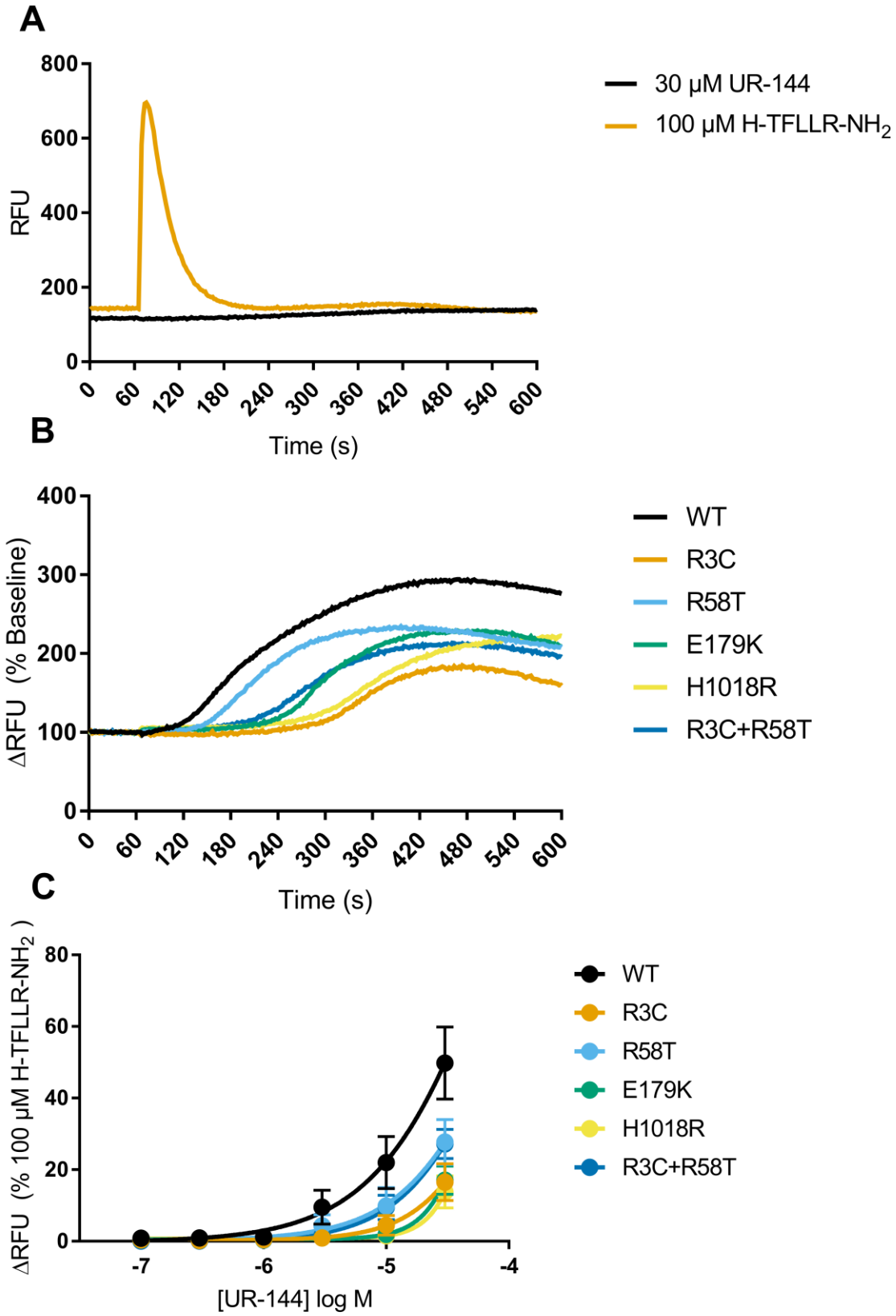

Figure 5:7 – Activation of hTRPA1 variants by the synthetic cannabinoid UR-144: A – Raw trace data illustrating the response of HEK293 WT cells to 30 µM UR-144 and 100 µM H-TFLLR-NH_2. B – Baseline normalised trace data illustrating the response of hTRPA1 variants to 30 µM UR-144. C – Concentration response relationship of UR-144 at hTRPA1 variants. Data represent the mean ± SEM of 5 independent determinations performed in duplicate.

5.2.7 XLR-11

Addition of XLR-11 to HEK293 cells expressing hTRPA1 variants elicited a robust, concentration dependant increase in Ca_i, but did not elevate Ca_i in HEK293 WT cells (Figure 5:8). The effect observed at [XLR-11] of 30 µM ranged from 44 ± 3 % of 100 µM H-TFLLR-NH_2 at R3C+R58T and R3C to 67 ± 10 at the WT (Table 5:12). There was no statistically significant difference between the effect observed at any hTRPA1 variant compared to the WT (Table 5:12).

Table 5:12 – Effect of 30 µM XLR-11 at hTRPA1 variants: Maximal effect was calculated individually for each replicate and pooled together. Data represent the mean ± SEM of 5 independent determinations performed in duplicate. Fold change was calculated as variant/WT where significant, indicated by a two-tailed t test, ns = not significant.

TRPA1	Effect at 30 µM (% 100 µM H-TFLLR-NH_2)	t (df = 8)	p	Fold Change
WT	67 ± 10	NA	NA	NA
R3C	44 ± 3	2.218	0.0574	ns
R58T	56 ± 5	1.028	0.334	ns
E179K	51 ± 4	1.462	0.1819	ns
H1018R	52 ± 6	1.295	0.2315	ns
R3C+R58T	44 ± 3	2.291	0.0512	ns

The effect observed at [XLR-11] of 10 µM ranged from 30 ± 2 % of H-TFLLR-NH_2 at R3C+R58T to 48 ± 6 at the WT (Table 5:13). There was a statistically significant difference between the effect observed at R3C and R3C+R58T when compared to the WT. These represent a 0.77 and 0.63-fold change, respectively (Table 5:13).

Table 5:13 – Effect of 10 µM XLR-11 on hTRPA1 variants: Effect at [XLR-11] of 10 µM was calculated individually for each replicate and pooled together. Data represent the mean ± SEM of 5 independent determinations performed in duplicate. Fold change was calculated as variant/WT where significant, indicated by a two-tailed t test, ns = not significant.

TRPA1	Effect at 10 µM (% 100 µM H-TFLLR-NH_2)	t (df = 8)	p	Fold Change
WT	48 ± 6	NA	NA	NA
R3C	31 ± 4	2.375	0.0449	0.77
R58T	37 ± 3	1.668	0.1339	ns
E179K	38 ± 3	1.58	0.1528	ns
H1018R	33 ± 4	2.08	0.0711	ns
R3C+R58T	30 ± 2	2.894	0.0201	0.63

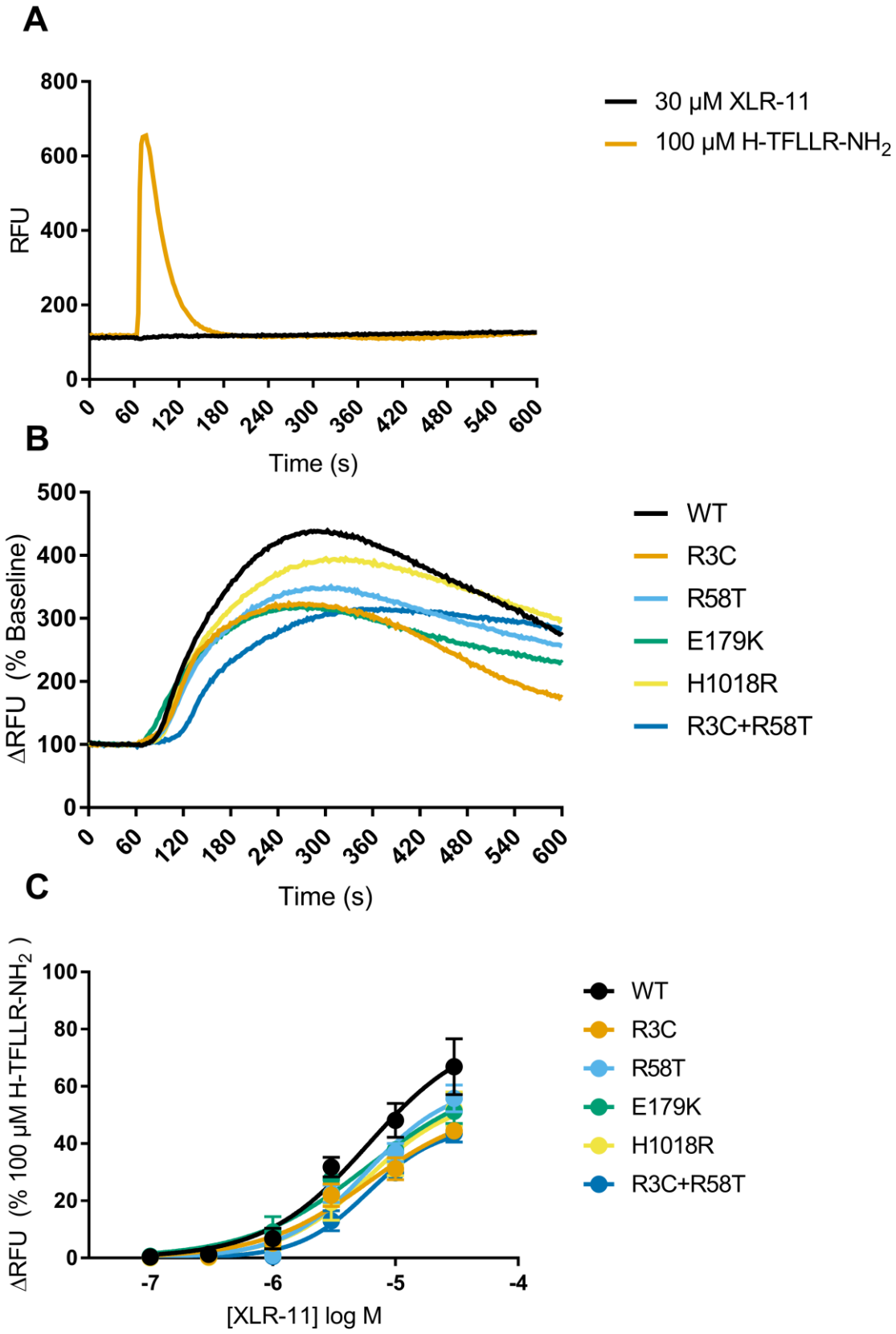

Figure 5:8 – Activation of hTRPA1 variants by the synthetic cannabinoid XLR-11: A – Raw trace data illustrating the response of HEK293 WT cells to 30 µM XLR-11 and 100 µM H-TFLLR-NH_2. B – Baseline normalised trace data illustrating the response of hTRPA1 variants to 30 µM XLR-11. C – Concentration response relationship of XLR-11 at hTRPA1 variants. Data represent the mean ± SEM of 5 independent determinations performed in duplicate.

5.2.8 UR-144 Compared to XLR-11

XLR-11 appeared to exhibit greater relative potency at variants of hTRPA1 when compared to UR-144 in our assay (Table 5:14, Figure 5:9). Comparing the effect at 30 µM between the two, there were statistically significant differences at R3C, R58T, E179K and H1018R (Table 5:15). These represent a 2.75, 2, 3 and 3.71-fold change, respectively (Table 5:14). Comparing the effect at 10 µM, there were statistically significant differences at all hTRPA1 variants tested (Table 5:15). The fold change ranged from 2.18 at the WT to 33 at H1018R (Table 5:14).

Table 5:14 – Effect at 30 µM and 10 µM of UR-144 and XLR-11 at hTRPA1 variants: Effect at 30 µM and 10 µM was calculated individually for each replicate and pooled together. Data represent the mean ± SEM of 5 independent determinations performed in duplicate. Fold change was calculated as XLR-11/UR-144 where statistically significant, as indicated by Sidak's test for multiple comparisons.

TRPA1	Effect at 30 µM (% 100 µM H-TFLLR-NH_2)			Effect at 10 µM (% 100 µM H-TFLLR-NH_2)		
	UR-144	**XLR-11**	**Fold Change**	**UR-144**	**XLR-11**	**Fold Change**
WT	50 ± 10	67 ± 10	ns	22 ± 7	48 ± 6	2.18
R3C	16 ± 5	44 ± 3	2.75	4 ± 3	31 ± 4	7.75
R58T	28 ± 6	56 ± 5	2.00	10 ± 5	37 ± 3	3.70
E179K	17 ± 4	51 ± 4	3.00	2 ± 0.6	38 ± 3	19.00
H1018R	14 ± 4	52 ± 6	3.71	1 ± 0.4	33 ± 4	33.00
R3C+R58T	27 ± 4	44 ± 3	ns	9 ± 3	30 ± 2	3.33

Table 5:15 – Statistics output comparing the effect of XLR-11 to UR-144 at hTRPA1 variants: A two-way ANOVA with Sidak's test for multiple comparisons was conducted to test for statistically significant differences between the effect at 30 µM and 10 µM of XLR-11 compared to UR-144 at each hTRPA1 variant.

UR-144 vs. XLR-11	Effect at 30 µM		Effect at 10 µM	
	t (df = 48)	**p**	**t (df = 48)**	**p**
WT	2.069	0.2365	4.665	0.0001
R3C	3.387	0.0085	4.773	0.0001
R58T	3.4	0.0082	4.814	<0.0001
E179K	4.158	0.0008	6.385	<0.0001
H1018R	4.637	0.0002	5.611	<0.0001
R3C+R58T	1.985	0.2781	3.621	0.0042

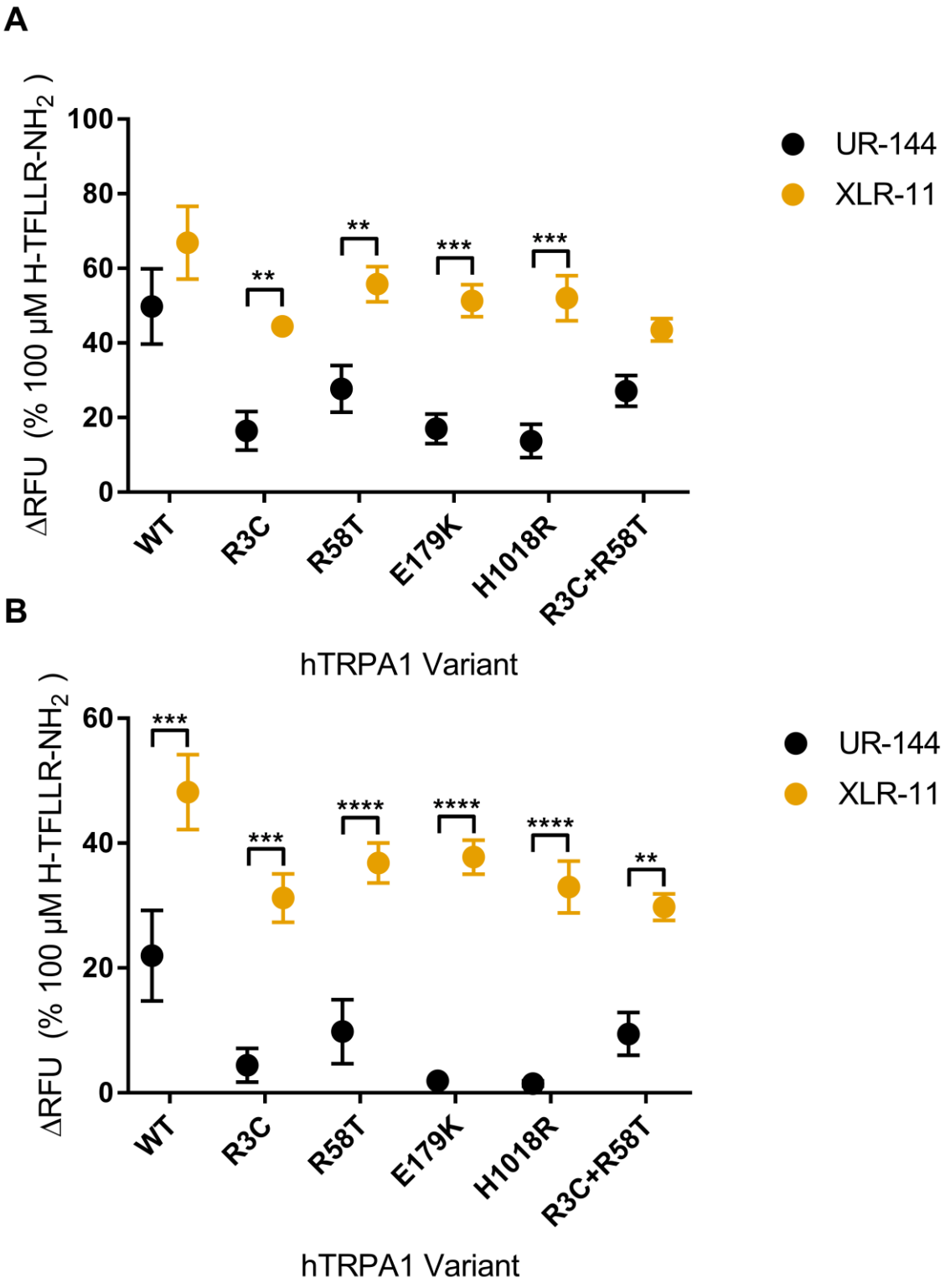

Figure 5:9 – Effect of UR-144 and XLR-11 at hTRPA1 variants: A – The effect of UR-144 and XLR-11 at 30 µM at hTRPA1 variants. B – The effect of UR-144 and XLR-11 at 10 µM at hTRPA1 variants. Data represent the mean ± SEM of 5 independent determinations performed in duplicate. Asterisks indicate significance at the $p < 0.05$ level.

5.2.9 5-OH

Addition of 5-OH to HEK293 cells expressing hTRPA1 variants produced a concentration dependant increase in Ca_i and did not elevate Ca_i in HEK293 WT cells (Figure 5:10). The effect of 30 µM 5-OH at hTRPA1 variants ranged from 51 ± 10 % of 100 µM H-TFLLR-NH_2 at H1018R to 84 ± 14 at the WT (Table 5:16). There was no statistically significant difference between the effect observed at any hTRPA1 variant when compared to the WT (Table 5:16).

Table 5:16 – Effect of 30 µM 5-OH at hTRPA1 variants: Maximal effect was calculated individually for each replicate and pooled together. Data represent the mean ± SEM of 5 independent determinations performed in duplicate. Fold change was calculated as variant/WT where significant, indicated by a two-tailed t test, ns = not significant.

TRPA1	Effect at 30 µM (% 100 µM H-TFLLR-NH_2)	t (df = 8)	p	Fold Change
WT	84 ± 14	NA	NA	NA
R3C	65 ± 8	1.253	0.2456	ns
R58T	86 ± 16	0.0908	0.9299	ns
E179K	60 ± 8	1.565	0.1561	ns
H1018R	51 ± 10	1.954	0.0865	ns
R3C+R58T	69 ± 7	0.9619	0.3643	ns

The effect observed at [5-OH] of 10 µM ranged from 15 ± % 100 µM H-TFLLR-NH_2 at H1018R to 41 ± 13 at R58T (Table 5:17). There was no statistically significant difference between the effect observed at any hTRPA1 variant when compared to the WT (Table 5:17).

Table 5:17 – Effect of 10 µM 5-OH at hTRPA1 variants: Effect at [5-OH] of 10 µM was calculated individually for each replicate and pooled together. Data represent the mean ± SEM of 5 independent determinations performed in duplicate. Fold change was calculated as variant/where significant, indicated by a two-tailed t test, ns = not significant.

TRPA1	Effect at 10 µM (% 100 µM H-TFLLR-NH_2)	t (df = 8)	p	Fold Change
WT	32 ± 16	NA	NA	NA
R3C	20 ± 8	0.6648	0.5249	ns
R58T	41 ± 13	0.4365	0.674	ns
E179K	27 ± 10	0.275	0.7903	ns
H1018R	15 ± 8	0.9788	0.3563	ns
R3C+R58T	27 ± 8	0.3107	0.764	ns

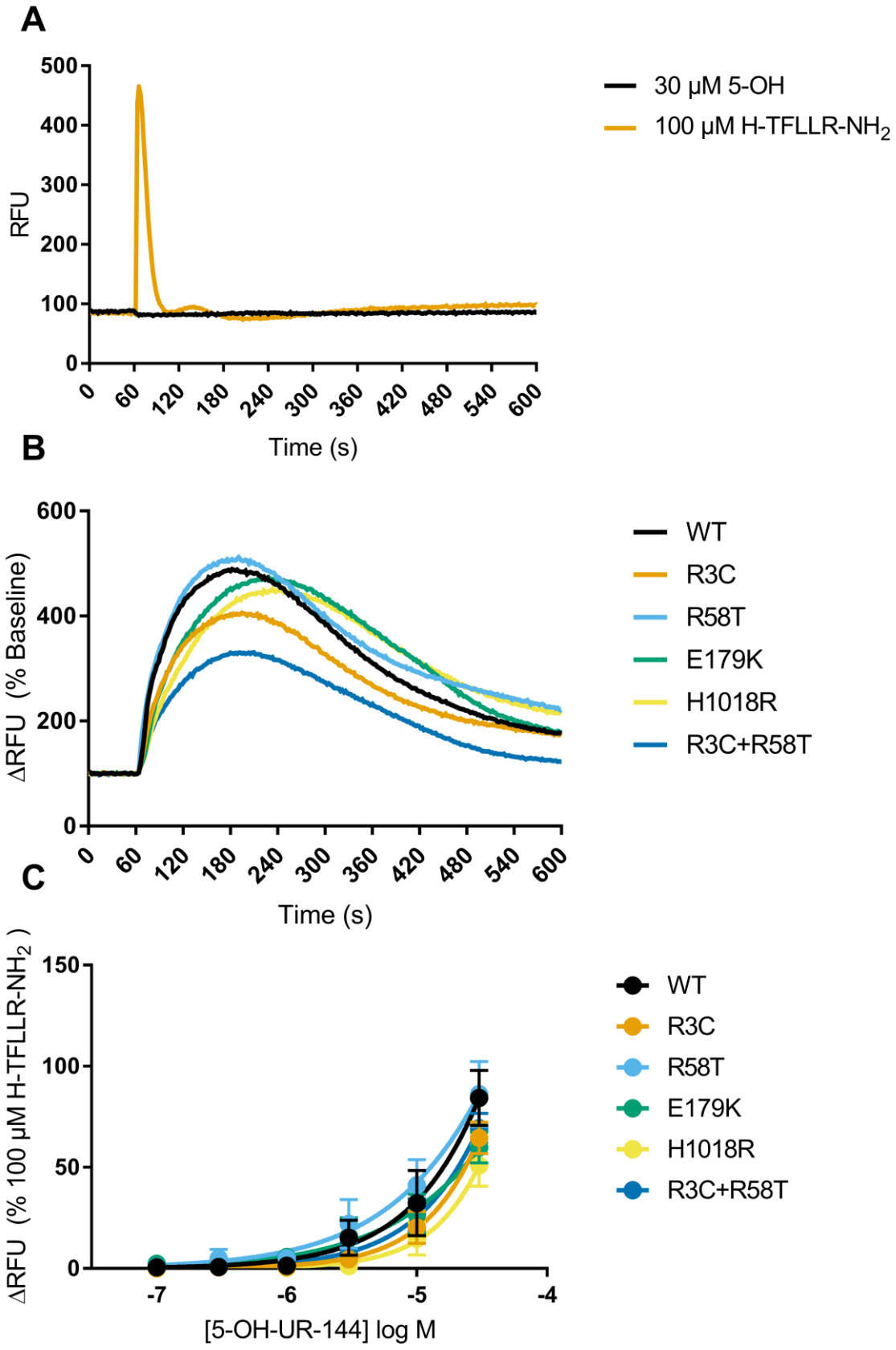

Figure 5:10 – Activation of hTRPA1 variants by the 5-hydroxypentyl metabolite of UR-144 and XLR-11: A – Raw trace data illustrating the response of HEK293 WT cells to 30 µM 5-OH and 100 µM H-TFLLR-NH_2. B – Baseline normalised trace data illustrating the response of hTRPA1 variants to 30 µM 5-OH. C – Concentration response relationship of 5-OH at hTRPA1 variants. Data represent the mean ± SEM of 5 independent determinations performed in duplicate.

5.2.10 5-OH Compared to Parent Compounds

The 5-hydroxypentyl metabolite of UR-144 and XLR-11 appeared to exhibit higher efficacy and potency in our assay (Figure 5:11). Comparing the 5-hydroxypentyl metabolite to the parent compound UR-144, there was a statistically significant increase in the effect at 30 µM at all hTRPA1 variants assayed (Table 5:18). The fold change ranged from 1.68 at the WT to 4.06 at R3C (Table 5:19). At 10 µM, there were statistically significant differences between the two compounds at R58T and E179K, representing 4.10 and 13.50-fold changes, respectively (Table 5:18, Table 5:19).

Table 5:18 – Statistics output comparing the effect of 5-OH to UR-144 at hTRPA1 variants: A two-way ANOVA with Tukey's test for multiple comparisons was conducted to test for statistically significant differences between the effect of 5-OH compared to its parent compound at each hTRPA1 variant.

5-OH vs. UR-144	Effect at 30 µM		Effect at 10 µM	
	q (df = 72)	p	q (df = 72)	p
WT	4.346	0.0083	1.464	0.5571
R3C	6.058	0.0002	2.262	0.2524
R58T	7.37	<0.0001	4.467	0.0065
E179K	5.388	0.0008	3.583	0.0355
H1018R	4.68	0.0041	1.87	0.3875
R3C+R58T	5.313	0.001	2.46	0.1977

Table 5:19 –Effect at 30 µM and 10 µM of UR-144 and its 5-hydroxypentyl metabolite at hTRPA1 variants: Effect at 30 µM and 10 µM was calculated individually for each replicate and pooled together. Data represent the mean ± SEM of 5 independent determinations performed in duplicate. Fold change was calculated as 5-OH/UR-144 where statistically significant, as indicated by Tukey's test for multiple comparisons, ns = not significant.

TRPA1	Maximal Effect (% 100 µM H-TFLLR-NH_2)			Effect at 10 µM (% 100 µM H-TFLLR-NH_2)		
	UR-144	5-OH	Fold Change	UR-144	5-OH	Fold Change
WT	50 ± 10	84 ± 14	1.68	22 ± 7	32 ± 16	ns
R3C	16 ± 5	65 ± 8	4.06	4 ± 3	20 ± 8	ns
R58T	28 ± 6	86 ± 16	3.07	10 ± 5	41 ± 13	4.10
E179K	17 ± 4	60 ± 8	3.53	2 ± 0.6	27 ± 10	13.50
H1018R	14 ± 4	51 ± 10	3.64	1 ± 0.4	15 ± 8	ns
R3C+R58T	27 ± 4	69 ± 7	2.56	9 ± 3	27 ± 8	ns

Comparing the 5-hydroxypentyl metabolite to its parent compound, XLR-11, there was a statistically significant increase in maximal effect at R58T, representing a 1.54-fold change (Table 5:20, Table 5:21). There was no statistically significant difference between the two compounds at a concentration of 10 µM at any of the hTRPA1 variants (Table 5:20).

Table 5:20 – Statistics output comparing the effect of 5-OH to XLR-11 at hTRPA1 variants: A two-way ANOVA with Tukey's test for multiple comparisons was conducted to test for statistically significant differences between the effect of 5-OH compared to its parent compound at each hTRPA1 variant.

5-OH vs. XLR-11	Effect at 30 µM		Effect at 10 µM	
	q (df = 72)	p	q (df = 72)	p
WT	2.196	0.2728	2.262	0.2524
R3C	2.538	0.1787	1.551	0.5193
R58T	3.837	0.0224	0.6216	0.8991
E179K	1.067	0.732	1.517	0.534
H1018R	0.1397	0.9946	2.612	0.1619
R3C+R58T	3.25	0.0625	0.4326	0.9498

Table 5:21 – Effect at 30 µM and 10 µM of XLR-11 and its 5-hydroxypentyl metabolite at hTRPA1 variants: Effect at 30 µM and 10 µM was calculated individually for each replicate and pooled together. Data represent the mean ± SEM of 5 independent determinations performed in duplicate. Fold change was calculated as 5-OH/UR-144 where statistically significant, as indicated by Tukey's test for multiple comparisons, ns = not significant.

TRPA1	Effect at 30 µM (% 100 µM H-TFLLR-NH_2)			Effect at 10 µM (% 100 µM H-TFLLR-NH_2)		
	XLR-11	5-OH	Fold Change	XLR-11	5-OH	Fold Change
WT	67 ± 10	84 ± 14	ns	48 ± 6	32 ± 16	ns
R3C	44 ± 3	65 ± 8	ns	31 ± 4	20 ± 8	ns
R58T	56 ± 5	86 ± 16	1.54	37 ± 3	41 ± 13	ns
E179K	51 ± 4	60 ± 8	ns	38 ± 3	27 ± 10	ns
H1018R	52 ± 6	51 ± 10	ns	33 ± 4	15 ± 8	ns
R3C+R58T	44 ± 3	69 ± 7	ns	30 ± 2	27 ± 8	ns

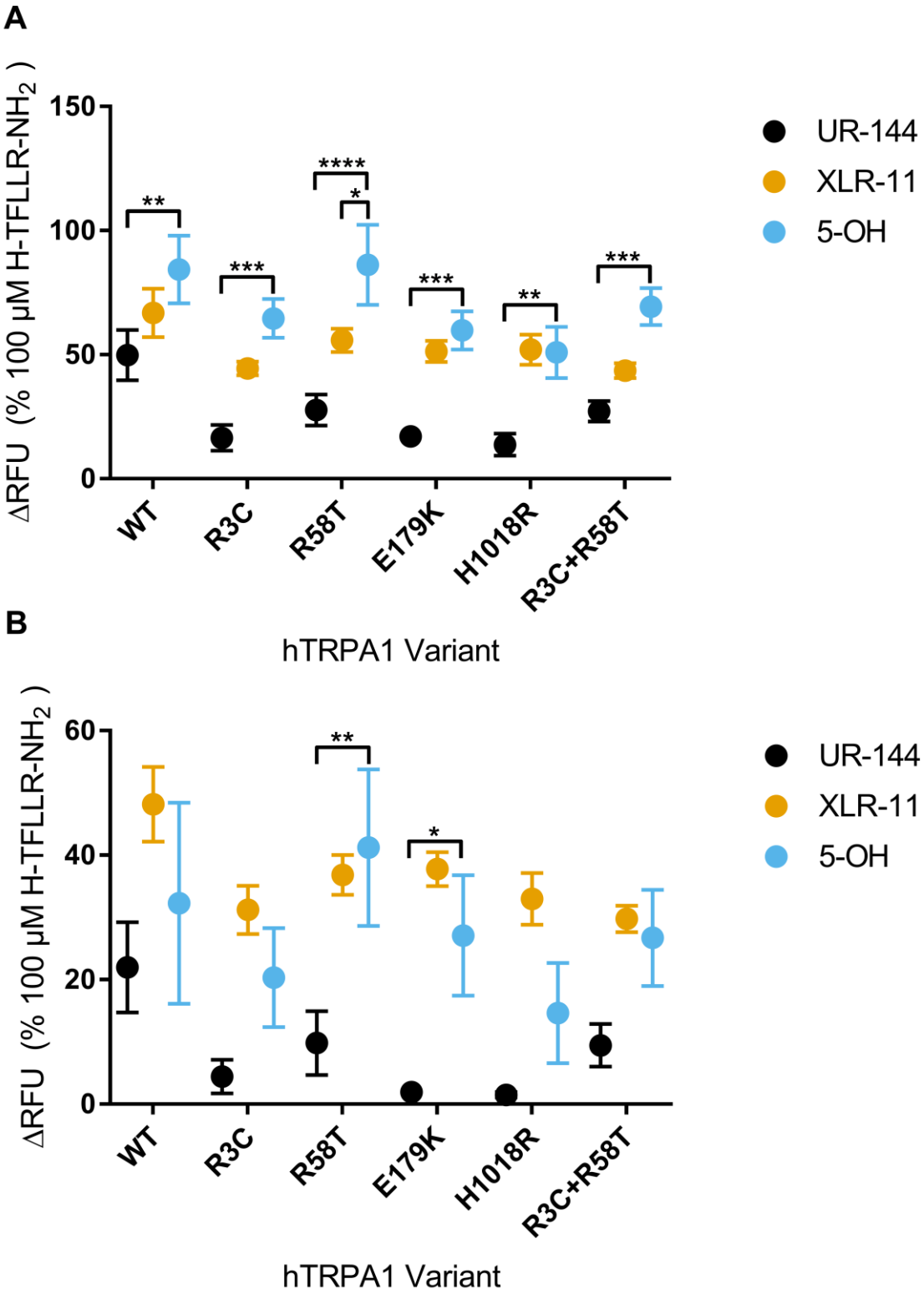

Figure 5:11 – Effect of UR-144, XLR-11 and the common 5-hydroxypentyl metabolite on hTRPA1 variants: A – The effect of UR-144, XLR-11 and the common 5-hydroxypentyl metabolite at 30 µM at hTRPA1 variants. B – The effect of UR-144, XLR-11 and the common 5-hydroxypentyl metabolite at 10 µM at hTRPA1 variants. Data represent the mean ± SEM of 5 independent determinations performed in duplicate. Asterisks indicate significance at the $p < 0.05$ level.

5.2.11 THC Compared to Synthetic Cannabinoids

At a concentration of 30 µM, THC exhibited greater activity at hTRPA1 variants when compared to all other synthetic cannabinoids tested (Table 5:22). At the WT, THC exhibited 1.5 to 3.6-fold greater activity than the synthetic compounds. At the WT, THC ≈ 5-OH > MDMB-CHMICA > XLR-11 > UR-144 > 5F-PB-22 > PB-22. At R3C, THC exhibited 2 to 4-fold greater activity than the synthetic compounds. For R3C, THC ≈ MDMB-CHMICA, 5F-PB-22, XLR-11, 5-OH > PB-22 > UR-144. At R58T, THC exhibited 2 to 3-fold greater activity than the synthetic compounds. For R58T, THC ≈ MDMB-CHMICA, 5F-PB-22, XLR-11, 5-OH > PB-22 > UR-144. At E179K, THC exhibited 2 to 4-fold greater activity than the synthetic compounds. For E179K, THC ≈ MDMB-CHMICA, XLR-11, 5-OH > 5F-PB-22, PB-22, UR-144. At H1018R, THC exhibited 2 to 5-fold greater activity than the synthetic compounds. For H1018R, THC ≈ MDMB-CHMICA, XLR-11, 5-OH > 5F-PB-22 > PB-22 > UR-144. At R3C+R58T, THC exhibited 2 to 5-fold greater activity than the synthetic compounds. For R3C+R58T, THC ≈ MDMB-CHMICA, 5-OH > XLR-11 > 5F-PB-22 > UR-144 > PB-22.

At a concentration of 10 µM, THC exhibited 3 to 11-fold greater activity than the synthetic compounds at the WT (Table 5:23). For the WT, THC ≈ MDMB-CHMICA, XLR-11, 5-OH > UR-144 > 5F-PB-22 > PB-22. There was no significant difference between THC and the synthetic compounds at R3C. At R58T, THC exhibited 4.7-fold greater activity than UR-144. AT E179K, THC exhibited less than half the activity of MDMB-CHMICA. There was no significant difference between THC and the synthetic compounds at H1018R. At R3C+R58T, THC exhibited 9 to 26-fold greater activity than the synthetic compounds. For R3C+R58T, THC ≈ MDMB-CHMICA, XLR-11, 5-OH > 5F-PB-22 > PB-22 > UR-144.

Table 5:22 – Effect of 30 µM THC compared to 30 µM synthetic cannabinoids at hTRPA1 variants: Effect at a drug concentration of 30 µM was calculated individually for each replicate and pooled together. Data represent the mean ± SEM of 5 independent determinations performed in duplicate. Fold change was calculated as THC/synthetic where statistically significant, indicated by Bonferroni's multiple comparisons test.

Comparison	Mean of Difference (% 100 µM H-TFLLR-NH_2)	Fold Change	t (df = 168)	p
WT				
THC vs. MDMB-CHMICA	33 ± 11	1.48	3.008	0.0182
THC vs. PB-22	73 ± 11	3.59	6.674	<0.0001
THC vs. 5F-PB-22	69 ± 11	3.13	6.299	<0.0001
THC vs. UR-144	52 ± 11	2.04	4.707	<0.0001
THC vs. XLR-11	35 ± 11	1.52	3.149	0.0117
THC vs. 5-OH	17 ± 11	ns	1.558	0.7273
R3C				
THC vs. MDMB-CHMICA	2 ± 11	ns	0.1745	>0.9999
THC vs. PB-22	32 ± 11	2.07	2.913	0.0244
THC vs. 5F-PB-22	27 ± 11	ns	2.485	0.0837
THC vs. UR-144	45 ± 11	3.74	4.127	0.0003
THC vs. XLR-11	17 ± 11	ns	1.577	0.7002
THC vs. 5-OH	-3 ± 11	ns	0.2616	>0.9999
R58T				
THC vs. MDMB-CHMICA	22 ± 11	ns	2.003	0.2806
THC vs. PB-22	39 ± 11	1.91	3.554	0.003
THC vs. 5F-PB-22	27 ± 11	ns	2.449	0.0921
THC vs. UR-144	54 ± 11	2.95	4.931	<0.0001
THC vs. XLR-11	26 ± 11	ns	2.371	0.1133
THC vs. 5-OH	-4 ± 11	ns	0.4089	>0.9999
E179K				
THC vs. MDMB-CHMICA	-13 ± 11	ns	1.19	>0.9999
THC vs. PB-22	31 ± 11	2.08	2.862	0.0285
THC vs. 5F-PB-22	30 ± 11	1.99	2.737	0.0412
THC vs. UR-144	43 ± 11	3.55	3.95	0.0007
THC vs. XLR-11	9 ± 11	ns	0.8189	>0.9999
THC vs. 5-OH	1 ± 11	ns	0.04609	>0.9999
H1018R				
THC vs. MDMB-CHMICA	13 ± 11	ns	1.192	>0.9999
THC vs. PB-22	44 ± 11	2.39	3.98	0.0006
THC vs. 5F-PB-22	30 ± 11	1.68	2.765	0.0379
THC vs. UR-144	61 ± 11	5.46	5.594	<0.0001
THC vs. XLR-11	23 ± 11	ns	2.102	0.2222
THC vs. 5-OH	24 ± 11	ns	2.203	0.1735
R3C+R58T				
THC vs. MDMB-CHMICA	27 ± 11	ns	2.441	0.0942
THC vs. PB-22	62 ± 11	4.60	5.66	<0.0001
THC vs. 5F-PB-22	51 ± 11	2.85	4.699	<0.0001
THC vs. UR-144	52 ± 11	3.75	4.754	<0.0001
THC vs. XLR-11	36 ± 11	1.82	3.259	0.0081
THC vs. 5-OH	10 ± 11	ns	0.9043	>0.9999

Table 5:23 – The effect of 10 µM THC compared to 10 µM synthetic cannabinoids at hTRPA1 variants: Effect at a drug concentration of 10 µM was calculated individually for reach replicate and pooled together. Data represent the mean ± SEM of 5 independent determinations performed in duplicate. Fold change was calculated as THC/synthetic where statistically significant, as indicated by Bonferroni's multiple comparisons test.

Comparison	Mean of Difference (% 100 µM H-TFLLR-NH_2)	Fold Change	t (df = 168)	p
WT				
THC vs. MDMB-CHMICA	2 ± 9	ns	0.2481	>0.9999
THC vs. PB-22	51 ± 9	10.97	5.471	<0.0001
THC vs. 5F-PB-22	37 ± 9	2.96	3.985	0.0006
THC vs. UR-144	34 ± 9	2.57	3.673	0.0019
THC vs. XLR-11	8 ± 9	ns	0.8779	>0.9999
THC vs. 5-OH	24 ± 9	ns	2.575	0.0654
R3C				
THC vs. MDMB-CHMICA	-18 ± 9	ns	1.879	0.3719
THC vs. PB-22	16 ± 9	ns	1.743	0.4989
THC vs. 5F-PB-22	7 ± 9	ns	0.7757	>0.9999
THC vs. UR-144	23 ± 9	ns	2.455	0.0907
THC vs. XLR-11	-4 ± 9	ns	0.4051	>0.9999
THC vs. 5-OH	7 ± 9	ns	0.7582	>0.9999
R58T				
THC vs. MDMB-CHMICA	2 ± 9	ns	0.1969	>0.9999
THC vs. PB-22	23 ± 9	ns	2.463	0.0888
THC vs. 5F-PB-22	10 ± 9	ns	1.042	>0.9999
THC vs. UR-144	36 ± 9	4.66	3.839	0.0011
THC vs. XLR-11	9 ± 9	ns	0.9539	>0.9999
THC vs. 5-OH	5 ± 9	ns	0.4877	>0.9999
E179K				
THC vs. MDMB-CHMICA	-31 ± 9	0.46	3.309	0.0069
THC vs. PB-22	16 ± 9	ns	1.726	0.5168
THC vs. 5F-PB-22	12 ± 9	ns	1.233	>0.9999
THC vs. UR-144	24 ± 9	ns	2.589	0.0628
THC vs. XLR-11	-12 ± 9	ns	1.237	>0.9999
THC vs. 5-OH	-1 ± 9	ns	0.09877	>0.9999
H1018R				
THC vs. MDMB-CHMICA	-24 ± 9	ns	2.516	0.0768
THC vs. PB-22	12 ± 9	ns	1.302	>0.9999
THC vs. 5F-PB-22	2 ± 9	ns	0.2349	>0.9999
THC vs. UR-144	22 ± 9	ns	2.355	0.1179
THC vs. XLR-11	-9 ± 9	ns	1.006	>0.9999
THC vs. 5-OH	9 ± 9	ns	0.9526	>0.9999
R3C+R58T				
THC vs. MDMB-CHMICA	-1 ± 9	ns	0.06582	>0.9999
THC vs. PB-22	34 ± 9	8.56	3.656	0.0021
THC vs. 5F-PB-22	26 ± 9	3.05	2.781	0.0362
THC vs. UR-144	29 ± 9	26.03	3.133	0.0122
THC vs. XLR-11	9 ± 9	ns	0.9636	>0.9999
THC vs. 5-OH	12 ± 9	ns	1.288	>0.9999

6 DISCUSSION

The principle finding of this study is that recently identified, high concern synthetic cannabinoids, function as agonists of hTRPA1, and that these agonist responses differ at polymorphic variants of hTRPA1. All synthetic cannabinoid compounds tested in this study activated hTRPA1 variants. Our data is consistent with previous work from our lab illustrating hTRPA1 activation by PB-22, UR-144, XLR-11 and 5-OH [230]. However, the previous study found that 5F-PB-22 exhibited no activity at hTRPA1. Our data demonstrates a robust, concentration dependant Ca_i elevation upon addition of 5F-PB-22. We do not have a simple explanation for this, however, we used a different HEK293 TRPA1 clone to the previous work, used buffer with a lower concentration of potassium, induced TRPA1 expression using a higher concentration of tetracycline (4 $\mu g.mL^{-1}$ opposed to 2 $\mu g.mL^{-1}$) and used different FBS for cell culture. This is the first study to demonstrate the activation of hTRPA1 by the synthetic cannabinoid MDMB-CHMICA, and indicates that hTRPA1 activity is preserved in more recent synthetic cannabinoid compounds. For each interaction observed, we can be confident that recorded effects are dependent on the expression of hTRPA1, as none of the synthetic cannabinoid compounds produced a measurable increase in Ca_i in untransfected HEK293 WT cells. Additionally, we can be reasonably certain that the differences in agonist response across hTRPA1 variants were not due to differences in protein expression. The 293 Flp-In™ T-REx™ expression system ensures that a single copy of the gene of interest is integrated in to the same position for each cell line.

Whether or not variations in hTRPA1 affected channel activation by synthetic cannabinoids differed between compounds, as did the magnitude of the difference. For MDMB-CHMICA, the variation between activity at all hTRPA1 variants at any given concentration was less than 30%. No hTRPA1 variant exhibited activity significantly different from the WT when treated with MDMB-CHMICA, at any given concentration. The activity of PB-22 at hTRPA1 was

largely unaffected by channel variants, save for R58T. At [PB-22] of 30μM, R58T resulted in a 1.56-fold increase in channel activity compared to the WT. This increase was more profound at [PB-22] of 10 μM, where the fold change over WT was 5.6. 5F-PB-22, structurally identical to PB-22 save for a terminal fluorine on the pentyl chain, was affected by hTRPA1 variations in a manner similar to PB-22. At [5F-PB-22] of 30 μM, R58T resulted in 1.72-fold increased activity over WT. However, unlike PB-22, hTRPA1 activity in the presence of 10 μM 5F-PB-22 was unaffected by all channel variants tested.

The activity of UR-144 and XLR-11 were affected by variations in hTRPA1, however, in a manner unlike PB-22 and 5F-PB-22. At [UR-144] of 30 μM, R3C, E179K and H1018R all significantly affected activity compared to the WT. Unlike PB-22 and 5F-PB-22 however, the hTRPA1 variants exhibited 0.28 to 0.34-fold less activity than the WT. At [UR-144] of 10 μM, activity at E179K and H1018R is almost abolished compared to the WT. XLR-11, structurally identical to UR-144 save for a terminal fluorine on the pentyl chain, was affected by hTRPA1 variants in a manner unlike UR-144. At [XLR-11] of 30 μM, there was no significant difference between activity at any hTRPA1 variant compared to the WT. At [XLR-11] of 10 μM, R3C and R3C+R58T exhibited 0.77 and 0.63-fold changes, respectively. The common 5-hydoxypentyl metabolite was not affected by variations in hTRPA1 at any given concentration.

Synthetic cannabinoid compounds featuring bioisoteric fluorine substitution have become increasingly popular in recent years, with evidence suggesting these compounds are more potent than their non-fluorinated parents [98, 246]. In the present study, we have investigated two pairs of terminally fluorinated synthetic cannabinoids and their terminally methylated parents; PB-22/5F-PB-22 and UR-144/XLR-11. Terminal fluorination of PB-22 has been shown to increase potency by approximately 2-fold at $CB_{1,}$ but also decrease CB_1 selectivity [98]. At all hTRPA1 variants studied, there was no significant difference between the activity of PB-22 and 5F-PB-22. Terminal fluorination of UR-144 (yielding XLR-11) has been shown

to increase potency approximately 4-fold at CB_1 [98]. This is reflected in our experiments in hTRPA1 variants. At a concentration of 30 µM, XLR-11 exhibited 3 to 4-fold greater activity relative to UR-144, at all hTRPA1 variants other than the WT and R3C+R58T. At a concentration of 10 µM, XLR-11 was more potent at all hTRPA1 variants relative to UR-144, with fold changes from 2 at the WT to 33 at H1018R. While only two bioisoteric fluorine pairs were examined in the present study, these data suggest the structure activity relationships of synthetic cannabinoids at the CB receptors do not necessarily reflect those at hTRPA1.

The metabolites of synthetic cannabinoid compounds have been reported to have a variety of effects at the CB receptors. Monohydroxylated metabolites of the compound JWH-018 retain CB_1 receptor activity, equal to that of the parent compound [247]. These metabolites also retain the parent compounds activity at the CB_2 receptor [248]. Glucuronidated metabolites of JWH-018 have been reported to act as neutral antagonists of the CB_1 receptor [249]. The 5-OH metabolite common to UR-144 and XLR-11 retains CB_1 receptor activity, but is significantly less potent than both of its parent compounds and exhibits a significant shift in CB_2 preference [98]. This is in agreement with recent studies published on 5-OH metabolites of other synthetic cannabinoids [250]. At hTRPA1, the 5-OH metabolite retained the activity of its parent compounds. This activity was not affected at any given concentration by hTRPA1 polymorphisms. Contrary to the effect at CB_1 however, 5-OH was a more potent agonist than both parent compounds. At a concentration of 30 µM, 5-OH was 2 to 4-fold more potent, relative to UR-144, at all hTRPA1 variants. At 10 µM, 5-OH was 4 and 14-fold more potent at R58T and E179K, respectively. Compared to XLR-11, 5-OH exhibited 1.5-fold greater activity at R58T, at a concentration of R58T. These data suggest that drug metabolism may increase activity at hTRPA1 over the parent compounds, and are not congruent with the effect at the CB receptors. This may contribute to the overall physiological profile of synthetic cannabinoids.

WT hTRPA1 and all variants were activated by THC, which is in agreement with previous studies [104, 112]. At a concentration of 30 µM, the activity of THC was not affected by hTRPA1 polymorphisms. At R3C and R58T, THC activity at a concentration of 10 µM was half that of the WT. While synthetic cannabinoids exhibit higher efficacy and potency than THC at the CB receptors, the opposite appears true at hTRPA1 [96-99, 250]. The effects of the THC were either equal to or greater than the synthetic compounds at hTRPA1. In our assay, THC (30 µM) exhibited 1.5 to 5 fold greater activity at some hTRPA1 variants when compared to MDMB-CHMICA, PB-22, 5F-PB-22, UR-144 and XLR-11. THC and 5-OH appeared to have similar activity across all hTRPA1 variants at 30 µM. There were fewer differences at [THC] of 10 µM, however, the differences are of greater magnitude. THC exhibited 9 to 11-fold greater activity than PB-22 and 3 to 9-fold greater activity than 5F-PB-22 at the WT and R3C+R58T. Compared to UR-144, THC exhibited 3 to 26 fold greater activity at some hTRPA1 mutants. Interestingly, at E179K, THC exhibited half the activity of MDMB-CHMICA. These data suggest that possible TRPA1 mediated toxic effects of synthetic cannabinoids are not the result of increased activity at the receptor when compared to THC.

While THC appears more potent than the synthetic cannabinoids in our assays, it is unclear at what concentration these drugs are when they reach their physiological targets, and where they distribute throughout the body. The contribution of other potential targets, such as TRPV1, is also unclear. Synthetic cannabinoids are sprayed on to supposedly inert plant material for consumption, however, it is possible that the plant material contains aromatic agonists of TRPA1. Commonly used herb material includes members of the Damiana and Lamiaceae family [251]. Particularly interesting are the members of the Lamiaceae family, which includes the thymol producing genera thymus [252-255]. Thymol is a known activator of hTRPA1, with the possibility for an additive or synergistic effect when combined with sprayed-on synthetic cannabinoid material [256]. This theory could be examined in future by

pre-incubating a population of hTRPA1 expressing HEK293 cells with thymol, before addition of a synthetic cannabinoid. Considering the wide range of plant derived, aromatic compounds with which TRPA1 interacts with, it is reasonable to imagine the possibility of other interactions occurring at TRPA1 between synthetic cannabinoids and aromatic compounds.

The expression of TRPA1 in the lungs affords many opportunities for it to come in to contact with inhaled synthetic cannabinoid products. The inhalation of noxious and toxic substances can cause the release of proinflammatory peptides, decrease respiration rates and cause coughing and bronchoconstriction in a TRPA1 mediated fashion, a property which is exploited by tear gas agents [220, 257-260]. In a number of reported cases of acute synthetic cannabinoid intoxication, measurable quantities of the drug have been found in the blood hours and days after first exposure [62, 65, 66, 76-79, 81, 82, 87, 92, 94]. TRPA1 is expressed in the vasculature and in nerve fibres that enervate the heart, where it mediates vasodilation, changes in blood pressure and local blood flow [209, 211]. Considering many adverse reactions to synthetic cannabinoid exposure include some form of respiratory or cardiovascular distress, it is reasonable to believe these affects may be, in part, mediated by TRPA1 activation [71, 73, 76-78, 91]. It is worth noting the presence of TRPA1 in the CNS; while its functions are as yet unclear, the interaction between SCRA's at TRPA1 in the CNS cannot be discounted [261, 262].

In our assay, there was no difference in hTRPA1 activity between channel variants when treated with the prototypic, electrophilic agonists cinnamaldehyde and AITC. These data are in contrast with a study published in 2015. TRPA1 activity and the effect of channel polymorphisms was examined using three different agonists; AITC, a prototypic, electrophilic agonist; 3,5-ditert butylphenol (DTBP), a non-electrophilic agonist and coal fly ash (CFA) particles, an insoluble product of combustion [110]. Data published on R3C and R58T suggest that these two mutants increase sensitivity to AITC (150 μM), DTBP (250 μM) and

CFA (2.3mg.mL^{-1}) by 170% and 200%, respectively, when compared to WT [110]. The double mutant of R3C/R58T shows a 20% increase in sensitivity to all three agonists. E179K exhibits a small change in response to CFA, but a negligible change to both AITC and DTBP [110]. H1018R results in a 70% increased response to CFA, but negligible changes to AITC and DTBP [110]. We were not able to observe any appreciable shift in activation by AITC at R3C or R58T, and did not investigate DTBP or CFA. However, our results do agree with the findings at H1018R and E179K. The reason for these differences in the conclusions may be due to the methodology of the two studies. Namely, our study performed at physiological body temperature (37°C), whereas the Deering-Rice et. al. 2015 study is performed at room temperature, at which the channel is more readily activated, consistent with one of its roles as a noxious cold sensor [110, 263]{Laursen, 2014 #23}. The Deering-Rice study also uses a single [AITC] of 150 µM for measuring calcium influx, rather than generating concentration response curves. It is interesting to note the effects of hTRPA1 variants on synthetic cannabinoid activation are not congruent with the effects, or lack thereof, on electrophilic agonists. This supports the notion that TRPA1 has at least one other binding site at which non-electrophilic agonists can act and that synthetic cannabinoid activation occurs independently of the cysteine rich linker region [202, 230, 235, 264]. Non-electrophilic agonists of TRPA1, such as menthol and DTBP, are known to interact with S873 and T874 residues on the 5th transmembrane domain [110, 265]. Our data cannot suggest whether or not synthetic cannabinoids interact with these residues, however, future experiments could investigate this using S873 and T874 mutants.

Carvacrol, the non-electrophilic agonist chosen in this study, activated hTRPA1 with a profile similar to that of an electrophilic agonist. Unlike DTBP, there was no significant effect of the R3C, R58T or E179K mutations on activity at hTRPA1 [110]. R3C+R58T increased sensitivity to DTBP by 20%, but decreased sensitivity to carvacrol in our assay [110]. Carvacrol has been shown to rapidly activate and then desensitise rat TRPA1 in HEK293

cells, and it has been reported that it does not elevate Ca_i in WT HEK293 cells [266]. In our assay, carvacrol produced a prolonged response in HEK293 cells expressing hTRPA1, with little desensitisation. However, carvacrol unexpectedly elicited large increases in Ca_i in WT HEK293 cells in our assay. The response in WT HEK293 cells was unlike the response in HEK293 TRPA1 cells. The response was not as prolonged, rather displaying a sharp increase and rapid desensitisation in a fashion similar to a GPCR like PAR-1. While it is unlikely carvacrol was acting at PAR-1, this could be examined via addition of H-TFLLR-NH_2 and carvacrol to the same population of cells, back to back in the same assay. Carvacrol has been shown to activate hTRPV3, as well as activate peroxisome proliferator-activated receptors (PPAR) α/γ and supress cyclooxygenase-2 (COX-2) expression [266, 267]. These interactions are, however, unlikely to be the cause of the observed response in HEK293 WT cells. A specific GPCR for carvacrol may exist, as a eugenol sensitive, mouse G protein-coupled olfactory receptor has been shown to interact with a number of aromatic compounds that share the simple benzene ring structure of carvacrol [268]. While HEK293 cells express a large number of endogenous GPCR's, none are olfactory in nature, and the binding partner for carvacrol on HEK293 WT cells in our assay remains unknown [242]. However, the differences between the findings of our study and that of Xu et. al. 2006 further illustrate the well-recognised phenotypic differences between nominally similar cell lines grown in different laboratories.

The present study investigated the effect of probenecid on hTRPA1 in a no-wash calcium assay. Probenecid at a concentration of 1mM was used in a Fura-2 AM based study of TRPA1 and authors make no mention of any effect the probenecid had on their assay, negative or otherwise [269]. A later study investigated the influence of probenecid in Fluo-4 AM and Fura-2 AM based assays of TRPA1 [240]. The authors report a significant increase in the EC_{50} of TRPA1 agonists ATIC, cinnamaldehyde, N-methyl malemide (NMM) and menthol in experiments where 2mM probenecid was added to the dye during incubation [240].

Specifically, they report the EC_{50} of cinnamaldehyde on hTRPA1 expressed in Chinese Hamster Ovary (CHO) cells to be 26 µM without probenecid and 144 µM with probenecid [240]. They do note, however, that probenecid is crucial for dye loading with Fura-2 in CHO cells. With Fluo-4 and CHO cells, probenecid significantly increases the assay window [240]. Probenecid has a similar effect on both dyes in STC-1 cells [240]. Similar results were seen in a study investigating the regulation of TRPA1 and TRPM8 by SRC-tyrosine kinase inhibitor [111]. The authors found that concentrations of probenecid above 1mM and up to 2.5mM inhibited both TRPM8 and TRPA1 mediated responses using Fluo-3 dye [111]. Low concentrations of probenecid (0.13 mM) did not affect assay results, however, the authors opted to omit probenecid from further experiments, as it seemed to have no tangible benefit to the assay [111].

In our assay, we saw no effect of 2.5 mM probenecid on the EC_{50} of cinnamaldehyde, it was 32 ± 2 µM without probenecid and 31 ± 2 µM with probenecid. Additionally, probenecid was needed to increase the dynamic range of the assay, with the maximum response to cinnamaldehyde 3 fold greater in cells incubated with probenecid than without. The difference may be due to the probenecid used in each experiment. In the present study, a pre-weighed, water soluble, sodium salt of probenecid is used, which is readily dissolved in assay buffer and does not require any further buffering. The probenecid used in the previous studies is a form poorly soluble in water, instead requiring the use of chloroform or sodium hydroxide and then appropriate pH buffering.

In conclusion, the present study demonstrates the activation of hTRPA1 by synthetic cannabinoids, and illustrates that these effects differ at polymorphic variants of hTRPA1. These data illustrate that structure activity relationships established so far of synthetic cannabinoids at CB receptors are not congruent with TRPA1. Terminal fluorination leads to increased potency at both CB receptors and TRPA1. However, the 5-OH metabolite is known to have decreased potency at CB_1 than its parents, with the opposite being true for TRPA1.

THC has been shown to activate hTRPA1 to a greater degree than synthetic compounds, suggesting that potential TRPA1 mediated synthetic cannabinoid toxicity is not due to relative potency. The effects of hTRPA1 polymorphisms on synthetic cannabinoid agonist activity were not seen in prototypic, electrophilic agonists, perhaps due to the difference in binding sites. The interaction between non-CB mediated interactions, channel polymorphisms and drug metabolism renders the issue of synthetic cannabinoid toxicity multi-faceted and highly individualised.

APPENDIX A – GENE PRODUCTS, MATERIALS AND REAGENTS

i. List of Materials and Reagents

Product	Company and Product Number
T75 Flasks	Corning, Inc., Corning, NY, USA – Cat No. 13-680-65, Manufacturer No. 353136
DMEM - High Glucose	Sigma-Aldrich Pty. Ltd., Castle Hill, NSW, Australia – Cat No. D6429
L-15	Life Technologies Australia Pty. Ltd., Scoresby, VIC, Australia – Cat. No. 11415064
Trypsin/EDTA	Sigma-Aldrich Pty. Ltd., Castle Hill, NSW, Australia – Cat No. T3924
FBS	SAFC Biosciences Pty. Ltd., Brooklyn, VIC, Australia – Cat. No. 12003C
PenStrep	Life Technologies Australia Pty. Ltd., Scoresby, VIC, Australia – Cat. No. 15140122
PBS	Life Technologies Australia Pty. Ltd., Scoresby, VIC, Australia – Cat. No. 20012027
HEK 293 Flp-In T-Rex	Life Technologies Australia Pty. Ltd., Scoresby, VIC, Australia – Cat. No. R78007
Blasticidin	InvivoGen, San Diego, California, USA – Cat. No. ant-bl
Zeocin	InvivoGen, San Diego, California, USA – Cat. No. ant-zn
Hygromycin B Gold	InvivoGen, San Diego, California, USA – Cat. No. ant-hg-1
FLIPR Calcium 5 Assay Kit	Molecular Devices, Sunnyvale, CA, USA – Cat. No. R8185
Probenecid	Biotium, Inc., Hayward, CA, USA – Cat. No. 50027
PAR-1 Agonist	Auspep Pty. Ltd., Tullamarine, VIC, Australia – Cat. No. 2660
Cinnamaldehyde	Sigma-Aldrich Pty. Ltd., Castle Hill, NSW, Australia – Cat. No. W228613
FuGENE HD	Promega Corporation, Madison, WI, USA – Cat. No. E231
pOG44	Life Technologies Australia Pty. Ltd., Scoresby, VIC, Australia – Cat. No. V600520
DMSO - General Use	Sigma-Aldrich Pty. Ltd., Castle Hill, NSW, Australia – Cat. No. D8418
BSA - Lyophilized Powder	Sigma-Aldrich Pty. Ltd., Castle Hill, NSW, Australia – Cat. No. A7030
V-bottomed Drug Plate	Greiner Bio-One GmbH, Frickenhausen, Germany – Cat. No. M2686, Manufacturer No. 651101
DMSO - Freezing Media	Sigma-Aldrich Pty. Ltd., Castle Hill, NSW, Australia – Cat. No. D2650
Carvacrol	Toronto Research Chemicals, Toronto, ON, Canada – Cat. No. C184600
AITC	Sigma-Aldrich Pty. Ltd., Castle Hill, NSW, Australia – Cat. No. 377430
GraphPad Prism	GraphPad Software, La Jolla, CA, USA, www.graphpad.com
Softmax Pro v5.4	Molecular Devices, Sunnyvale, CA, USA

ii. Map of the pcDNA™5/FRT/TO vector, found in the pcDNA™5/FRT/TO user manual (Invitrogen Corporation, Carlsbad, CA, USA)

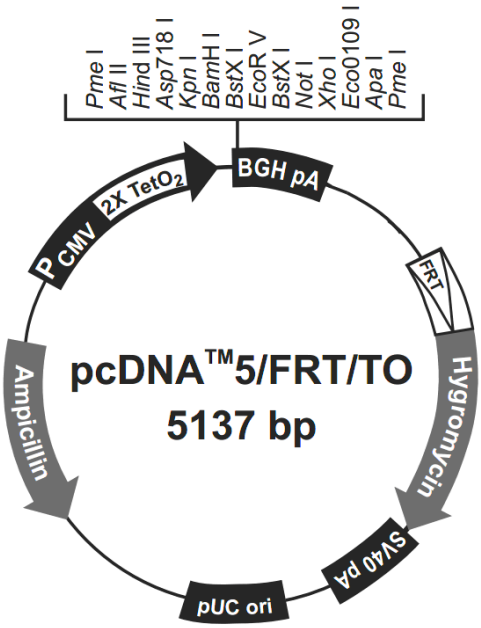

iii. Mutant hTRPA1 construct sequence information, provided by GenScript

>Mutant: R3C Cloning Site: KpnI – NotI
GGTACCGCCACCATGAAATGCAGCCTGCGAAAAATGTGGCGGCCCGGCGAAAAGAAGGA
ACCTCAGGGGGTCGTGTATGAAGATGTGCCAGATGATACTGAGGACTTTAAAGAATCACT
GAAGGTGGTCTTCGAGGGCTCCGCTTACGGACTGCAGAACTTCAACAAGCAGAAGAAAC
TGAAGCGATGCGACGATATGGATACCTTCTTTCTGCACTATGCCGCTGCAGAGGGCCAGA
TCGAGCTGATGGAAAAGATTACTCGGGACTCCAGCCTGGAGGTGCTGCACGAAATGGAC
GATTACGGAAACACCCCTCTGCATTGTGCAGTGGAGAAAAATCAGATCGAAAGCGTCAA
GTTTCTGCTGTCTCGAGGCGCCAACCCCAATCTGCGTAACTTCAATATGATGGCCCCTCTG
CACATTGCTGTGCAGGGAATGAACAATGAAGTGATGAAGGTCCTGCTGGAACATAGGAC
AATCGACGTGAATCTGGAGGGGGAAAACGGTAATACTGCAGTCATCATTGCCTGCACCAC
AAACAATTCTGAGGCTCTGCAGATTCTGCTGAAGAAAGGCGCAAAGCCATGCAAAAGTA
ACAAGTGGGGATGTTTTCCCATCCACCAGGCCGCTTTCAGTGGCTCAAAGGAGTGTATGG
AAATCATTCTGAGGTTTGGGGAGGAACACGGTTACTCTCGGCAGCTGCATATCAACTTCA
TGAACAATGGGAAGGCCACTCCACTGCACCTGGCTGTGCAGAACGGCGACCTGGAGATG
ATCAAAATGTGCCTGGACAATGGCGCCCAGATTGATCCCGTGGAAAAGGGACGGTGTAC
CGCCATTCATTTTGCAGCCACCCAGGGAGCTACAGAGATCGTGAAGCTGATGATTTCTAG
TTACTCCGGGAGCGTGGACATCGTCAATACTACCGATGGTTGCCACGAGACCATGCTGCA
TAGAGCTTCTCTGTTCGACCACCATGAACTGGCAGATTATCTGATCAGTGTGGGCGCCGA
CATCAACAAGATTGATTCTGAGGGACGCAGTCCACTGATCCTGGCTACAGCATCTGCCAG
TTGGAACATTGTGAATCTGCTGCTGAGCAAAGGGGCCCAGGTCGACATTAAGGATAACTT
TGGTCGAAATTTCCTGCACCTGACTGTGCAGCAGCCATACGGGCTGAAAAATCTGCGTCC
CGAGTTTATGCAGATGCAGCAGATCAAGGAGCTGGTCATGGATGAAGACAACGATGGTT
GCACCCCTCTGCATTATGCTTGTAGGCAGGGCGGACCAGGCAGCGTGAACAATCTGCTGG
GCTTCAACGTGTCCATCCACTCAAAGTCCAAAGACAAGAAATCTCCTCTGCATTTCGCTG
CAAGTTACGGGAGAATCAACACTTGCCAGCGCCTGCTGCAGGACATTTCTGATACCCGGC
TGCTGAATGAGGGCGACCTGCACGGAATGACCCCACTGCATCTGGCCGCTAAAAACGGA

CACGATAAGGTGGTCCAGCTGCTGCTGAAGAAAGGGGCCCTGTTCCTGTCCGACCATAAC
GGTTGGACAGCTCTGCACCATGCAAGCATGGGCGGCTATACTCAGACCATGAAAGTGATC
CTGGACACTAACCTGAAGTGTACCGATAGGCTGGACGAGGATGGCAATACTGCTCTGCAC
TTTGCAGCCCGGGAAGGACATGCTAAGGCAGTGGCCCTGCTGCTGTCACACAACGCCGAT
ATCGTCCTGAATAAGCAGCAGGCATCCTTCCTGCACCTGGCCCTGCATAATAAGAGAAAA
GAGGTGGTCCTGACAATCATTAGGTCCAAACGGTGGGACGAATGCCTGAAGATCTTTAGC
CACAACTCTCCTGGCAACAAGTGTCCAATCACCGAGATGATTGAATACCTGCCAGAGTGC
ATGAAGGTGCTGCTGGATTTCTGTATGCTGCATTCAACAGAGGACAAATCCTGCCGCGAT
TACTACATCGAATACAACTTCAAGTATCTGCAGTGTCCTCTGGAGTTCACCAAGAAAACA
CCAACTCAGGACGTGATCTACGAACCCCTGACAGCCCTGAACGCTATGGTCCAGAACAAT
CGAATCGAGCTGCTGAATCACCCCGTGTGCAAAGAATACCTGCTGATGAAGTGGCTGGCA
TATGGCTTTCGTGCCCATATGATGAATCTGGGCTCTTATTGTCTGGGACTGATCCCCATGA
CCATTCTGGTGGTCAACATTAAGCCTGGGATGGCTTTCAACAGCACCGGTATCATTAATG
AGACAAGTGACCACTCAGAAATCCTGGATACAACTAACTCTTACCTGATCAAGACATGCA
TGATTCTGGTGTTTCTGTCATCCATCTTCGGGTATTGTAAAGAGGCTGGTCAGATTTTTCA
GCAGAAGAGGAACTACTTCATGGATATCTCCAATGTGCTGGAGTGGATCATCTACACCAC
AGGGATCATTTTTGTGCTGCCCCTGTTCGTCGAAATCCCTGCCCATCTGCAGTGGCAGTGC
GGTGCTATTGCAGTGTACTTTTATTGGATGAACTTCCTGCTGTACCTGCAGAGGTTTGAGA
ATTGTGGCATCTTCATTGTGATGCTGGAAGTCATCCTGAAGACACTGCTGCGGAGTACTG
TGGTCTTCATTTTTCTGCTGCTGGCCTTTGGACTGTCATTCTATATCCTGCTGAATCTGCAG
GATCCCTTCTCCTCTCCCCTGCTGAGTATCATTCAGACATTCTCAATGATGCTGGGCGACA
TCAACTACAGAGAGAGCTTTCTGGAACCTTATCTGCGCAATGAGCTGGCCCACCCAGTGC
TGTCCTTCGCTCAGCTGGTCAGCTTTACTATCTTCGTGCCCATTGTCCTGATGAACCTGCT
GATCGGGCTGGCTGTGGGTGACATTGCAGAGGTCCAGAAACACGCTAGCCTGAAGAGAA
TCGCAATGCAGGTGGAGCTGCATACATCTCTGGAAAAGAAACTGCCTCTGTGGTTTCTGA
GAAAAGTGGATCAGAAGAGTACTATTGTCTACCCCAATAAGCCTCGCTCAGGCGGAATGC
TGTTCCATATCTTCTGCTTTCTGTTCTGTACCGGCGAGATCAGACAGGAAATTCCTAACGC
CGATAAGTCCCTGGAGATGGAAATTCTGAAGCAGAAATATCGCCTGAAAGACCTGACTTT
CCTGCTGGAGAAGCAGCACGAACTGATCAAACTGATCATTCAGAAGATGGAGATCATTA
GCGAGACCGAAGACGATGACTCCCATTGTAGCTTTCAGGACCGATTCAAGAAAGAGCAG
ATGGAACAGCGTAACTCCCGTTGGAATACCGTCCTGCGTGCCGTGAAAGCTAAGACCCAT
CATCTGGAACCATAAGCGGCCGC

>Mutant: R58T Cloning Site: KpnI – NotI
GGTACCGCCACCATGAAAAGAAGCCTGCGAAAAATGTGGCGGCCCGGCGAAAAGAAGG
AACCTCAGGGGGTCGTGTATGAAGATGTGCCAGATGATACTGAGGACTTTAAAGAATCAC
TGAAGGTGGTCTTCGAGGGCTCCGCTTACGGACTGCAGAACTTCAACAAGCAGAAGAAA
CTGAAGACCTGCGACGATATGGATACCTTCTTTCTGCACTATGCCGCTGCAGAGGGCCAG
ATCGAGCTGATGGAAAAGATTACTCGGGACTCCAGCCTGGAGGTGCTGCACGAAATGGA
CGATTACGGAAACACCCCTCTGCATTGTGCAGTGGAGAAAAATCAGATCGAAAGCGTCA
AGTTTCTGCTGTCTCGAGGCGCCAACCCCAATCTGCGTAACTTCAATATGATGGCCCCTCT
GCACATTGCTGTGCAGGGAATGAACAATGAAGTGATGAAGGTCCTGCTGGAACATAGGA
CAATCGACGTGAATCTGGAGGGGGAAAACGGTAATACTGCAGTCATCATTGCCTGCACCA
CAAACAATTCTGAGGCTCTGCAGATTCTGCTGAAGAAAGGCGCAAAGCCATGCAAAAGT
AACAAGTGGGGATGTTTTCCCATCCACCAGGCCGCTTTCAGTGGCTCAAAGGAGTGTATG
GAAATCATTCTGAGGTTTGGGGAGGAACACGGTTACTCTCGGCAGCTGCATATCAACTTC
ATGAACAATGGGAAGGCCACTCCACTGCACCTGGCTGTGCAGAACGGCGACCTGGAGAT
GATCAAAATGTGCCTGGACAATGGCGCCCAGATTGATCCCGTGGAAAAGGGACGGTGTA
CCGCCATTCATTTTGCAGCCACCCAGGGAGCTACAGAGATCGTGAAGCTGATGATTTCTA
GTTACTCCGGGAGCGTGGACATCGTCAATACTACCGATGGTTGCCACGAGACCATGCTGC
ATAGAGCTTCTCTGTTCGACCACCATGAACTGGCAGATTATCTGATCAGTGTGGGCGCCG
ACATCAACAAGATTGATTCTGAGGGACGCAGTCCACTGATCCTGGCTACAGCATCTGCCA
GTTGGAACATTGTGAATCTGCTGCTGAGCAAAGGGGCCCAGGTCGACATTAAGGATAACT
TTGGTCGAAATTTCCTGCACCTGACTGTGCAGCAGCCATACGGGCTGAAAAATCTGCGTC

CCGAGTTTATGCAGATGCAGCAGATCAAGGAGCTGGTCATGGATGAAGACAACGATGGT
TGCACCCCTCTGCATTATGCTTGTAGGCAGGGCGGACCAGGCAGCGTGAACAATCTGCTG
GGCTTCAACGTGTCCATCCACTCAAAGTCCAAAGACAAGAAATCTCCTCTGCATTTCGCT
GCAAGTTACGGGAGAATCAACACTTGCCAGCGCCTGCTGCAGGACATTTCTGATACCCGG
CTGCTGAATGAGGGCGACCTGCACGGAATGACCCCACTGCATCTGGCCGCTAAAAACGG
ACACGATAAGGTGGTCCAGCTGCTGCTGAAGAAAGGGGCCCTGTTCCTGTCCGACCATAA
CGGTTGGACAGCTCTGCACCATGCAAGCATGGGCGGCTATACTCAGACCATGAAAGTGAT
CCTGGACACTAACCTGAAGTGTACCGATAGGCTGGACGAGGATGGCAATACTGCTCTGCA
CTTTGCAGCCCGGGAAGGACATGCTAAGGCAGTGGCCCTGCTGCTGTCACACAACGCCGA
TATCGTCCTGAATAAGCAGCAGGCATCCTTCCTGCACCTGGCCCTGCATAATAAGAGAAA
AGAGGTGGTCCTGACAATCATTAGGTCCAAACGGTGGGACGAATGCCTGAAGATCTTTAG
CCACAACTCTCCTGGCAACAAGTGTCCAATCACCGAGATGATTGAATACCTGCCAGAGTG
CATGAAGGTGCTGCTGGATTTCTGTATGCTGCATTCAACAGAGGACAAATCCTGCCGCGA
TTACTACATCGAATACAACTTCAAGTATCTGCAGTGTCCTCTGGAGTTCACCAAGAAAAC
ACCAACTCAGGACGTGATCTACGAACCCCTGACAGCCCTGAACGCTATGGTCCAGAACAA
TCGAATCGAGCTGCTGAATCACCCCGTGTGCAAAGAATACCTGCTGATGAAGTGGCTGGC
ATATGGCTTTCGTGCCCATATGATGAATCTGGGCTCTTATTGTCTGGGACTGATCCCCATG
ACCATTCTGGTGGTCAACATTAAGCCTGGGATGGCTTTCAACAGCACCGGTATCATTAAT
GAGACAAGTGACCACTCAGAAATCCTGGATACAACTAACTCTTACCTGATCAAGACATGC
ATGATTCTGGTGTTTCTGTCATCCATCTTCGGGTATTGTAAAGAGGCTGGTCAGATTTTTC
AGCAGAAGAGGAACTACTTCATGGATATCTCCAATGTGCTGGAGTGGATCATCTACACCA
CAGGGATCATTTTTGTGCTGCCCCTGTTCGTCGAAATCCCTGCCCATCTGCAGTGGCAGTG
CGGTGCTATTGCAGTGTACTTTTATTGGATGAACTTCCTGCTGTACCTGCAGAGGTTTGAG
AATTGTGGCATCTTCATTGTGATGCTGGAAGTCATCCTGAAGACACTGCTGCGGAGTACT
GTGGTCTTCATTTTTCTGCTGCTGGCCTTTGGACTGTCATTCTATATCCTGCTGAATCTGCA
GGATCCCTTCTCCTCTCCCCTGCTGAGTATCATTCAGACATTCTCAATGATGCTGGGCGAC
ATCAACTACAGAGAGAGCTTTCTGGAACCTTATCTGCGCAATGAGCTGGCCCACCCAGTG
CTGTCCTTCGCTCAGCTGGTCAGCTTTACTATCTTCGTGCCCATTGTCCTGATGAACCTGCT
GATCGGGCTGGCTGTGGGTGACATTGCAGAGGTCCAGAAACACGCTAGCCTGAAGAGAA
TCGCAATGCAGGTGGAGCTGCATACATCTCTGGAAAAGAAACTGCCTCTGTGGTTTCTGA
GAAAAGTGGATCAGAAGAGTACTATTGTCTACCCCAATAAGCCTCGCTCAGGCGGAATGC
TGTTCCATATCTTCTGCTTTCTGTTCTGTACCGGCGAGATCAGACAGGAAATTCCTAACGC
CGATAAGTCCCTGGAGATGGAAATTCTGAAGCAGAAATATCGCCTGAAAGACCTGACTTT
CCTGCTGGAGAAGCAGCACGAACTGATCAAACTGATCATTCAGAAGATGGAGATCATTA
GCGAGACCGAAGACGATGACTCCCATTGTAGCTTTCAGGACCGATTCAAGAAAGAGCAG
ATGGAACAGCGTAACTCCCGTTGGAATACCGTCCTGCGTGCCGTGAAAGCTAAGACCCAT
CATCTGGAACCATAAGCGGCCG

>Mutant: E179K Cloning Site: KpnI – NotI
GGTACCGCCACCATGAAAAGAAGCCTGCGAAAAATGTGGCGGCCCGGCGAAAAGAAGG
AACCTCAGGGGGTCGTGTATGAAGATGTGCCAGATGATACTGAGGACTTTAAAGAATCAC
TGAAGGTGGTCTTCGAGGGCTCCGCTTACGGACTGCAGAACTTCAACAAGCAGAAGAAA
CTGAAGCGATGCGACGATATGGATACCTTCTTTCTGCACTATGCCGCTGCAGAGGGCCAG
ATCGAGCTGATGGAAAAGATTACTCGGGACTCCAGCCTGGAGGTGCTGCACGAAATGGA
CGATTACGGAAACACCCCTCTGCATTGTGCAGTGGAGAAAAATCAGATCGAAAGCGTCA
AGTTTCTGCTGTCTCGAGGCGCCAACCCCAATCTGCGTAACTTCAATATGATGGCCCCTCT
GCACATTGCTGTGCAGGGAATGAACAATGAAGTGATGAAGGTCCTGCTGGAACATAGGA
CAATCGACGTGAATCTGGAGGGGGAAAACGGTAATACTGCAGTCATCATTGCCTGCACCA
CAAACAATTCTAAAGCTCTGCAGATTCTGCTGAAGAAAGGCGCAAAGCCATGCAAAAGT
AACAAGTGGGGATGTTTTCCCATCCACCAGGCCGCTTTCAGTGGCTCAAAGGAGTGTATG
GAAATCATTCTGAGGTTTGGGGAGGAACACGGTTACTCTCGGCAGCTGCATATCAACTTC
ATGAACAATGGGAAGGCCACTCCACTGCACCTGGCTGTGCAGAACGGCGACCTGGAGAT
GATCAAAATGTGCCTGGACAATGGCGCCCAGATTGATCCCGTGGAAAAGGGACGGTGTA
CCGCCATTCATTTTGCAGCCACCCAGGGAGCTACAGAGATCGTGAAGCTGATGATTTCTA

GTTACTCCGGGAGCGTGGACATCGTCAATACTACCGATGGTTGCCACGAGACCATGCTGC
ATAGAGCTTCTCTGTTCGACCACCATGAACTGGCAGATTATCTGATCAGTGTGGGCGCCG
ACATCAACAAGATTGATTCTGAGGGACGCAGTCCACTGATCCTGGCTACAGCATCTGCCA
GTTGGAACATTGTGAATCTGCTGCTGAGCAAAGGGGCCCAGGTCGACATTAAGGATAACT
TTGGTCGAAATTTCCTGCACCTGACTGTGCAGCAGCCATACGGGCTGAAAAATCTGCGTC
CCGAGTTTATGCAGATGCAGCAGATCAAGGAGCTGGTCATGGATGAAGACAACGATGGT
TGCACCCCTCTGCATTATGCTTGTAGGCAGGGCGGACCAGGCAGCGTGAACAATCTGCTG
GGCTTCAACGTGTCCATCCACTCAAAGTCCAAAGACAAGAAATCTCCTCTGCATTTCGCT
GCAAGTTACGGGAGAATCAACACTTGCCAGCGCCTGCTGCAGGACATTTCTGATACCCGG
CTGCTGAATGAGGGCGACCTGCACGGAATGACCCCACTGCATCTGGCCGCTAAAAACGG
ACACGATAAGGTGGTCCAGCTGCTGCTGAAGAAAGGGGCCCTGTTCCTGTCCGACCATAA
CGGTTGGACAGCTCTGCACCATGCAAGCATGGGCGGCTATACTCAGACCATGAAAGTGAT
CCTGGACACTAACCTGAAGTGTACCGATAGGCTGGACGAGGATGGCAATACTGCTCTGCA
CTTTGCAGCCCGGGAAGGACATGCTAAGGCAGTGGCCCTGCTGCTGTCACACAACGCCGA
TATCGTCCTGAATAAGCAGCAGGCATCCTTCCTGCACCTGGCCCTGCATAATAAGAGAAA
AGAGGTGGTCCTGACAATCATTAGGTCCAAACGGTGGGACGAATGCCTGAAGATCTTTAG
CCACAACTCTCCTGGCAACAAGTGTCCAATCACCGAGATGATTGAATACCTGCCAGAGTG
CATGAAGGTGCTGCTGGATTTCTGTATGCTGCATTCAACAGAGGACAAATCCTGCCGCGA
TTACTACATCGAATACAACTTCAAGTATCTGCAGTGTCCTCTGGAGTTCACCAAGAAAAC
ACCAACTCAGGACGTGATCTACGAACCCCTGACAGCCCTGAACGCTATGGTCCAGAACAA
TCGAATCGAGCTGCTGAATCACCCCGTGTGCAAAGAATACCTGCTGATGAAGTGGCTGGC
ATATGGCTTTCGTGCCCATATGATGAATCTGGGCTCTTATTGTCTGGGACTGATCCCCATG
ACCATTCTGGTGGTCAACATTAAGCCTGGGATGGCTTTCAACAGCACCGGTATCATTAAT
GAGACAAGTGACCACTCAGAAATCCTGGATACAACTAACTCTTACCTGATCAAGACATGC
ATGATTCTGGTGTTTCTGTCATCCATCTTCGGGTATTGTAAAGAGGCTGGTCAGATTTTTC
AGCAGAAGAGGAACTACTTCATGGATATCTCCAATGTGCTGGAGTGGATCATCTACACCA
CAGGGATCATTTTTGTGCTGCCCCTGTTCGTCGAAATCCCTGCCCATCTGCAGTGGCAGTG
CGGTGCTATTGCAGTGTACTTTTATTGGATGAACTTCCTGCTGTACCTGCAGAGGTTTGAG
AATTGTGGCATCTTCATTGTGATGCTGGAAGTCATCCTGAAGACACTGCTGCGGAGTACT
GTGGTCTTCATTTTTCTGCTGCTGGCCTTTGGACTGTCATTCTATATCCTGCTGAATCTGCA
GGATCCCTTCTCCTCTCCCCTGCTGAGTATCATTCAGACATTCTCAATGATGCTGGGCGAC
ATCAACTACAGAGAGAGCTTTCTGGAACCTTATCTGCGCAATGAGCTGGCCCACCCAGTG
CTGTCCTTCGCTCAGCTGGTCAGCTTTACTATCTTCGTGCCCATTGTCCTGATGAACCTGCT
GATCGGGCTGGCTGTGGGTGACATTGCAGAGGTCCAGAAACACGCTAGCCTGAAGAGAA
TCGCAATGCAGGTGGAGCTGCATACATCTCTGGAAAAGAAACTGCCTCTGTGGTTTCTGA
GAAAAGTGGATCAGAAGAGTACTATTGTCTACCCCAATAAGCCTCGCTCAGGCGGAATGC
TGTTCCATATCTTCTGCTTTCTGTTCTGTACCGGCGAGATCAGACAGGAAATTCCTAACGC
CGATAAGTCCCTGGAGATGGAAATTCTGAAGCAGAAATATCGCCTGAAAGACCTGACTTT
CCTGCTGGAGAAGCAGCACGAACTGATCAAACTGATCATTCAGAAGATGGAGATCATTA
GCGAGACCGAAGACGATGACTCCCATTGTAGCTTTCAGGACCGATTCAAGAAAGAGCAG
ATGGAACAGCGTAACTCCCGTTGGAATACCGTCCTGCGTGCCGTGAAAGCTAAGACCCAT
CATCTGGAACCATAAGCGGCCGC

>Mutant: H1018R Cloning Site: KpnI – NotI
GGTACCGCCACCATGAAAAGAAGCCTGCGAAAAATGTGGCGGCCCGGCGAAAAGAAGG
AACCTCAGGGGGTCGTGTATGAAGATGTGCCAGATGATACTGAGGACTTTAAAGAATCAC
TGAAGGTGGTCTTCGAGGGCTCCGCTTACGGACTGCAGAACTTCAACAAGCAGAAGAAA
CTGAAGCGATGCGACGATATGGATACCTTCTTTCTGCACTATGCCGCTGCAGAGGGCCAG
ATCGAGCTGATGGAAAAGATTACTCGGGACTCCAGCCTGGAGGTGCTGCACGAAATGGA
CGATTACGGAAACACCCCTCTGCATTGTGCAGTGGAGAAAAATCAGATCGAAAGCGTCA
AGTTTCTGCTGTCTCGAGGCGCCAACCCCAATCTGCGTAACTTCAATATGATGGCCCCTCT
GCACATTGCTGTGCAGGGAATGAACAATGAAGTGATGAAGGTCCTGCTGGAACATAGGA
CAATCGACGTGAATCTGGAGGGGGAAAACGGTAATACTGCAGTCATCATTGCCTGCACCA
CAAACAATTCTGAGGCTCTGCAGATTCTGCTGAAGAAAGGCGCAAAGCCATGCAAAAGT

AACAAGTGGGGATGTTTTCCCATCCACCAGGCCGCTTTCAGTGGCTCAAAGGAGTGTATG
GAAATCATTCTGAGGTTTGGGGAGGAACACGGTTACTCTCGGCAGCTGCATATCAACTTC
ATGAACAATGGGAAGGCCACTCCACTGCACCTGGCTGTGCAGAACGGCGACCTGGAGAT
GATCAAAATGTGCCTGGACAATGGCGCCCAGATTGATCCCGTGGAAAAGGGACGGTGTA
CCGCCATTCATTTTGCAGCCACCCAGGGAGCTACAGAGATCGTGAAGCTGATGATTTCTA
GTTACTCCGGGAGCGTGGACATCGTCAATACTACCGATGGTTGCCACGAGACCATGCTGC
ATAGAGCTTCTCTGTTCGACCACCATGAACTGGCAGATTATCTGATCAGTGTGGGCGCCG
ACATCAACAAGATTGATTCTGAGGGACGCAGTCCACTGATCCTGGCTACAGCATCTGCCA
GTTGGAACATTGTGAATCTGCTGCTGAGCAAAGGGGCCCAGGTCGACATTAAGGATAACT
TTGGTCGAAATTTCCTGCACCTGACTGTGCAGCAGCCATACGGGCTGAAAAATCTGCGTC
CCGAGTTTATGCAGATGCAGCAGATCAAGGAGCTGGTCATGGATGAAGACAACGATGGT
TGCACCCCTCTGCATTATGCTTGTAGGCAGGGCGGACCAGGCAGCGTGAACAATCTGCTG
GGCTTCAACGTGTCCATCCACTCAAAGTCCAAAGACAAGAAATCTCCTCTGCATTTCGCT
GCAAGTTACGGGAGAATCAACACTTGCCAGCGCCTGCTGCAGGACATTTCTGATACCCGG
CTGCTGAATGAGGGCGACCTGCACGGAATGACCCCACTGCATCTGGCCGCTAAAAACGG
ACACGATAAGGTGGTCCAGCTGCTGCTGAAGAAAGGGGCCCTGTTCCTGTCCGACCATAA
CGGTTGGACAGCTCTGCACCATGCAAGCATGGGCGGCTATACTCAGACCATGAAAGTGAT
CCTGGACACTAACCTGAAGTGTACCGATAGGCTGGACGAGGATGGCAATACTGCTCTGCA
CTTTGCAGCCCGGGAAGGACATGCTAAGGCAGTGGCCCTGCTGCTGTCACACAACGCCGA
TATCGTCCTGAATAAGCAGCAGGCATCCTTCCTGCACCTGGCCCTGCATAATAAGAGAAA
AGAGGTGGTCCTGACAATCATTAGGTCCAAACGGTGGGACGAATGCCTGAAGATCTTTAG
CCACAACTCTCCTGGCAACAAGTGTCCAATCACCGAGATGATTGAATACCTGCCAGAGTG
CATGAAGGTGCTGCTGGATTTCTGTATGCTGCATTCAACAGAGGACAAATCCTGCCGCGA
TTACTACATCGAATACAACTTCAAGTATCTGCAGTGTCCTCTGGAGTTCACCAAGAAAAC
ACCAACTCAGGACGTGATCTACGAACCCCTGACAGCCCTGAACGCTATGGTCCAGAACAA
TCGAATCGAGCTGCTGAATCACCCCGTGTGCAAAGAATACCTGCTGATGAAGTGGCTGGC
ATATGGCTTTCGTGCCCATATGATGAATCTGGGCTCTTATTGTCTGGGACTGATCCCCATG
ACCATTCTGGTGGTCAACATTAAGCCTGGGATGGCTTTCAACAGCACCGGTATCATTAAT
GAGACAAGTGACCACTCAGAAATCCTGGATACAACTAACTCTTACCTGATCAAGACATGC
ATGATTCTGGTGTTTCTGTCATCCATCTTCGGGTATTGTAAAGAGGCTGGTCAGATTTTTC
AGCAGAAGAGGAACTACTTCATGGATATCTCCAATGTGCTGGAGTGGATCATCTACACCA
CAGGGATCATTTTTGTGCTGCCCCTGTTCGTCGAAATCCCTGCCCATCTGCAGTGGCAGTG
CGGTGCTATTGCAGTGTACTTTTATTGGATGAACTTCCTGCTGTACCTGCAGAGGTTTGAG
AATTGTGGCATCTTCATTGTGATGCTGGAAGTCATCCTGAAGACACTGCTGCGGAGTACT
GTGGTCTTCATTTTTCTGCTGCTGGCCTTTGGACTGTCATTCTATATCCTGCTGAATCTGCA
GGATCCCTTCTCCTCTCCCCTGCTGAGTATCATTCAGACATTCTCAATGATGCTGGGCGAC
ATCAACTACAGAGAGAGCTTTCTGGAACCTTATCTGCGCAATGAGCTGGCCCACCCAGTG
CTGTCCTTCGCTCAGCTGGTCAGCTTTACTATCTTCGTGCCCATTGTCCTGATGAACCTGCT
GATCGGGCTGGCTGTGGGTGACATTGCAGAGGTCCAGAAACACGCTAGCCTGAAGAGAA
TCGCAATGCAGGTGGAGCTGCATACATCTCTGGAAAAGAAACTGCCTCTGTGGTTTCTGA
GAAAAGTGGATCAGAAGAGTACTATTGTCTACCCCAATAAGCCTCGCTCAGGCGGAATGC
TGTTCCGTATCTTCTGCTTTCTGTTCTGTACCGGCGAGATCAGACAGGAAATTCCTAACGC
CGATAAGTCCCTGGAGATGGAAATTCTGAAGCAGAAATATCGCCTGAAAGACCTGACTTT
CCTGCTGGAGAAGCAGCACGAACTGATCAAACTGATCATTCAGAAGATGGAGATCATTA
GCGAGACCGAAGACGATGACTCCCATTGTAGCTTTCAGGACCGATTCAAGAAAGAGCAG
ATGGAACAGCGTAACTCCCGTTGGAATACCGTCCTGCGTGCCGTGAAAGCTAAGACCCAT
CATCTGGAACCATAAGCGGCCGC

>Mutant: R3C+R58T Cloning Site: KpnI – NotI
GGTACCGCCACCATGAAATGCAGCCTGCGAAAAATGTGGCGGCCCGGCGAAAAGAAGGA
ACCTCAGGGGGTCGTGTATGAAGATGTGCCAGATGATACTGAGGACTTTAAAGAATCACT
GAAGGTGGTCTTCGAGGGCTCCGCTTACGGACTGCAGAACTTCAACAAGCAGAAGAAAC
TGAAGACCTGCGACGATATGGATACCTTCTTTCTGCACTATGCCGCTGCAGAGGGCCAGA
TCGAGCTGATGGAAAAGATTACTCGGGACTCCAGCCTGGAGGTGCTGCACGAAATGGAC

GATTACGGAAACACCCCTCTGCATTGTGCAGTGGAGAAAAATCAGATCGAAAGCGTCAA
GTTTCTGCTGTCTCGAGGCGCCAACCCCAATCTGCGTAACTTCAATATGATGGCCCCTCTG
CACATTGCTGTGCAGGGAATGAACAATGAAGTGATGAAGGTCCTGCTGGAACATAGGAC
AATCGACGTGAATCTGGAGGGGGAAAACGGTAATACTGCAGTCATCATTGCCTGCACCAC
AAACAATTCTGAGGCTCTGCAGATTCTGCTGAAGAAAGGCGCAAAGCCATGCAAAAGTA
ACAAGTGGGGATGTTTTCCCATCCACCAGGCCGCTTTCAGTGGCTCAAAGGAGTGTATGG
AAATCATTCTGAGGTTTGGGGAGGAACACGGTTACTCTCGGCAGCTGCATATCAACTTCA
TGAACAATGGGAAGGCCACTCCACTGCACCTGGCTGTGCAGAACGGCGACCTGGAGATG
ATCAAAATGTGCCTGGACAATGGCGCCCAGATTGATCCCGTGGAAAAGGGACGGTGTAC
CGCCATTCATTTTGCAGCCACCCAGGGAGCTACAGAGATCGTGAAGCTGATGATTTCTAG
TTACTCCGGGAGCGTGGACATCGTCAATACTACCGATGGTTGCCACGAGACCATGCTGCA
TAGAGCTTCTCTGTTCGACCACCATGAACTGGCAGATTATCTGATCAGTGTGGGCGCCGA
CATCAACAAGATTGATTCTGAGGGACGCAGTCCACTGATCCTGGCTACAGCATCTGCCAG
TTGGAACATTGTGAATCTGCTGCTGAGCAAAGGGGCCCAGGTCGACATTAAGGATAACTT
TGGTCGAAATTTCCTGCACCTGACTGTGCAGCAGCCATACGGGCTGAAAAATCTGCGTCC
CGAGTTTATGCAGATGCAGCAGATCAAGGAGCTGGTCATGGATGAAGACAACGATGGTT
GCACCCCTCTGCATTATGCTTGTAGGCAGGGCGGACCAGGCAGCGTGAACAATCTGCTGG
GCTTCAACGTGTCCATCCACTCAAAGTCCAAAGACAAGAAATCTCCTCTGCATTTCGCTG
CAAGTTACGGGAGAATCAACACTTGCCAGCGCCTGCTGCAGGACATTTCTGATACCCGGC
TGCTGAATGAGGGCGACCTGCACGGAATGACCCCACTGCATCTGGCCGCTAAAAACGGA
CACGATAAGGTGGTCCAGCTGCTGCTGAAGAAAGGGGCCCTGTTCCTGTCCGACCATAAC
GGTTGGACAGCTCTGCACCATGCAAGCATGGGCGGCTATACTCAGACCATGAAAGTGATC
CTGGACACTAACCTGAAGTGTACCGATAGGCTGGACGAGGATGGCAATACTGCTCTGCAC
TTTGCAGCCCGGGAAGGACATGCTAAGGCAGTGGCCCTGCTGCTGTCACACAACGCCGAT
ATCGTCCTGAATAAGCAGCAGGCATCCTTCCTGCACCTGGCCCTGCATAATAAGAGAAAA
GAGGTGGTCCTGACAATCATTAGGTCCAAACGGTGGGACGAATGCCTGAAGATCTTTAGC
CACAACTCTCCTGGCAACAAGTGTCCAATCACCGAGATGATTGAATACCTGCCAGAGTGC
ATGAAGGTGCTGCTGGATTTCTGTATGCTGCATTCAACAGAGGACAAATCCTGCCGCGAT
TACTACATCGAATACAACTTCAAGTATCTGCAGTGTCCTCTGGAGTTCACCAAGAAAACA
CCAACTCAGGACGTGATCTACGAACCCCTGACAGCCCTGAACGCTATGGTCCAGAACAAT
CGAATCGAGCTGCTGAATCACCCCGTGTGCAAAGAATACCTGCTGATGAAGTGGCTGGCA
TATGGCTTTCGTGCCCATATGATGAATCTGGGCTCTTATTGTCTGGGACTGATCCCCATGA
CCATTCTGGTGGTCAACATTAAGCCTGGGATGGCTTTCAACAGCACCGGTATCATTAATG
AGACAAGTGACCACTCAGAAATCCTGGATACAACTAACTCTTACCTGATCAAGACATGCA
TGATTCTGGTGTTTCTGTCATCCATCTTCGGGTATTGTAAAGAGGCTGGTCAGATTTTTCA
GCAGAAGAGGAACTACTTCATGGATATCTCCAATGTGCTGGAGTGGATCATCTACACCAC
AGGGATCATTTTTGTGCTGCCCCTGTTCGTCGAAATCCCTGCCCATCTGCAGTGGCAGTGC
GGTGCTATTGCAGTGTACTTTTATTGGATGAACTTCCTGCTGTACCTGCAGAGGTTTGAGA
ATTGTGGCATCTTCATTGTGATGCTGGAAGTCATCCTGAAGACACTGCTGCGGAGTACTG
TGGTCTTCATTTTTCTGCTGCTGGCCTTTGGACTGTCATTCTATATCCTGCTGAATCTGCAG
GATCCCTTCTCCTCTCCCCTGCTGAGTATCATTCAGACATTCTCAATGATGCTGGGCGACA
TCAACTACAGAGAGAGCTTTCTGGAACCTTATCTGCGCAATGAGCTGGCCCACCCAGTGC
TGTCCTTCGCTCAGCTGGTCAGCTTTACTATCTTCGTGCCCATTGTCCTGATGAACCTGCT
GATCGGGCTGGCTGTGGGTGACATTGCAGAGGTCCAGAAACACGCTAGCCTGAAGAGAA
TCGCAATGCAGGTGGAGCTGCATACATCTCTGGAAAAGAAACTGCCTCTGTGGTTTCTGA
GAAAAGTGGATCAGAAGAGTACTATTGTCTACCCCAATAAGCCTCGCTCAGGCGGAATGC
TGTTCCATATCTTCTGCTTTCTGTTCTGTACCGGCGAGATCAGACAGGAAATTCCTAACGC
CGATAAGTCCCTGGAGATGGAAATTCTGAAGCAGAAATATCGCCTGAAAGACCTGACTTT
CCTGCTGGAGAAGCAGCACGAACTGATCAAACTGATCATTCAGAAGATGGAGATCATTA
GCGAGACCGAAGACGATGACTCCCATTGTAGCTTTCAGGACCGATTCAAGAAAGAGCAG
ATGGAACAGCGTAACTCCCGTTGGAATACCGTCCTGCGTGCCGTGAAAGCTAAGACCCAT
CATCTGGAACCATAAGCGGCCGC

APPENDIX B – STATISTICS SUMMARIES

i. One-way ANOVA Table – effect of TRPA1 polymorphisms on the maximal effect of cinnamaldehyde (Section 3.2.2)

	Sum of Squares	df	Mean Square	F(DFn, DFd)	p
Treatment (between columns)	29832	5	5966	F (5, 24) = 2.122	P=0.0974
Residual (within columns)	67466	24	2811		
Total	97298	29			

ii. One-way ANOVA Table – effect of TRPA1 polymorphisms on the EC_{50} of cinnamaldehyde (Section 3.2.2)

	Sum of Squares	df	Mean Square	F(DFn, DFd)	p
Treatment (between columns)	4.903E-10	5	9.807E-11	F (5, 24) = 1.967	P=0.1203
Residual (within columns)	1.197E-09	24	4.986E-11		
Total	1.687E-09	29			

iii. One-way ANOVA Table – effect of TRPA1 polymorphisms on the maximal effect of H-TFLLR-NH_2 (Section 3.2.2)

	Sum of Squares	df	Mean Square	F (DFn, DFd)	p
Treatment (between columns)	2923	5	584.6	F (5, 30) = 0.319	P=0.8976
Residual (within columns)	54977	30	1833		
Total	57900	35			

iv. One-way ANOVA Table – effect of TRPA1 polymorphisms on the EC_{50} of H-TFLLR-NH_2 (Section 3.2.2)

	Sum of Squares	df	Mean Square	F (DFn, DFd)	p
Treatment (between columns)	9.377E-12	5	1.875E-12	F (5, 30) = 0.6692	P=0.6498
Residual (within columns)	8.407E-11	30	2.802E-12		
Total	9.345E-11	35			

v. Two-way ANOVA Table – difference of maximal effect of 1mM AITC and CA between TRPA1 polymorphisms (Section 4.2.2)

	Sum of Squares (Type III)	df	Mean Square	F (DFn, DFd)	p
Interaction	4961	5	992.1	F (5, 47) = 1.213	P=0.3180
hTRPA1 Variant	3552	5	710.4	F (5, 47) = 0.8682	P=0.5095
Agonist	21574	1	21574	F (1, 47) = 26.37	P<0.0001
Residual	38456	47	818.2		

vi. Two-way ANOVA Table – difference of maximal effect of PB-22 and 5F-PB-22 at hTRPA1 variants (Section 5.2.5)

	Sum of Squares	df	Mean Square	F(DFn, DFd)	p
Interaction	302.2	5	60.45	F (5, 48) = 0.4496	P=0.8115
hTRPA1 Variant	4046	5	809.2	F (5, 48) = 6.018	P=0.0002
Drug	885.5	1	885.5	F (1, 48) = 6.586	P=0.0135
Residual	6454	48	134.5		

vii. Two-way ANOVA Table – difference of 10 µM PB-22 and 5F-PB-22 at hTRPA1 variants (Section 5.2.5)

	Sum of Squares	df	Mean Square	F(DFn, DFd)	p
Interaction	148.2	5	29.63	F (5, 48) = 0.268	P=0.9284
hTRPA1 Variant	2614	5	522.8	F (5, 48) = 4.728	P=0.0014
Drug	1456	1	1456	F (1, 48) = 13.17	P=0.0007
Residual	5307	48	110.6		

viii. Two-way ANOVA Table – difference of maximal effect of UR-144 and XLR-11 at hTRPA1 variants (Section 5.2.8)

	Sum of Squares	df	Mean Square	F(DFn, DFd)	p
Interaction	983.9	5	196.8	F (5, 48) = 1.156	P=0.3445
hTRPA1 Variant	5279	5	1056	F (5, 48) = 6.202	P=0.0002
Drug	10938	1	10938	F (1, 48) = 64.25	P<0.0001
Residual	8171	48	170.2		

ix. Two-way ANOVA Table – difference of 10 µM UR-144 and XLR-11 at hTRPA1 variants (Section 5.2.8)

	Sum of Squares	df	Mean Square	F(DFn, DFd)	p
Interaction	345.6	5	69.12	F (5, 48) = 0.8777	P=0.5032
hTRPA1 Variant	2232	5	446.4	F (5, 48) = 5.668	P=0.0003
Drug	11710	1	11710	F (1, 48) = 148.7	P<0.0001
Residual	3780	48	78.75		

x. Two-way ANOVA Table – difference of 30 µM 5-OH, UR-144 and XLR-11 at hTRPA1 variants

	Sum of Squares	df	Mean Square	F(DFn, DFd)	p
Interaction	2386	10	238.6	F (10, 72) = 0.7573	P=0.6686
TRPA1 Variant	8688	5	1738	F (5, 72) = 5.515	P=0.0002
Drug	29381	2	14690	F (2, 72) = 46.62	P<0.0001
Residual	22687	72	315.1		

xi. Two-way ANOVA Table – difference of 10 µM 5-OH, UR-144 and XLR-11 at hTRPA1 variants

	Sum of Squares	df	Mean Square	F(DFn, DFd)	p
Interaction	1347	10	134.7	F (10, 72) = 0.5456	P=0.8519
TRPA1 Variant	3367	5	673.4	F (5, 72) = 2.728	P=0.0259
Drug	12189	2	6094	F (2, 72) = 24.69	P<0.0001
Residual	17773	72	246.8		

xii. Two-way ANOVA Table – difference of 30 µM THC compared to all synthetic cannabinoids

	Sum of Squares	df	Mean Square	F(DFn, DFd)	p
Interaction	12537	30	417.9	F (30, 168) = 1.392	P=0.0990
hTRPA1 Variant	9901	5	1980	F (5, 168) = 6.598	P<0.0001
Drug	72454	6	12076	F (6, 168) = 40.23	P<0.0001
Residual	50423	168	300.1		

xiii. Two-way ANOVA Table – difference of 10 µM THC compared to all synthetic cannabinoids

	Sum of Squares	df	Mean Square	F(DFn, DFd)	p
Interaction	7309	30	243.6	F (30, 168) = 1.111	P=0.3290
hTRPA1 Variant	5488	5	1098	F (5, 168) = 5.004	P=0.0003
Drug	37761	6	6294	F (6, 168) = 28.69	P<0.0001
Residual	36852	168	219.4		

REFERENCES

1. Russo, E.B., *History of Cannabis and Its Preparations in Saga, Science, and Sobriquet.* Chemistry & Biodiversity, 2007. **4**(8): p. 1614-1648.
2. ElSohly, M.A. and W. Gul, *Constituents of Cannabis Sativa*, in *Handbook of Cannabis*. 2014, Oxford University Press: Oxford.
3. Russo, E.B., *The Pharmacological History of Cannabis*, in *Handbook of Cannabis*. 2014, Oxford University Press: Oxford.
4. Ware, M.A., *Synthetic Psychoactive Cannabinoids Licensed as Medicines*, in *Handbook of Cannabis*. 2014, Oxford University Press: Oxford.
5. Maas, A.I.R., et al., *Efficacy and safety of dexanabinol in severe traumatic brain injury: results of a phase III randomised, placebo-controlled, clinical trial.* The Lancet Neurology, 2006. **5**(1): p. 38-45.
6. Burstein, S.H., *Ajulemic acid (CT3): a potent analog of the acid metabolites of THC.* Current Pharmaceutical Design, 2000. **6**(13): p. 1339-45.
7. Mattes, R.D., et al., *Bypassing the first-pass effect for the therapeutic use of cannabinoids.* Pharmacology Biochemistry and Behavior, 1993. **44**(3): p. 745-747.
8. Diasio, R.B., D.S. Ettinger, and B.E. Satterwhite, *Oral Levonantradol in the Treatment of Chemotherapy-Induced Emesis: Preliminary Observations.* The Journal of Clinical Pharmacology, 1981. **21**(S1): p. 81S-85S.
9. Pain, S., *A potted history.* Nature, 2015. **525**(7570): p. S10-S11.
10. Nurmikko, T.J., et al., *Sativex successfully treats neuropathic pain characterised by allodynia: A randomised, double-blind, placebo-controlled clinical trial.* PAIN, 2007. **133**(1-2-3): p. 210-220.
11. Novotna, A., et al., *A randomized, double-blind, placebo-controlled, parallel-group, enriched-design study of nabiximols* (Sativex(®)), as add-on therapy, in subjects with refractory spasticity caused by multiple sclerosis.* European Journal Of Neurology, 2011. **18**(9): p. 1122-1131.
12. Kavia, R.B.C., et al., *Randomized controlled trial of Sativex to treat detrusor overactivity in multiple sclerosis.* Multiple Sclerosis (Houndmills, Basingstoke, England), 2010. **16**(11): p. 1349-1359.
13. Blake, D.R., et al., *Preliminary assessment of the efficacy, tolerability and safety of a cannabis-based medicine (Sativex) in the treatment of pain caused by rheumatoid arthritis.* Rheumatology (Oxford, England), 2006. **45**(1): p. 50-52.
14. Mechoulam, R. and Y. Gaoni, *Recent Advances in the Chemistry of Hashish*, in *Fortschritte der Chemie Organischer Naturstoffe / Progress in the Chemistry of*

Organic Natural Products / Progrès dans la Chimie des Substances Organiques Naturelles, L. Zechmeister, Editor. 1967, Springer Vienna: Vienna. p. 175-213.

15. Howlett, A.C., et al., *International Union of Pharmacology. XXVII. Classification of Cannabinoid Receptors.* Pharmacological Reviews, 2002. **54**(2): p. 161-202.
16. Pertwee, R.G., *The pharmacology of cannabinoid receptors and their ligands: an overview.* International Journal of Obesity, 2006. **30**(S1): p. S13-S18.
17. Pagotto, U., et al., *The Emerging Role of the Endocannabinoid System in Endocrine Regulation and Energy Balance.* Endocrine Reviews, 2006. **27**(1): p. 73-100.
18. Devane, W.A., et al., *Isolation and structure of a brain constituent that binds to the cannabinoid receptor.* Science, 1992. **258**(5090): p. 1946.
19. Mechoulam, R., et al., *Identification of an endogenous 2-monoglyceride, present in canine gut, that binds to cannabinoid receptors.* Biochemical Pharmacology, 1995. **50**(1): p. 83-90.
20. Sugiura, T., et al., *2-Arachidonoylgylcerol: A Possible Endogenous Cannabinoid Receptor Ligand in Brain.* Biochemical and Biophysical Research Communications, 1995. **215**(1): p. 89-97.
21. Panikashvili, D., et al., *CB1 cannabinoid receptors are involved in neuroprotection via NF-κB inhibition.* Journal of Cerebral Blood Flow & Metabolism, 2005. **25**(4): p. 477-484.
22. van der Stelt, M. and V. Di Marzo, *The endocannabinoid system in the basal ganglia and in the mesolimbic reward system: implications for neurological and psychiatric disorders.* European Journal of Pharmacology, 2003. **480**(1): p. 133-150.
23. Varvel, S.A. and A.H. Lichtman, *Evaluation of CB₁ Receptor Knockout Mice in the Morris Water Maze.* Journal of Pharmacology and Experimental Therapeutics, 2002. **301**(3): p. 915.
24. Victoria, E.M. and A.-G. Edda, *Cannabinoid System as a Potential Target for Drug Development in the Treatment of Cardiovascular Disease.* Current Vascular Pharmacology, 2003. **1**(3): p. 301-313.
25. *World Drug Report 2016*. 2016, United Nations publication, Sales No. E.16.X1.7.
26. Winstock, A., et al., *Global Drug Survey - Global Overview and Highlights*, in *Global Drug Survey*. 2017.
27. *National Drug Strategy Household Survey 2016: detailed findings*, in *Drug Satistics Series*. 2017, Australian Institute of Health and Welfare: Canberra.
28. Curran, H.V. and C.J.A. Morgan, *Desired and Undesired Effects of Cannabis on the Human Mind and Psychological Well-Being*, in *Handbook of Cannabis*. 2014, Oxford University Press: Oxford.

29. Dekker, N., D.H. Linszen, and L. De Haan, *Reasons for cannabis use and effects of cannabis use as reported by patients with psychotic disorders.* Psychopathology, 2009. **42**(6): p. 350-60.
30. Gill, K.E., et al., *Reasons for Cannabis Use Among Youths at Ultra High Risk for Psychosis.* Early Intervention In Psychiatry, 2015. **9**(3): p. 207-210.
31. Lachenmeier, D.W. and J. Rehm, *Comparative risk assessment of alcohol, tobacco, cannabis and other illicit drugs using the margin of exposure approach.* Scientific Reports, 2015. **5**: p. 8126.
32. Grotenhermen, F., *Nonpsychological Adverse Effects*, in *Handbook of Cannabis*. 2014, Oxford University Press: Oxford.
33. Hancock-Allen, J.B., et al., *Notes from the Field: Death Following Ingestion of an Edible Marijuana Product--Colorado, March 2014.* MMWR Morbidity and Mortality Weekly Report, 2015. **64**(28): p. 771-2.
34. Hall, W. and L. Degenhardt, *Harm Reduction Policies for Cannabis*, in *Handbook of Cannabis*. 2014, Oxford University Press: Oxford.
35. Lloyd, B., et al., *Trends in Alcohol and Drug-Related Ambulance Attendances in Victoria: 2013/14*, in *Ambo Project: Alcohol and Drug Related Ambulance Attendances*. 2015: Fitzroy, Victoria. p. 212.
36. Roxburgh, A. and L. Burns, *Drug-related hospital stays in Australia 1993-2013.* Sydney: National Drug and Alcohol Research Centre, 2013.
37. Fisher, B.A., et al., *Cardiovascular complications induced by cannabis smoking: a case report and review of the literature.* Emergency Medicine Journal, 2005. **22**(9): p. 679-80.
38. Casier, I., et al., *Is recent cannabis use associated with acute coronary syndromes?* Acta Cardiologica, 2014. **69**(2): p. 131-136.
39. Thomas, B.F., et al., *Cannabinoid Designer Drugs: Effects and Forensics*, in *Handbook of Cannabis*. 2014, Oxford University Press: Oxford.
40. Pertwee, R.G., et al., *International Union of Basic and Clinical Pharmacology. LXXIX. Cannabinoid Receptors and Their Ligands: Beyond CB(1) and CB(2).* Pharmacological Reviews, 2010. **62**(4): p. 588-631.
41. Seely, K.A., et al., *Marijuana-based Drugs: Innovative Therapeutics or Designer Drugs of Abuse?* Molecular Interventions, 2011. **11**(1): p. 36-51.
42. Tabrizi, M.A. and P.G. Baraldi, *Chapter 62 - Chemistry of Cannabinoid Receptor Agonists A2 - Preedy, V.R*, in *Handbook of Cannabis and Related Pathologies*. 2017, Academic Press: San Diego. p. 592-605.

43. *Synthetic cannabinoids in Europe*, in *Perspectives on Drugs*. 2016, European Monitoring Centre for Drugs and Addiction.
44. *Understanding the 'Spice' phenomenon*, in *Thematic Papers*. 2009, European Monitoring Centre for Drugs and Drug Addiction: Luxembourg.
45. Chin, C.-n., et al., *The Third Transmembrane Helix of the Cannabinoid Receptor Plays a Role in the Selectivity of Aminoalkylindoles for CB2, Peripheral Cannabinoid Receptor.* Journal of Pharmacology and Experimental Therapeutics, 1999. **291**(2): p. 837.
46. Weissman, A., G.M. Milne, and L.S.J. Melvin, *Cannabimimetic activity from CP-47,497, a derivative of 3-phenylcyclohexanol.* The Journal of Pharmacology and Experimental Therapeutics, 1982(0022-3565 (Print)): p. 516-523.
47. Mechoulam, R., et al., *Enantiomeric cannabinoids: stereospecificity of psychotropic activity.* Experientia, 1988. **44**(9): p. 762-764.
48. *European Drug Report 2016: Trends and Developments*. 2016, European Monitoring Centre for Drugs and Drug Addiction: Publications Office of the European Union, Luxembourg.
49. *Special Report: Synthetic Cannabinoids and Synthetic Cathinones Reported in NFLIS, 2013-2015*. 2016, U.S. Drug Enforcement Administration: Springfield, VA 22152.
50. Castaneto, M.S., et al., *Synthetic Cannabinoids: Epidemiology, Pharmacodynamics, and Clinical Implications.* Drug and Alcohol Dependence, 2014. **0**: p. 12-41.
51. Hu, X., et al., *College students and use of K2: an emerging drug of abuse in young persons.* Substance Abuse Treatment, Prevention, and Policy, 2011. **6**: p. 16-16.
52. Vandrey, R., et al., *A survey study to characterize use of Spice products (synthetic cannabinoids).* Drug and Alcohol Dependence, 2012. **120**(1-3): p. 238-241.
53. Gunderson, E.W., et al., *A Survey of Synthetic Cannabinoid Consumption by Current Cannabis Users.* Substance abuse : official publication of the Association for Medical Education and Research in Substance Abuse, 2014. **35**(2): p. 184-189.
54. Barratt, M.J., V. Cakic, and S. Lenton, *Patterns of synthetic cannabinoid use in Australia.* Drug & Alcohol Review, 2013. **32**(2): p. 141-146.
55. Sutherland, R., et al., *Motivations for new psychoactive substance use among regular psychostimulant users in Australia.* The International Journal of Drug Policy, 2017. **43**: p. 23-32.
56. Dresen, S., et al., *Development and validation of a liquid chromatography-tandem mass spectrometry method for the quantitation of synthetic cannabinoids of the aminoalkylindole type and methanandamide in serum and its application to forensic samples.* Journal of Mass Spectrometry, (1096-9888 (Electronic)).

57. *Synthetic cannabinoids in Europe (Perspectives on drugs)*, in *Perspectives on Drugs (PODs)*. 2017, European Monitoring Centre for Drugs and Drug Addiction.
58. Johnston, L.D., et al., *Monitoring the Future national survey results on drug use: 1975-2014: Overview, key findings on adolescent drug use*. 2015, Institute for Social Research, The University of Michigan. : Ann Arbor.
59. Meyyappan, C., L. Ford, and A. Vale, *Poisoning due to MDMB-CHMICA, a synthetic cannabinoid receptor agonist.* Clinical Toxicology (Phila), 2017. **55**(2): p. 151-152.
60. Dobaja, M., et al., *Occupational transdermal poisoning with synthetic cannabinoid cumyl-PINACA.* Clinical Toxicology, 2017. **55**(3): p. 193-195.
61. Barcelo, B., et al., *Acute intoxication caused by synthetic cannabinoids 5F-ADB and MMB-2201: A case series.* Forensic Science International, 2017.
62. Westin, A.A., et al., *Sudden Cardiac Death Following Use of the Synthetic Cannabinoid MDMB-CHMICA.* Journal of Analytical Toxicology, 2016. **40**(1): p. 86-7.
63. Tournebize, J., V. Gibaja, and J.P. Kahn, *Acute effects of synthetic cannabinoids: Update 2015.* Substance Abuse, 2016: p. 1-23.
64. Springer, Y.P., et al., *Increase in adverse reactions associated with use of synthetic cannabinoids — Anchorage,Alaska,2015–2016.* Morbidity and Mortality Weekly Report, 2016. **65**(40): p. 1108-1111.
65. Shanks, K.G., W. Clark, and G. Behonick, *Death Associated With the Use of the Synthetic Cannabinoid ADB-FUBINACA.* Journal of Analytical Toxicology, 2016. **40**(3): p. 236-9.
66. Shanks, K.G. and G.S. Behonick, *Death after use of the synthetic cannabinoid 5F-AMB.* Forensic Science International, 2016. **262**: p. e21-4.
67. Seywright, A., et al., *Analysis and clinical findings of cases positive for the novel synthetic cannabinoid receptor agonist MDMB-CHMICA.* Clinical Toxicology (Phila), 2016. **54**(8): p. 632-7.
68. Raheemullah, A. and T.N. Laurence, *Repeated Thrombosis After Synthetic Cannabinoid Use.* The Journal of Emergency Medicine, 2016. **51**(5): p. 540-543.
69. Klavz, J., M. Gorenjak, and M. Marinsek, *Suicide attempt with a mix of synthetic cannabinoids and synthetic cathinones: Case report of non-fatal intoxication with AB-CHMINACA, AB-FUBINACA, alpha-PHP, alpha-PVP and 4-CMC.* Forensic Science International, 2016. **265**: p. 121-4.
70. Katz, K.D., et al., *Case Series of Synthetic Cannabinoid Intoxication from One Toxicology Center.* Western Journal of Emergency Medicine, 2016. **17**(3): p. 290-4.

71. Hill, S.L., et al., *Clinical toxicity following analytically confirmed use of the synthetic cannabinoid receptor agonist MDMB-CHMICA. A report from the Identification Of Novel psychoActive substances (IONA) study.* Clinical Toxicology (Phila), 2016. **54**(8): p. 638-43.
72. Clements-Nolle, K., et al., *Prevalence and Correlates of Any and Frequent Synthetic Cannabinoid Use in a Representative Sample of High School Students.* Substance Use & Misuse, 2016. **51**(9): p. 1139-46.
73. Backberg, M., et al., *Analytically Confirmed Intoxications Involving MDMB-CHMICA from the STRIDA Project.* Journal of Medical Toxicology, 2016.
74. Angerer, V., et al., *Reply to 'Sudden Cardiac Death Following Use of the Synthetic Cannabinoid MDMB-CHMICA'.* Journal of Analytical Toxicology, 2016. **40**(3): p. 240-2.
75. Adams, A.J., et al., *"Zombie" Outbreak Caused by the Synthetic Cannabinoid AMB-FUBINACA in New York.* New England Journal of Medicine, 2016.
76. Adamowicz, P. and J. Gieron, *Acute intoxication of four individuals following use of the synthetic cannabinoid MAB-CHMINACA.* Clinical Toxicology (Phila), 2016. **54**(8): p. 650-4.
77. Adamowicz, P., *Fatal intoxication with synthetic cannabinoid MDMB-CHMICA.* Forensic Science International, 2016. **261**: p. e5-10.
78. Abouchedid, R., et al., *Acute Toxicity Associated with Use of 5F-Derivations of Synthetic Cannabinoid Receptor Agonists with Analytical Confirmation.* Journal of Medical Toxicology, 2016. **12**(4): p. 396-401.
79. Tyndall, J.A., et al., *An outbreak of acute delirium from exposure to the synthetic cannabinoid AB-CHMINACA.* Clinical Toxicology (Phila), 2015. **53**(10): p. 950-6.
80. Trecki, J., R.R. Gerona, and M.D. Schwartz, *Synthetic Cannabinoid–Related Illnesses and Deaths.* New England Journal of Medicine, 2015. **373**(2): p. 103-107.
81. Thornton, S.L., et al., *Unintentional Pediatric Exposure to a Synthetic Cannabinoid (AB-PINACA) Resulting in Coma and Intubation.* Annals of Emergency Medicine, 2015. **66**(3): p. 343-4.
82. Schwartz, M.D., et al., *A Common Source Outbreak of Severe Delirium Associated with Exposure to the Novel Synthetic Cannabinoid ADB-PINACA.* The Journal of Emergency Medicine, 2015. **48**(5): p. 573-80.
83. Sampson, C.S., S.M. Bedy, and T. Carlisle, *Withdrawal seizures seen in the setting of synthetic cannabinoid abuse.* The American Journal of Emergency Medicine, 2015. **33**(11): p. 1712 e3.

84. Rose, D.Z., et al., *Hemorrhagic stroke following use of the synthetic marijuana "spice".* Neurology, 2015. **85**(13): p. 1177-1179.
85. Obafemi, A.I., et al., *Cluster of Acute Toxicity from Ingestion of Synthetic Cannabinoid-Laced Brownies.* Journal of Medical Toxicology, 2015. **11**(4): p. 426-9.
86. Hess, C., et al., *Death due to diabetic ketoacidosis: Induction by the consumption of synthetic cannabinoids?* Forensic Science International, 2015. **257**: p. e6-11.
87. Hasegawa, K., et al., *Postmortem distribution of MAB-CHMINACA in body fluids and solid tissues of a human cadaver.* Forensic Science International, 2015. **33**(2): p. 380-387.
88. Gerostamoulos, D., O.H. Drummer, and N.W. Woodford, *Deaths linked to synthetic cannabinoids.* Forensic Science, Medicine, and Pathology, 2015. **11**(3): p. 478.
89. Davis, C. and D. Boddington, *Teenage cardiac arrest following abuse of synthetic cannabis.* Heart Lung and Circulation, 2015. **24**(10): p. e162-3.
90. Besli, G.E., et al., *Synthetic Cannabinoid Abuse in Adolescents: A Case Series.* The Journal of Emergency Medicine, 2015. **49**(5): p. 644-50.
91. Monte, A.A., et al., *An outbreak of exposure to a novel synthetic cannabinoid.* New England Journal of Medicine, 2014. **370**(4): p. 389-90.
92. Hasegawa, K., et al., *Identification and quantitation of 5-fluoro-ADB, one of the most dangerous synthetic cannabinoids, in the stomach contents and solid tissues of a human cadaver and in some herbal products.* Forensic Toxicology, 2014. **33**(1): p. 112-121.
93. Gugelmann, H., et al., *'Crazy Monkey' poisons man and dog: Human and canine seizures due to PB-22, a novel synthetic cannabinoid.* Clinical Toxicology (Phila), 2014. **52**(6): p. 635-8.
94. Behonick, G., et al., *Four postmortem case reports with quantitative detection of the synthetic cannabinoid, 5F-PB-22.* Journal of Analytical Toxicology, 2014. **38**(8): p. 559-62.
95. Efe, T.H., et al., *Atrial fibrillation following synthetic cannabinoid abuse.* Turk Kardiyol Dern Ars, 2017. **45**(4): p. 362-364.
96. Banister, S.D., et al., *Pharmacology of Valinate and tert-Leucinate Synthetic Cannabinoids 5F-AMBICA, 5F-AMB, 5F-ADB, AMB-FUBINACA, MDMB-FUBINACA, MDMB-CHMICA, and Their Analogues.* ACS Chemical Neuroscience, 2016. **7**(9): p. 1241-54.
97. Banister, S.D., et al., *Pharmacology of Indole and Indazole Synthetic Cannabinoid Designer Drugs AB-FUBINACA, ADB-FUBINACA, AB-PINACA, ADB-PINACA, 5F-*

AB-PINACA, 5F-ADB-PINACA, ADBICA, and 5F-ADBICA. ACS Chemical Neuroscience, 2015. **6**(9): p. 1546-1559.

98. Banister, S.D., et al., *Effects of Bioisosteric Fluorine in Synthetic Cannabinoid Designer Drugs JWH-018, AM-2201, UR-144, XLR-11, PB-22, 5F-PB-22, APICA, and STS-135.* ACS Chemical Neuroscience, 2015. **6**(8): p. 1445-1458.
99. Longworth, M., et al., *The pharmacology of cumyl-carboxamide synthetic cannabinoid new psychoactive substances (NPS) CUMYL-BICA, CUMYL-PICA, CUMYL-5F-PICA, CUMYL-5F-PINACA, and their analogues.* ACS Chemical Neuroscience, 2017.
100. Pertwee, R.G. and M.G. Cascio, *Known Pharmacological Actions of Delta-9-Tetrahydrocannabinol and of Four Other Chemical Constituents of Cannabis that Activate Cannabinoid Receptors*, in *Handbook of Cannabis*. 2014, Oxford University Press: Oxford.
101. Pertwee, R.G., *Receptors and Channels Targeted by Synthetic Cannabinoid Receptor Agonists and Antagonists.* Current Medicinal Chemistry, 2010. **17**(14): p. 1360-1381.
102. De Petrocellis, L. and V. Di Marzo, *Non-CB1, non-CB2 receptors for endocannabinoids, plant cannabinoids, and synthetic cannabimimetics: focus on G-protein-coupled receptors and transient receptor potential channels.* Journal of Neuroimmune Pharmacology, 2010. **5**(1): p. 103-21.
103. De Petrocellis, L., et al., *Effects of cannabinoids and cannabinoid-enriched Cannabis extracts on TRP channels and endocannabinoid metabolic enzymes.* British Journal of Pharmacology, 2011. **163**(7): p. 1479-1494.
104. De Petrocellis, L., et al., *Plant-derived cannabinoids modulate the activity of transient receptor potential channels of ankyrin type-1 and melastatin type-8.* The Journal of Pharmacology and Experimental Therapeutics, 2008. **325**(3): p. 1007-15.
105. O'Sullivan, S.E., et al., *Novel time-dependent vascular actions of Delta9-tetrahydrocannabinol mediated by peroxisome proliferator-activated receptor gamma.* Biochemical and Biophysical Research Communications, 2005. **337**(3): p. 824-31.
106. Andersson, D.A., et al., *TRPA1 mediates spinal antinociception induced by acetaminophen and the cannabinoid Δ9-tetrahydrocannabiorcol.* Nature Communications, 2011. **2**: p. 551.
107. Qin, N., et al., *TRPV2 Is Activated by Cannabidiol and Mediates CGRP Release in Cultured Rat Dorsal Root Ganglion Neurons.* The Journal of Neuroscience, 2008. **28**(24): p. 6231.

108. Gyombolai, P., et al., *Mutations in the 'DRY' motif of the CB1 cannabinoid receptor result in biased receptor variants.* Journal of Molecular Endocrinology, 2015. **54**(1): p. 75-89.
109. Montell, C., *A mint of mutations in TRPM8 leads to cool results.* Nature Neuroscience, 2006. **9**(4): p. 466-468.
110. Deering-Rice, C.E., et al., *Activation of Transient Receptor Potential Ankyrin-1 by Insoluble Particulate Material and Association with Asthma.* American Journal of Respiratory Cell and Molecular Biology, 2015. **53**(6): p. 893-901.
111. Morgan, K., et al., *Human TRPM8 and TRPA1 pain channels, including a gene variant with increased sensitivity to agonists (TRPA1 R797T), exhibit differential regulation by SRC-tyrosine kinase inhibitor.* Bioscience Reports, 2014. **34**(4).
112. Jordt, S.-E., et al., *Mustard oils and cannabinoids excite sensory nerve fibres through the TRP channel ANKTM1.* Nature, 2004. **427**(6971): p. 260-265.
113. Backes, C., et al., *New insights into the genetics of glioblastoma multiforme by familial exome sequencing.* Oncotarget, 2015. **6**(8): p. 5918-5931.
114. Gallo, V., et al., *TRPA1 gene polymorphisms and childhood asthma.* Pediatric Allergy and Immunology, 2016.
115. Kremeyer, B., et al., *A gain-of-function mutation in TRPA1 causes familial episodic pain syndrome.* Neuron, 2010. **66**(5): p. 671-80.
116. Morgan, K., L.R. Sadofsky, and A.H. Morice, *Genetic variants affecting human TRPA1 or TRPM8 structure can be classified in vitro as 'well expressed', 'poorly expressed' or 'salvageable'.* Bioscience Reports, 2015. **35**(5).
117. Uhl, G.R., et al., *Menthol preference among smokers: association with TRPA1 variants.* Nicotine & Tobacco Research, 2011. **13**(12): p. 1311-5.
118. Venkatachalam, K. and C. Montell, *TRP channels.* Annu Rev Biochem, 2007. **76**: p. 387-417.
119. Li, M., Y. Yu, and J. Yang, *Structural Biology of TRP Channels*, in *Transient Receptor Potential Channels*, M.S. Islam, Editor. 2010, Springer Netherlands.
120. Montell, C. and G.M. Rubin, *Molecular characterization of the drosophila trp locus: A putative integral membrane protein required for phototransduction.* Neuron, 1989. **2**(4): p. 1313-1323.
121. Cosens, D.J. and A. Manning, *Abnormal Electroretinogram from a Drosophila Mutant.* Nature, 1969. **224**: p. 285-287.
122. Sun, M., et al., *Mucolipidosis type IV is caused by mutations in a gene encoding a novel transient receptor potential channel.* Human Molecular Genetics, 2000. **9**(17): p. 2471-2478.

123. Mochizuki, T., et al., *PKD2, a Gene for Polycystic Kidney Disease That Encodes an Integral Membrane Protein.* Science, 1996. **272**(5266): p. 1339-1342.
124. Bassi, M.T., et al., *Cloning of the Gene Encoding a Novel Integral Membrane Protein, Mucolipidin—and Identification of the Two Major Founder Mutations Causing Mucolipidosis Type IV.* American Journal of Human Genetics, 2000. **67**(5): p. 1110-1120.
125. Bargal, R., et al., *Identification of the gene causing mucolipidosis type IV.* Nat Genet, 2000. **26**(1): p. 118-123.
126. Walker, R.G., A.T. Willingham, and C.S. Zuker, *A Drosophila Mechanosensory Transduction Channel.* Science, 2000. **287**(5461): p. 2229.
127. Palmer, C.P., et al., *A TRP homolog in Saccharomyces cerevisiae forms an intracellular Ca(2+)-permeable channel in the yeast vacuolar membrane.* Proceedings of the National Academy of Sciences of the United States of America, 2001. **98**(14): p. 7801-7805.
128. Kaleta, M. and C. Palmer, *TRP Channels in Yeast*, in *Transient Receptor Potential Channels*, M.S. Islam, Editor. 2010, Springer Netherlands: Netherlands.
129. Denis, V. and M.S. Cyert, *Internal Ca(2+) release in yeast is triggered by hypertonic shock and mediated by a TRP channel homologue.* The Journal of Cell Biology, 2002. **156**(1): p. 29-34.
130. Palmer, Christopher P., E. Aydar, and Mustafa B A. Djamgoz, *A microbial TRP-like polycystic-kidney-disease-related ion channel gene.* Biochemical Journal, 2005. **387**(Pt 1): p. 211-219.
131. Aydar, E. and C.P. Palmer, *Polycystic kidney disease channel and synaptotagmin homologues play roles in schizosaccharomyces pombe cell wall synthesis/repair and membrane protein trafficking.* Journal of Membrane Biology, 2009. **229**(3): p. 141-52.
132. Gaudet, R., *Structural Insights into the Functon of TRP Channels*, in *TRP Ion Channel Function in Sensory Transduction and Cellular Signalling Cascades*, W.B. Liedtke and S. Heller, Editors. 2006, CRC Press/Taylor & Francis.
133. Jaquemar, D., T. Schenker, and B. Trueb, *An Ankyrin-like Protein with Transmembrane Domains Is Specifically Lost after Oncogenic Transformation of Human Fibroblasts.* Journal of Biological Chemistry, 1999. **274**(11): p. 7325-7333.
134. Gaudet, R., *A primer on ankyrin repeat function in TRP channels and beyond.* Molecular bioSystems, 2008. **4**(5): p. 372-379.
135. Mosavi, L.K., et al., *The ankyrin repeat as molecular architecture for protein recognition.* Protein Science : A Publication of the Protein Society, 2004. **13**(6): p. 1435-1448.

136. Liao, M., et al., *Structure of the TRPV1 ion channel determined by electron cryo-microscopy.* Nature, 2013. **504**(7478): p. 107-12.
137. Phelps, C.B., et al., *Structural analyses of the ankyrin repeat domain of TRPV6 and related TRPV ion channels.* Biochemistry, 2008. **47**(8): p. 2476-84.
138. Shi, D.J., et al., *Crystal structure of the N-terminal ankyrin repeat domain of TRPV3 reveals unique conformation of finger 3 loop critical for channel function.* Protein Cell, 2013. **4**(12): p. 942-50.
139. Sullivan, J.M., et al., *Novel mutations highlight the key role of the ankyrin repeat domain in TRPV4-mediated neuropathy.* Neurology Genetics, 2015. **1**(4): p. e29.
140. McCleverty, C.J., et al., *Crystal structure of the human TRPV2 channel ankyrin repeat domain.* Protein Science, 2006. **15**(9): p. 2201-6.
141. Feng, S., *TRPC Channel Structure and Properties*, in *Transient Receptor Potential Canonical Channels and Brain Diseases*, Y. Wang, Editor. 2017, Springer Netherlands: Dordrecht. p. 9-23.
142. Zhu, M.X., *Multiple roles of calmodulin and other Ca2+-binding proteins in the functional regulation of TRP channels.* Pflügers Archiv, 2005. **451**(1): p. 105-115.
143. Tang, J., et al., *Identification of Common Binding Sites for Calmodulin and Inositol 1,4,5-Trisphosphate Receptors on the Carboxyl Termini of Trp Channels.* The Journal of biological chemistry, 2001. **276**(24): p. 21303-21310.
144. Lau, S.Y., E. Procko, and R. Gaudet, *Distinct properties of Ca2+-calmodulin binding to N- and C-terminal regulatory regions of the TRPV1 channel.* J Gen Physiol, 2012. **140**(5): p. 541-55.
145. Holakovska, B., et al., *Calmodulin and S100A1 protein interact with N terminus of TRPM3 channel.* The Journal of Biological Chemistry, 2012. **287**(20): p. 16645-55.
146. Zhang, Z., et al., *Activation of Trp3 by inositol 1,4,5-trisphosphate receptors through displacement of inhibitory calmodulin from a common binding domain.* Proceedings of the National Academy of Sciences, 2001. **98**(6): p. 3168-3173.
147. Yogi, A., et al., *Aldosterone signaling through transient receptor potential melastatin 7 cation channel (TRPM7) and its alpha-kinase domain.* Cell Signal, 2013. **25**(11): p. 2163-75.
148. Thebault, S., et al., *Role of the alpha-kinase domain in transient receptor potential melastatin 6 channel and regulation by intracellular ATP.* Journal of Biological Chemistry, 2008. **283**(29): p. 19999-20007.
149. Scharenberg, A.M., *TRPM2 and TRPM7: channel/enzyme fusions to generate novel intracellular sensors.* Pflügers Archiv, 2005. **451**(1): p. 220-227.

150. Vergarajauregui, S., J.A. Martina, and R. Puertollano, *Identification of the penta-EF-hand protein ALG-2 as a Ca2+-dependent interactor of mucolipin-1*. Journal of Biological Chemistry, 2009. **284**(52): p. 36357-66.
151. Allen, M.D., et al., *A high-resolution structure of the EF-hand domain of human polycystin-2.* Protein Science, 2014. **23**(9): p. 1301-8.
152. Zheng, J., *Molecular mechanism of TRP channels.* Comprehensive Physiology, 2013. **3**(1): p. 221-42.
153. Wu, L.J., T.B. Sweet, and D.E. Clapham, *International Union of Basic and Clinical Pharmacology. LXXVI. Current Progress in the Mammalian TRP Ion Channel Family.* Pharmacological Reviews, 2010. **62**(3): p. 381-404.
154. Atoyan, R., D. Shander, and N.V. Botchkareva, *Non-neuronal expression of transient receptor potential type A1 (TRPA1) in human skin.* Journal of Investigative Dermatology, 2009. **129**(9): p. 2312-5.
155. Oancea, E., J.T. Wolfe, and D.E. Clapham, *Functional TRPM7 channels accumulate at the plasma membrane in response to fluid flow.* Circulation Research, 2006. **98**(2): p. 245-53.
156. Wagner, T.F.J., et al., *Transient receptor potential M3 channels are ionotropic steroid receptors in pancreatic [beta] cells.* Nat Cell Biol, 2008. **10**(12): p. 1421-1430.
157. Nijenhuis, T., *Localization and Regulation of the Epithelial Ca2+ Channel TRPV6 in the Kidney*. Journal of the American Society of Nephrology, 2003. **14**(11): p. 2731-2740.
158. Hoenderop, J.G.J., et al., *Molecular Identification of the Apical Ca2+Channel in 1,25-Dihydroxyvitamin D3-responsive Epithelia.* Journal of Biological Chemistry, 1999. **274**(13): p. 8375-8378.
159. Birder, L., et al., *Activation of urothelial transient receptor potential vanilloid 4 by 4alpha-phorbol 12,13-didecanoate contributes to altered bladder reflexes in the rat.* The Journal of Pharmacology and Experimental Therapeutics, 2007. **323**(1): p. 227-35.
160. Gevaert, T., et al., *Deletion of the transient receptor potential cation channel TRPV4 impairs murine bladder voiding.* The Journal of Clinical Investigation, 2007. **117**(11): p. 3453-3462.
161. Helliwell, R.J.A., et al., *Capsaicin sensitivity is associated with the expression of the vanilloid (capsaicin) receptor (VR1) mRNA in adult rat sensory ganglia.* Neuroscience Letters, 1998. **250**(3): p. 177-180.
162. Riccio, A., et al., *Essential role for TRPC5 in amygdala function and fear-related behavior*. Cell, 2009. **137**(4): p. 761-772.

163. Poole, D.P., et al., *Chapter 21 - Targeting of Transient Receptor Potential Channels in Digestive Disease A2 - Szallasi, Arpad*, in *TRP Channels as Therapeutic Targets*. 2015, Academic Press: Boston. p. 385-403.
164. Perez, C.A., et al., *A transient receptor potential channel expressed in taste receptor cells.* Nat Neurosci, 2002. **5**(11): p. 1169-1176.
165. Link, T.M., et al., *TRPV2 plays a pivotal role in macrophage particle binding and phagocytosis.* Nature immunology, 2010. **11**(3): p. 232-239.
166. Vetter, I. and R.J. Lewis, *Natural Product Ligands of TRP Channels*, in *Transient Receptor Potential Channels*, M.S. Islam, Editor. 2010, Springer Netherlands.
167. Caterina, M.J., et al., *The capsaicin receptor: a heat-activated ion channel in the pain pathway.* Nature, 1997. **389**(6653): p. 816-824.
168. Xu, H., et al., *Oregano, thyme and clove-derived flavors and skin sensitizers activate specific TRP channels.* Nat Neurosci, 2006. **9**(5): p. 628-635.
169. Bhuiyan, M.N.I., et al., *Constituents of the essential oil from leaves and buds of clove (Syzigium caryophyllatum (L.) Alston).* African Journal of Plant Science, 2010. **5**(11): p. 451-454.
170. Yang, B.H., et al., *Activation of Vanilloid Receptor 1 (VR1) by Eugenol.* Journal of Dental Research, 2003. **82**(10): p. 781-785.
171. Bandell, M., et al., *Noxious Cold Ion Channel TRPA1 Is Activated by Pungent Compounds and Bradykinin.* Neuron, 2004. **41**(6): p. 849-857.
172. McNamara, F.N., A. Randall, and M.J. Gunthorpe, *Effects of piperine, the pungent component of black pepper, at the human vanilloid receptor (TRPV1).* British Journal of Pharmacology, 2005. **144**(6): p. 781-790.
173. Peier, A.M., et al., *A TRP Channel that Senses Cold Stimuli and Menthol.* Cell, 2002. **108**(5): p. 705-715.
174. McKemy, D.D., W.M. Neuhausser, and D. Julius, *Identification of a cold receptor reveals a general role for TRP channels in thermosensation.* Nature, 2002. **416**(6876): p. 52-58.
175. Bautista, D.M., et al., *Pungent products from garlic activate the sensory ion channel TRPA1.* Proceedings of the National Academy of Sciences of the United States of America, 2005. **102**(34): p. 12248-12252.
176. Vogt-Eisele, A.K., et al., *Monoterpenoid agonists of TRPV3.* British Journal of Pharmacology, 2007. **151**(4): p. 530-40.
177. Smith, P.L., et al., *Bisandrographolide from Andrographis paniculata activates TRPV4 channels.* Journal of Biological Chemistry, 2006. **281**(40): p. 29897-904.

178. Watanabe, H., et al., *Activation of TRPV4 channels (hVRL-2/mTRP12) by phorbol derivatives.* Journal of Biological Chemistry, 2002. **277**(16): p. 13569-77.
179. Behrendt, H.J., et al., *Characterization of the mouse cold-menthol receptor TRPM8 and vanilloid receptor type-1 VR1 using a fluorometric imaging plate reader (FLIPR) assay.* British Journal of Pharmacology, 2004. **141**(4): p. 737-745.
180. Riera, C.E., et al., *Compounds from Sichuan and Melegueta peppers activate, covalently and non-covalently, TRPA1 and TRPV1 channels.* British Journal of Pharmacology, 2009. **157**(8): p. 1398-1409.
181. Bisogno, T., et al., *Molecular targets for cannabidiol and its synthetic analogues: effect on vanilloid VR1 receptors and on the cellular uptake and enzymatic hydrolysis of anandamide.* British Journal of Pharmacology, 2001. **134**(4): p. 845-852.
182. Neeper, M.P., et al., *Activation Properties of Heterologously Expressed Mammalian TRPV2: EVIDENCE FOR SPECIES DEPENDENCE.* Journal of Biological Chemistry, 2007. **282**(21): p. 15894-15902.
183. Bezanilla, F., *How membrane proteins sense voltage.* Nat Rev Mol Cell Biol, 2008. **9**(4): p. 323-332.
184. Voets, T., et al., *The principle of temperature-dependent gating in cold- and heat-sensitive TRP channels.* Nature, 2004. **430**(7001): p. 748-754.
185. Schoppa, N.E., et al., *The size of gating charge in wild-type and mutant Shaker potassium channels.* Science, 1992. **255**(5052): p. 1712.
186. Brauchi, S. and P. Orio, *Voltage Sensing in Thermo-TRP Channels*, in *Transient Receptor Potential Channels*, M.S. Islam, Editor. 2010, Springer Netherlands.
187. Karashima, Y., et al., *TRPA1 acts as a cold sensor in vitro and in vivo.* Proceedings of the National Academy of Sciences of the United States of America, 2009. **106**(4): p. 1273-1278.
188. Caterina, M.J., et al., *A capsaicin-receptor homologue with a high threshold for noxious heat.* Nature, 1999. **398**(6726): p. 436-441.
189. Peier, A.M., et al., *A Heat-Sensitive TRP Channel Expressed in Keratinocytes.* Science, 2002. **296**(5575): p. 2046-2049.
190. Moran, M.M., H. Xu, and D.E. Clapham, *TRP ion channels in the nervous system.* Current Opinion in Neurobiology, 2004. **14**(3): p. 362-369.
191. Caterina, M.J., *Transient receptor potential ion channels as participants in thermosensation and thermoregulation.* American Journal of Physiology - Regulatory, Integrative and Comparative Physiology, 2007. **292**(1): p. R64-R76.
192. McKemy, D.D., *How cold is it? TRPM8 and TRPA1 in the molecular logic of cold sensation.* Molecular Pain, 2005. **1**: p. 16-16.

193. Zimmermann, K., et al., *Transient receptor potential cation channel, subfamily C, member 5 (TRPC5) is a cold-transducer in the peripheral nervous system.* Proceedings of the National Academy of Sciences of the United States of America, 2011. **108**(44): p. 18114-18119.
194. Wu, L., et al., *Dual role of the TRPV4 channel as a sensor of flow and osmolality in renal epithelial cells.* American Journal of Physiology - Renal Physiology, 2007. **293**(5): p. F1699-F1713.
195. Liedtke, W., et al., *Vanilloid receptor-related osmotically activated channel (VR-OAC), a candidate vertebrate osmoreceptor.* Cell, 2000. **103**(3): p. 525-535.
196. Muraki, K., et al., *TRPV2 Is a Component of Osmotically Sensitive Cation Channels in Murine Aortic Myocytes.* Circulation Research, 2003. **93**(9): p. 829.
197. Numata, T., T. Shimizu, and Y. Okada, *TRPM7 is a stretch- and swelling-activated cation channel involved in volume regulation in human epithelial cells.* American Journal of Physiology - Cell Physiology, 2007. **292**(1): p. C460-C467.
198. Maroto, R., et al., *TRPC1 forms the stretch-activated cation channel in vertebrate cells.* Nat Cell Biol, 2005. **7**(2): p. 179-185.
199. Spassova, M.A., et al., *A common mechanism underlies stretch activation and receptor activation of TRPC6 channels.* Proceedings of the National Academy of Sciences of the United States of America, 2006. **103**(44): p. 16586-16591.
200. Morita, H., et al., *Membrane Stretch-Induced Activation of a TRPM4-Like Nonselective Cation Channel in Cerebral Artery Myocytes.* Journal of Pharmacological Sciences, 2007. **103**(4): p. 417-426.
201. *UniProtKB - O75762 (TRPA1_HUMAN)*. 2017 10/05/2017 [cited 2017 31/05]; Available from: http://www.uniprot.org/uniprot/O75762.
202. Laursen, W.J., S.N. Bagriantsev, and E.O. Gracheva, *TRPA1 channels: chemical and temperature sensitivity.* Current Topics in Membranes, 2014. **74**: p. 89-112.
203. Hinman, A., et al., *TRP channel activation by reversible covalent modification.* Proceedings of the National Academy of Sciences, 2006. **103**(51): p. 19564-19568.
204. Macpherson, L.J., et al., *Noxious compounds activate TRPA1 ion channels through covalent modification of cysteines.* Nature, 2007. **445**(7127): p. 541-5.
205. Zayats, V., et al., *Regulation of the transient receptor potential channel TRPA1 by its N-terminal ankyrin repeat domain.* Journal of Molecular Modeling, 2013. **19**(11): p. 4689-4700.
206. Cordero-Morales, J.F., E.O. Gracheva, and D. Julius, *Cytoplasmic ankyrin repeats of transient receptor potential A1 (TRPA1) dictate sensitivity to thermal and chemical*

stimuli. Proceedings of the National Academy of Sciences, 2011. **108**(46): p. E1184-E1191.

207. Paulsen, C.E., et al., *Structure of the TRPA1 ion channel suggests regulatory mechanisms.* Nature, 2015. **520**(7548): p. 511-7.
208. Story, G.M., et al., *ANKTM1, a TRP-like Channel Expressed in Nociceptive Neurons, Is Activated by Cold Temperatures.* Cell, 2003. **112**(6): p. 819-829.
209. Nilius, B., G. Appendino, and G. Owsianik, *The transient receptor potential channel TRPA1: from gene to pathophysiology.* Pflügers Archiv - European Journal of Physiology, 2012. **464**(5): p. 425-458.
210. Brozmanova, M., et al., *Preferential activation of the vagal nodose nociceptive subtype by TRPA1 agonists in the guinea pig esophagus.* Neurogastroenterology and motility : the official journal of the European Gastrointestinal Motility Society, 2011. **23**(10): p. e437-e445.
211. Pozsgai, G., et al., *Evidence for the pathophysiological relevance of TRPA1 receptors in the cardiovascular system in vivo.* Cardiovascular Research, 2010. **87**(4): p. 760-768.
212. Caceres, A.I., et al., *A sensory neuronal ion channel essential for airway inflammation and hyperreactivity in asthma.* Proceedings of the National Academy of Sciences, 2009. **106**(22): p. 9099-9104.
213. Büch, T.R.H., et al., *Functional expression of the transient receptor potential channel TRPA1, a sensor for toxic lung inhalants, in pulmonary epithelial cells.* Chemico-Biological Interactions, 2013. **206**(3): p. 462-471.
214. Nozawa, K., et al., *TRPA1 regulates gastrointestinal motility through serotonin release from enterochromaffin cells.* Proceedings of the National Academy of Sciences of the United States of America, 2009. **106**(9): p. 3408-3413.
215. Macpherson, L.J., et al., *The Pungency of Garlic: Activation of TRPA1 and TRPV1 in Response to Allicin.* Current Biology, 2005. **15**(10): p. 929-934.
216. Trevisani, M., et al., *4-Hydroxynonenal, an endogenous aldehyde, causes pain and neurogenic inflammation through activation of the irritant receptor TRPA1.* Proceedings of the National Academy of Sciences of the United States of America, 2007. **104**(33): p. 13519-13524.
217. Nilius, B., J. Prenen, and G. Owsianik, *Irritating channels: the case of TRPA1.* The Journal of Physiology, 2011. **589**(7): p. 1543-1549.
218. Andersson, D.A., et al., *Transient Receptor Potential A1 Is a Sensory Receptor for Multiple Products of Oxidative Stress.* The Journal of neuroscience : the official journal of the Society for Neuroscience, 2008. **28**(10): p. 2485-2494.

219. Bautista, D.M., et al., *TRPA1 Mediates the Inflammatory Actions of Environmental Irritants and Proalgesic Agents.* Cell, 2006. **124**(6): p. 1269-1282.
220. Andrè, E., et al., *Cigarette smoke–induced neurogenic inflammation is mediated by α,β-unsaturated aldehydes and the TRPA1 receptor in rodents.* The Journal of Clinical Investigation, 2008. **118**(7): p. 2574-2582.
221. Zygmunt, P.M., D.A. Andersson, and E.D. Högestätt, *Δ9-Tetrahydrocannabinol and Cannabinol Activate Capsaicin-Sensitive Sensory Nerves via a CB1 and CB2 Cannabinoid Receptor-Independent Mechanism.* The Journal of Neuroscience, 2002. **22**(11): p. 4720-4727.
222. Patacchini, R., C.A. Maggi, and A. Meli, *Capsaicin-like activity of some natural pungent substances on peripheral endings of visceral primary afferents.* Naunyn-Schmiedeberg's Archives of Pharmacology, 1990. **342**(1): p. 72-77.
223. Caterina, M.J., et al., *Impaired Nociception and Pain Sensation in Mice Lacking the Capsaicin Receptor.* Science, 2000. **288**(5464): p. 306-313.
224. Wilson, R.K., et al., *Effects of papaya seed extract and benzyl isothiocyanate on vascular contraction.* Life Sciences, 2002. **71**(5): p. 497-507.
225. Fernandes, E.S., M.A. Fernandes, and J.E. Keeble, *The functions of TRPA1 and TRPV1: moving away from sensory nerves.* British Journal of Pharmacology, 2012. **166**(2): p. 510-521.
226. !!! INVALID CITATION !!! {De Petrocellis, 2008 #101}.
227. Di Marzo, V. and L.D. Petrocellis, *Plant, synthetic, and endogenous cannabinoids in medicine.* Annual Review of Medicine, 2006. **57**: p. 553-74.
228. Qin, N., et al., *TRPV2 Is Activated by Cannabidiol and Mediates CGRP Release in Cultured Rat Dorsal Root Ganglion Neurons.* The Journal of Neuroscience, 2008. **28**(24): p. 6231-6238.
229. Akopian, A.N., et al., *Cannabinoids Desensitize Capsaicin and Mustard Oil Responses in Sensory Neurons via TRPA1 Activation.* The Journal of Neuroscience, 2008. **28**(5): p. 1064-1075.
230. Stuart, J.M., *The Pharmacology of Novel Illicit Synthetic Cannabinoids,* in *Australian School of Advanced Medicine*. 2015, Macquarie University. p. 329.
231. Binder, A., et al., *Transient Receptor Potential Channel Polymorphisms Are Associated with the Somatosensory Function in Neuropathic Pain Patients.* PLoS ONE, 2011. **6**(3): p. e17387.
232. Zhu, J., *Influence of polymorphisms of three TRP genes on pain sensitivity in neuropathic pain patients,* in *Faculty of Medicine*. 2009, University of Kiel.
233. Wong, B., *Points of view: Colour blindness.* Nature Methods, 2011. **8**(6): p. 441-441.

234. Redmond, W.J., et al., *Nordihydroguaiaretic acid activates hTRPA1 and modulates behavioral responses to noxious cold in mice.* Pharmacology Research & Perspectives, 2014. **2**(6): p. e00079.
235. Redmond, W.J., et al., *Ligand determinants of fatty acid activation of the pronociceptive ion channel TRPA1*. PeerJ, 2014. **2**: p. e248.
236. Arkin, M.R., et al., *FLIPR™ Assays for GPCR and Ion Channel Targets*, in *Assay Guidance Manual*, S. Sittamapalam, et al., Editors. 2012, Eli Lilly & Company and the National Center for Advancing Translational Sciences: Bethesda, Maryland.
237. S., S.K. and B.D. Neagle, *FLIPR: A New Instrument for Accurate, High Throughput Optical Screening.* Journal of Biomolecular Screening, 1996. **1**(2): p. 75-80.
238. Kahn, A.M. and E.J. Weinman, *Urate transport in the proximal tubule: in vivo and vesicle studies.* he American Journal of Physiology, 1985. **249**(6 Pt 2): p. 89-98.
239. Di Virgilio, F., T.H. Steinberg, and S.C. Silverstein, *Inhibition of Fura-2 sequestration and secretion with organic anion transport blockers.* Cell Calcium, 1990. **11**(2-3): p. 57-62.
240. McClenaghan, C., F. Zeng, and J.M. Verkuyl, *TRPA1 agonist activity of probenecid desensitizes channel responses: consequences for screening.* Assay and Drug Development Technologies, 2012. **10**(6): p. 533-41.
241. Bianchi, B.R., et al., *Species Comparison and Pharmacological Characterization of Human, Monkey, Rat, and Mouse TRPA1 Channels.* Journal of Pharmacology and Experimental Therapeutics, 2012. **341**(2): p. 360.
242. Atwood, B.K., et al., *Expression of G protein-coupled receptors and related proteins in HEK293, AtT20, BV2, and N18 cell lines as revealed by microarray analysis.* BMC Genomics, 2011. **12**: p. 14.
243. Vu, T.-K.H., et al., *Molecular cloning of a functional thrombin receptor reveals a novel proteolytic mechanism of receptor activation.* Cell, 1991. **64**(6): p. 1057-1068.
244. Wojtukiewicz, M.Z., et al., *Protease-activated receptors (PARs)—biology and role in cancer invasion and metastasis.* Cancer Metastasis Reviews, 2015. **34**: p. 775-796.
245. Ossovskaya, V.S. and N.W. Bunnett, *Protease-Activated Receptors: Contribution to Physiology and Disease.* Physiological Reviews, 2004. **84**(2): p. 579.
246. Wilkinson, S.M., S.D. Banister, and M. Kassiou, *Bioisosteric Fluorine in the Clandestine Design of Synthetic Cannabinoids.* Australian Journal of Chemistry, 2015. **68**(1): p. 4-8.
247. Brents, L.K., et al., *Phase I Hydroxylated Metabolites of the K2 Synthetic Cannabinoid JWH-018 Retain In Vitro and In Vivo Cannabinoid 1 Receptor Affinity and Activity*. PLoS ONE, 2011. **6**(7): p. e21917.

248. Rajasekaran, M., et al., *Human metabolites of synthetic cannabinoids JWH-018 and JWH-073 bind with high affinity and act as potent agonists at cannabinoid type-2 receptors.* Toxicology and applied pharmacology, 2013. **269**(2): p. 100-108.
249. Seely, K.A., et al., *A major glucuronidated metabolite of JWH-018 is a neutral antagonist at CB1 receptors.* Chemical research in toxicology, 2012. **25**(4): p. 825-827.
250. Longworth, M., et al., *Synthesis and Pharmacological profiling of the metabolites of synthetic cannabinoid drugs APICA, STS-135, ADB-PINACA, and 5F-ADB-PINACA.* ACS Chemical Neuroscience, 2017. **8**(8): p. 1673-1680.
251. Ogata, J., et al., *DNA sequence analyses of blended herbal products including synthetic cannabinoids as designer drugs.* Forensic Science International, 2013. **227**(1): p. 33-41.
252. Goodner, K.L., et al., *Aromatic profiles of Thymus hyemalis and Spanish T. vulgaris essential oils by GC–MS/GC–O.* Industrial Crops and Products, 2006. **24**(3): p. 264-268.
253. Lee, S.-J., et al., *Identification of volatile components in basil (Ocimum basilicum L.) and thyme leaves (Thymus vulgaris L.) and their antioxidant properties.* Food Chemistry, 2005. **91**(1): p. 131-137.
254. Bouchra, C., et al., *Chemical composition and antifungal activity of essential oils of seven Moroccan Labiatae against Botrytis cinerea Pers: Fr.* Journal of Ethnopharmacology, 2003. **89**(1): p. 165-169.
255. Moldão-Martins, M., et al., *Supercritical CO2 extraction of Thymus zygis L. subsp. sylvestris aroma.* The Journal of Supercritical Fluids, 2000. **18**(1): p. 25-34.
256. Haoxing, X., et al., *Oregano, thyme and clove-derived flavors and skin sensitizers activate specific TRP channels.* Nature Neuroscience, 2006. **9**(5): p. 628.
257. Bessac, B.F. and S.-E. Jordt, *Sensory Detection and Responses to Toxic Gases.* Proceedings of the American Thoracic Society, 2010. **7**(4): p. 269-277.
258. Birrell, M.A., et al., *TRPA1 Agonists Evoke Coughing in Guinea Pig and Human Volunteers.* American Journal of Respiratory and Critical Care Medicine, 2009. **180**(11): p. 1042-1047.
259. Bessac, B.F., et al., *Transient receptor potential ankyrin 1 antagonists block the noxious effects of toxic industrial isocyanates and tear gases.* The FASEB Journal, 2009. **23**(4): p. 1102-1114.
260. Brône, B., et al., *Tear gasses CN, CR, and CS are potent activators of the human TRPA1 receptor.* Toxicology and Applied Pharmacology, 2008. **231**(2): p. 150-156.

261. Shigetomi, E., et al., *TRPA1 Channels Are Regulators of Astrocyte Basal Calcium Levels and Long-Term Potentiation via Constitutive d-Serine Release.* The Journal of Neuroscience, 2013. **33**(24): p. 10143-10153.
262. Shigetomi, E., et al., *TRPA1 channels regulate astrocyte resting calcium levels and inhibitory synapse efficacy via GAT-3.* Nature neuroscience, 2012. **15**(1): p. 70-80.
263. Wang, S., et al., *Warmth suppresses and desensitizes damage-sensing ion channel TRPA1.* Molecular Pain, 2012. **8**: p. 22-22.
264. Peyrot Des Gachons, C., et al., *Unusual pungency from extra-virgin olive oil is attributable to restricted spatial expression of the receptor of oleocanthal.* The Journal of neuroscience : the official journal of the Society for Neuroscience, 2011. **31**(3): p. 999.
265. Xiao, B., et al., *Identification of the Transmembrane Domain Five as a Critical Molecular Determinant of Menthol Sensitivity in Mammalian TRPA1 Channels.* The Journal of neuroscience : the official journal of the Society for Neuroscience, 2008. **28**(39): p. 9640-9651.
266. Xu, H., et al., *Oregano, thyme and clove-derived flavors and skin sensitizers activate specific TRP channels.* Nature Neuroscience, 2006. **9**(5): p. 628-635.
267. Hotta, M., et al., *Carvacrol, a component of thyme oil, activates PPARα and γ and suppresses COX-2 expression.* Journal of Lipid Research, 2010. **51**(1): p. 132-139.
268. Katada, S., et al., *Structural Basis for a Broad But Selective Ligand Spectrum of a Mouse Olfactory Receptor: Mapping the Odorant-Binding Site.* The Journal of Neuroscience, 2005. **25**(7): p. 1806.
269. Andersson, D.A., et al., *Clioquinol and pyrithione activate TRPA1 by increasing intracellular Zn2+*. Proceedings of the National Academy of Sciences, 2009. **106**(20): p. 8374-8379.